Spatial distribution of dioxin deposition plumes in the vicinity of an incinerator using air dispersion coupled geostatistical model

by

Hoa Thi Trinh

A dissertation submitted in partial fulfillment
of the requirements for the degree of
Doctor of Philosophy
(Environmental Engineering)
in The University of Michigan
2009

Doctoral Committee:

Professor Peter Adriaens, Co-Chair

Associate Professor Christian M. Lastoskie, Co-Chair

Associate Professor Avery H. Demond

Associate Professor Olivier J. Jolliet

2009

To My Mom, Dad, Sisters and the Family

Acknowledgements

I am grateful to the continuous advices, encouragements and supports from Dr Peter Adriaens during my 5 years at the University of Michigan. I would like to thank Dr. Pierre Goovaerts at Biomedware, Ann Arbor, MI for the initial development of this study; for the great support to my following-up work and for the open guidance and discussions. I would want to thank to my committee members, professors and my colleagues at the University of Michigan Dioxin Exposure Study (UMDES) for exchanging information, discussions and conferences. I would like to express my profound respect to my family in Vietnam and to my friends for all the loving and caring. Lastly, I appreciate financial supports from Vietnam Education Foundation (VEF) for a graduate scholarship during my first two years and funding from the University of Michigan Dioxin Exposure Study for the last three years of my graduate study at the University of Michigan.

Table of Contents

List of Figures

List of Tables

Chapter 1

Introduction

Solid waste disposal is an ever increasing concern in a modern society, primarily addressed through landfill operations and incineration. The latter results in a large reduction of waste in terms of mass and volume, and has been an expensive alternative for hazardous waste disposal during the last decades. The high operating cost of an incinerator can be strategically offset by the benefit of energy generation, local transport, and a short reaction time, among other benefits*(1)*. Still, regulators strictly consider drawbacks of incineration such as incomplete combustion of waste, which leads to the formation and release of possible toxic chemicals to the environment. As a consequence, these releases potentially introduce exposure risks to these toxic chemicals for residents in the vicinity of an incinerator. Among the emissions from the incineration stacks, polychlorinated dibenzo-p- dioxins (PCDDs), polychlorinated dibenzo furans (PCDFs), and polychlorinated biphenyls (PCBs) generate the most concern due to their carcinogenic potential. Considerable research efforts have been directed towards estimating the levels of dioxin emissions from incinerators, their dispersion in air and distribution in soils and other environmental media, to inform regulatory thresholds *(2)*.

The distribution of dioxins from an incinerator in environmental media is often assessed by using air dispersion models such as ISCST3 (the old regulatory model) and

AERMOD (the new replacement model for ISCST3), developed by the US EPA. The model results include predictions for wet and dry particle deposition and concentrations of dioxins in soil with model inputs of incinerator stack emissions, particle size distributions and average long term meteorological data of the potentially impacted areas *(3, 4)*. However, there remains a discrepancy between the predictions and real measurements, partly due to uncertainties associated with the model assumptions and also due to the lack of information on emission profiles and loads of contaminants from the smoke stack. Among possible validation methods, preliminary results for the case study of the Dow Chemical Company incinerator complex in Midland, MI. suggested that the gap between model predictions and measured data could be improved by combining a geostatistical model with the air dispersion models to account for information from available soil data *(5, 6)*.

The Dow Chemical Company's incinerator complex 703 and complex 830 were brought into operation in the 50s and 60s to dispose various types of waste, including liquid waste, tars, containerized and loose solid waste *(7)*. Prior to 1970, the incineration process was fairly inefficient resulting in the formation, dispersion and deposition of higher concentrations of unintended by-products such as PCDD, PCDF, and PCBs. During the 1980s, various actions were taken by the facilities in an effort to significantly reduce air emissions *(8, 9)* through in-stack heat profile modification, resulting in the development of highly efficient incinerators (99.9999% PCDD/F reduction). In the case under study here, many soil sampling campaigns have been conducted in Midland by the US EPA, the Michigan Department of Environmental Quality (MDEQ) and the Dow Company itself to quantify levels of dioxin contamination in the area. The University of

Michigan Dioxin Exposure Study (UMDES) *(10)* was initiated in 2003 to determine exposure pathways to dioxins in the area, through an intensive data sampling campaign in soil, dust, vegetation and human blood. One of the outputs was to determine whether the level of dioxins and furans in soils has an association with the elevated level of dioxins and furans in the blood serum samples of local residents.

A component of the UMDES is to model the deposition plume from the Dow Chemical Plant incinerator to guide the soil sampling campaign*(11)*. The plume modeling seeks to provide information on the spatial distribution of dioxins, both in terms of total toxic equivalents (TEQs), and congener specific dioxins in soil with the following objectives:

(1) Develop a methodology to validate and update air dispersion models with newly collected soil samples;

(2) Compare the performance of the new air dispersion model (AERMOD) over that of ISCST3 in identifying dioxin deposition plumes and

(3) Apply the AERMOD coupled geostatistical model to specific dioxin congeners and

(4) To validate the congener modeling work.

References

(1) US. EPA Available: Exposure and Human Health Reassessment of 2,3,7,8-Tetrachlorodibenzo-p-Dioxin (TCDD) and Related Compounds National Academy Sciences (NAS) Review Draft. http://www.epa.gov/ncea/pdfs/dioxin/nas-review/pdfs/part1_vol1/dioxin_pt1_vol1_ch02_dec2003.pdf Accessed June 16, 2009.

(2) Lohmann, R.; Jones, K. C., Dioxins and furans in air and deposition: A review of levels, behaviour and processes. *Science of the Total Environment* **1998,** 219, (1), 53-81.

(3) US. EPA, User's Guide for the Industrial Source Complex (ISC 3) Dispersion Models **1995,** Vol. 1

(4) US. EPA, User's Guide for the AMS/EPA Regulatory Model - AERMOD. **2006**

(5) Goovaerts, P.; Trinh, H. T.; Demond, A.; Franzblau, A.; Garabrant, D.; Gillespie, B.; Lepkowski, J.; Adriaens, P., Geostatistical modeling of the spatial distribution of soil dioxins in the vicinity of an incinerator. 1. Theory and application to Midland, Michigan. *Environmental Science & Technology* **2008,** 42, (10), 3648-3654.

(6) Goovaerts, P.; Trinh, H. T.; Demond, A. H.; Towey, T.; Chang, S. C.; Gwinn, D.; Hong, B.; Franzblau, A.; Garabrant, D.; Gillespie, B. W.; Lepkowski, J.; Adriaens, P., Geostatistical modeling of the spatial distribution of soil dioxin in the vicinity of an incinerator. 2. Verification and calibration study. *Environmental Science & Technology* **2008,** 42, (10), 3655-3661.

(7) Trembly, M. G.; Amendola, G. A., Dow Chemical Building 703 incinerator exhaust and ambient air study. Final report. In 1987; p Pages: 308.

(8) US. EPA, Soil Screening Survey At Four Midwestern Sites **1985**, 163.

(9) MDEQ, Dow Hazardous Waste Facility Operating License Information In Michigan Department of Environmental Quality (MDEQ) 2009.

(10) UMDES Available: University of Michigan Dioxin Exposure Study. www.dioxin.org Accessed July 8,2009.

(11) Garabrant, D. H.; Franzblau, A.; Lepkowski, J.; Gillespie, B. W.; Adriaens, P.; Demond, A.; Ward, B.; LaDronka, K.; Hedgeman, E.; Knutson, K.; Zwica, L.; Olson, K.; Towey, T.; Chen, Q. X.; Hong, B. L., The University of Michigan Dioxin Exposure Study: Methods for an Environmental Exposure Study of Polychlorinated Dioxins, Furans, and Biphenyls. *Environmental Health Perspectives* **2009,** 117, (5), 803-810.

Chapter 2

Literature Review

2.1. Background on PCDDs and PCDFs

2.1.1. Characterizations of dioxins and furans

Polychlorinated dibenzo-p-dioxins (PCDD) and polychlorinated dibenzo furans (PCDF) comprise 75 dioxin congeners and 135 furan congeners substituted with up to 8 chlorine atoms. The congeners differ from each other by numbers and positions of halogenated substitutions in the aromatic rings. PCDD and PCDF are unintentionally produced as byproducts of many industrial processes and of combustion*(1)*.

The potential toxicity of all congeners is not the same, in part because of the variable planarity of the congeners which triggers differential binding with key metabolic enzymes (Steven Safe article on dioxin toxicity) . 2,3,7,8 TCDD is the best studied substance and is considered the most toxic compound as a probable carcinogen (dioxin reassessment report ref). The toxicity of other congeners is proportional to 2,3,7,8 TCDD and is expressed by way of a toxic equivalency factor (TEF), ranging from 0 to 1 according to the increasing level of toxicity. 2,3,7,8 TCDD is among the substances with a TEF of 1. The TEF schemes were proposed by a panel of experts based on the scientific

judgments using the most up-to-date data available. By multiplying the mass concentration and the TEF of each congener and summing the results, a total value termed Toxic Equivalents (TEQ) is obtained. There are several formulations of TEQ according to different TEF conventions, including I-TEFs, WHO 1988 TEFs 1998 and WHO 2005 TEFs, adopted by the US.EPA or the World Health Organization (Table 2.1) *(2, 3)*.

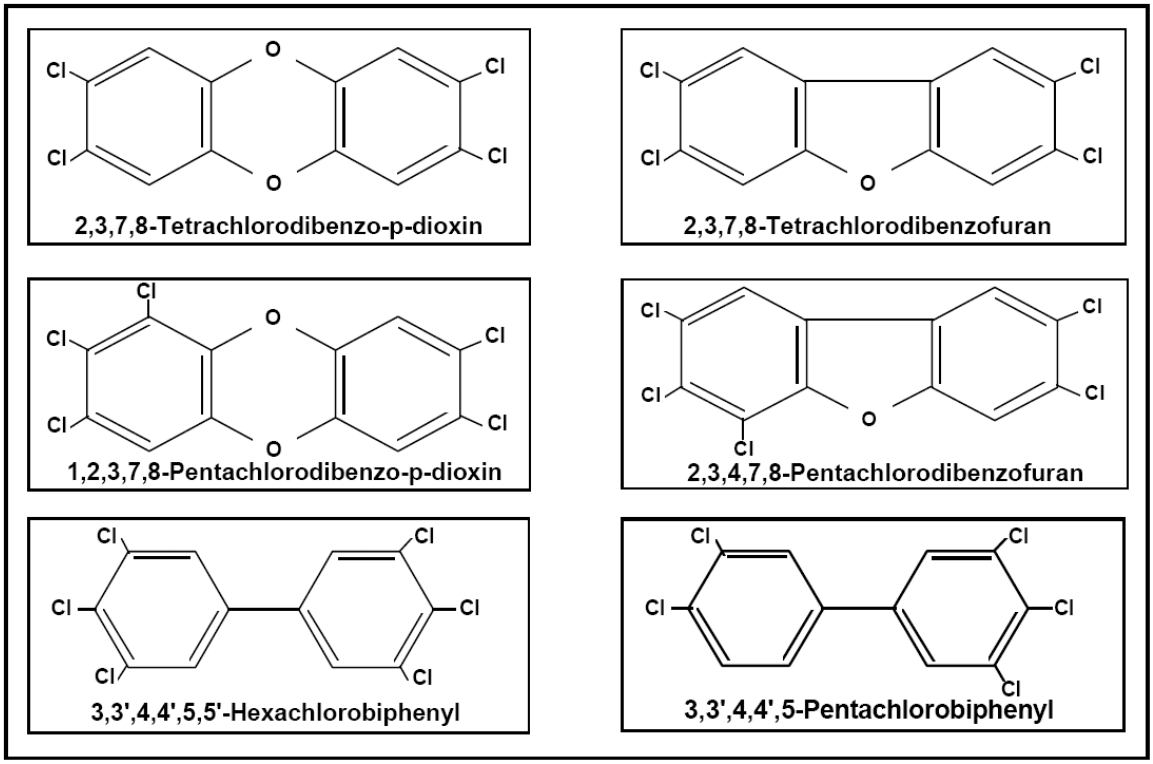

Figure 2.1 Chemical structure of 2,3,7,8-TCDD and its related compounds (adopted from Fiedler, H., 2003) *(4).*

The persistence and bioaccumulation of dioxins and furans results in these compounds being found in environmental compartments rich in organic matter such as sewage sludge, soil, sediment and biota (lipids). However, the occurrence of dioxins and

furans has been reported in every compartment, albeit at low concentrations, and they are known to be multimedia pollutants *(5)* because of their partitioning capability between media. Advances in analytical techniques have allowed for the detection of these compounds at trace and ultra-trace levels (ppt. or ng/kg to ppq of pg/kg) in most compartments.

The University of Michigan Dioxin Exposure Study (UMDES) collected and measured concentrations of total 29 congeners, including 12 PCBs. In this research, we omitted the contributions of PCBs in the mixture because PCBs were never produced at Dow Midland, and in the previous sampling campaigns no PCBs were measured and reported. The abbreviations of the 17 dioxins and furans are shown in table 1 and 2 and are consistently used throughout the study.

Table 2.1. The UMDES 17 dioxins and furans congeners and the WHO 1988, 2005 TEFs*(3)*.

			WHO 1998	
Chemicals	**Abbreviation**	**CAS-No.**	**TEF**	**WHO 2005 TEF**
2,3,7,8-TCDD	2,3,7,8-TCDD	1746-01-6	1	1
1,2,3,7,8-PentaCDD	1,2,3,7,8-PeCDD	40231-76-4	1	1
1,2,3,4,7,8-HexaCDD	1,2.3,4,7,8-HxCDD	39227-26-8	0.1	0.1
1,2,3,6,7,8-HexaCDD	1,2,3,6,7,8-HxCDD	57653-85-7	0.1	0.1
1,2,3,7,8,9-HexaCDD	1,2,3,7,8.9-HxCDD	19408-74-3	0.1	0.1
1,2,3,4,6,7,8-HeptaCDD	1,2,3,4,6,7,8-HpCDD	35822-46-9	0.01	0.01
OctaCDD	OCDD	3268-87-9	0.0001	0.0001
2,3,7,8-TetraCDF	2,3,7,8-TCDF	51207-31-9	0.1	0.1
1,2,3,7,8-PentaCDF	1,2,3,7,8-PeCDF	57117-41-6	0.05	0.03
2,3,4,7,8-PentaCDF	2,3,4,7,8-PeCDF	57117-44-9	0.5	0.3
1,2,3,4,7,8-HexaCDF	1,2,3,4,7,8-HxCDF	70658-26-9	0.1	0.1
1,2,3,6,7,8-HexaCDF	1,2,3,6,7,8-HxCDF	57117-44-9	0.1	0.1
1,2,3,7,8,9-HexaCDF	1,2,3,7,8,9-HxCDF	72918-21-9	0.1	0.1
2,3,4,6,7,8-HexaCDF	2,3,4,6,7,8-HxCDF	60851-34-5	0.1	0.1
1,2,3,4,6,7,8-HeptaCDF	1,2,3,4,6,7,8-HpCDF	67462-39-4	0.01	0.01
1,2,3,4,7,8,9-HeptaCDF	1,2,3,4,7,8,9-HpCDF	55673-89-7	0.01	0.01
OctaCDF	OCDF	39001-02-0	0.0001	0.0003

Table 1.2. Physical properties of the 17 dioxins and Furans (Webster and Mackay 2007)

		Molecular	Water	Vapor			
		Weight	Solubility	Pressure	Partition Coefficient		
Chemical code	**CAS-No.**	**(g/mol)**	**(g/m-cu)**	**(Pa)**	**Log Kow**	**log Koa**	**Log Kaw**
2378_TCDD	1746-01-6	322	1.93E-05	2.00E-07	6.8	9.670955	-1.43548
12378_PeCDD	40231-76-4	356.416	9.82E-05	5.80E-08	7.5	11.57097	-2.03549
123478_HxC	39227-26-8	390.861	0.000006	5.10E-09	7.8	11.6728	-1.9364
123678_HxCDD	57653-85-7	390.681	0.000006	4.80E-09	7.9	11.79913	-1.94957
123789_HxCDD	19408-74-3	390.681	0.000006	6.50E-09	8.02	11.78746	-1.88373
1234678_HpCDD	35822-46-9	425.308	2.40E-06	7.50E-10	8	12.27069	-2.13535
OCDD	3268-87-9	459.751	7.40E-08	1.10E-10	8.2	11.75956	-1.77978
2378_TCDF	51207-31-9	305.978	0.000419	2.00E-06	6.53	9.759739	-1.61487
12378_PeCDF	57117-41-6	340.418	0.0002	1.00E-06	6.99	10.15326	-1.58163
23478_PeCDF	57117-44-9	340.418	0.000236	3.50E-07	6.5	10.19108	-1.84554
123478_HxCDF	70658-26-9	374.863	8.25E-06	3.20E-08	7	10.23168	-1.61584
123678_HxCDF	57117-44-9	374.863	0.000008	2.90E-08	7.57	10.83106	-1.63053
123789_HxCDF	72918-21-9	374.863	0.000008	1.44E-08	7.76	11.3251	-1.78255
234678_HxCDF	60851-34-5	374.863	0.000008	2.60E-08	7.65	10.95849	-1.65424
1234678_HpCDF	67462-39-4	409.308	1.35E-06	4.70E-09	7.4	10.64043	-1.62022
1234789_HpCDF	55673-89-7	409.308	1.30E-06	6.20E-09	8.23	11.33375	-1.55187
OCDF	39001-02-0	443.753	1.16E-06	5.00E-10	8	12.11259	-2.0563

Table 2.1 Half-life of dioxins and furans in the environment (Webster and Mackay 2007)

	Half-life (hours)			
Chemical code	**Air**	**Water**	**Soil**	**Sediment**
2378_TCDD	170	550	17000	55000
12378_PeCDD	550	550	17000	55000
123478_HxCDD	550	1700	55000	55000
123678_HxCDD	550	1700	55000	55000
123789_HxCDD	550	1700	55000	55000
1234678_HpCDD	550	1700	55000	55000
OCDD	550	5500	55000	55000
2378_TCDF	170	550	17000	55000
12378_PeCDF	550	550	17000	55000
23478_PeCDF	550	550	17000	55000
123478_HxCDF	550	1700	17000	55000
123678_HxCDF	550	1700	17000	55000
123789_HxCDF	550	1700	17000	55000
234678_HxCDF	550	1700	17000	55000
1234678_HpCDF	550	1700	17000	55000
1234789_HpCDF	550	1700	17000	55000
OCDF	550	5500	55000	55000

2.1.2. Dioxin emission from waste incineration

Dioxins and furans are never intentionally produced but found as by-products in other industrial-chemical processes that involved the production of chlorinated organic compounds such as chlorophenols, chlorobenzenes and aliphatic chlorinated compounds as well as those using inorganic chlorinated compounds *(4)*. The presence of PCDDs and PCDFs was found in tri-, tetra- and penta-chlorophenols (PCPs) at various concentrations depending on the temperature and manufacturing conditions. TetraCDDs were reported at less than 0.1 ppm (part per million) in 2,4,5-trichlorophenol and its sodium salt, for example, and HxCDD concentrations were up to 520 ppm during 1975 to 1977 *(6)* and up to 2,320 ppm I-TEQ in PCP*(4)*. The pulp and paper mill industry and chemical industry were the major sources of dioxins and furans in the past. Point sources of dioxins and furans today are mainly the result of combustion processes, incineration in particular.

Incineration is the process of thermally decomposing wastes. During the thermal process, dioxins and furans can be formed under three possible mechanistic scenarios: (1) PCDDs and PCDFs are already in the feed wastes, are not altered during combustion and are emitted to the environment through the incinerator stack; (2) PCDD/PCDFs are formed from the precursors having similar aromatic ring structures as dioxins and furans (pre-dioxins such as PCBs, chlorinated phenols and chlorinated benzenes) in an incomplete combustion process; and (3) PCDD/PCDFs are synthesized *de novo*, a process that involves carbon, oxygen, hydrogen, chorine, and a transition metal catalyst in a heterogeneous reaction *(5, 7)*.

The formation rate of PCDDs and PCDFs during combustion is impacted by a number of factors, of which the following are considered most important: the overall

combustion efficiency, post-combustion flue gas temperatures and residence times, and the availability of surface catalytic sites to support PCDDs/PCDFs synthesis. The presence of chlorine from the feed has also significant influence *(7).*

Dioxins and furans emitted from municipal waste incinerators (MWI) are known to be the highest contributors (38% of total environmental releases) in the combustion categories, which also include backyard burning and medical waste incinerators *(7)*. Of all emission sources, air emission from combustion accounts for 71% of total environmental releases according to the 1995 inventory *(1)*. The concentration of PCDD/PCDFs emitted from a modern MWI is at 0.1 ng I-TEQ/m^3 as compared to the level of 5 and 50 ng I-TEQ/m^3 in the 1990s and 1970s, respectively *(1)*. To a lesser extent, hazardous waste incineration (HWI) is also a source of environmental release of dioxins and furans. The US Inventory reported levels of air emissions from hazardous waste incineration at 5.0, 5.8 and 3.5 gram TEQ_{WHO-98} for PCDDs and PCDFs in the reference year of 1987, 1995 and 2002/2004, as compared to 8877, 1250 and 12 g TEQ $_{WHO-98/DF}$ emitted from municipal waste incineration for the same years *(8)*. Air emissions from waste incineration has decreased significantly over last decades owing to the fact that control measured have been implemented*(9)* .

2.1.3. Historical emission of dioxins and furans

Findings in the late 70s about the ubiquitous presence of dioxins in environmental samples since “the advent of fires” *(10)* marked a starting point for decades of studies on every aspect of dioxins, such as source, emission, environmental fate and transport, toxicology, health effect etc. The US EPA conducted the National Dioxin Study in the early 80s and the U.S. Dioxin Inventory was first reported for the reference year of 1987,

and for the following years of 1995, 2000, 2002 and 2005 *(8)*. The temporal trend of dioxins however needs emission data for a longer time frame, in particular the years encapsulating when dioxin emissions peaked (early 1970s).

In an attempt to reconstruct the temporal trend of dioxins, scientists have been looking at the historical levels of dioxins in sediment cores in lakes and rivers. Analysis of sediment cores provides a signature of atmospheric deposition of dioxins. Studies in the US, especially in the Great Lakes region *(11)* and in Lake Green in upstate New York *(12)* found that the dioxin level in lake sediment arose slowly in the beginning of 1940s, peaked in the late 1960s and early 1970s, and declined afterward. Similar trends were observed in European studies *(13)* (Figure 2.2(a,b)).

Generally, dioxin emissions from incineration are poorly characterized due to the fact that sampling and analysis are comprehensive and expensive. However, the Dow Chemical Plant in Midland, MI has been subjected to various sampling campaigns and investigations. The company's early report of dioxins in environmental and ambient air samples was done in 1978 and published 2 years later in Science *(10)*. The US EPA and the MDEQ conducted the Michigan Dioxin Study on soil, wastewater, ambient air, and flue gas from the company's incinerator stacks *(14)*. Dyke and Amendola recently included the Dow Chemical Co.'s incinerators (among 18 hazardous waste incinerators across the US) in an inventory study, are reported the range of air releases from these facilities from 0.0038 g I-TEQ to 3.08 g I-TEQ for the year 2000 *(9)*. Current emission data are collected by the Air Monitoring Network of Michigan, reflecting the current deposition from the new incinerator complex, building 32, which was built as a replacement of buildings 703 and 830 in 2004 (Figure 2.3).

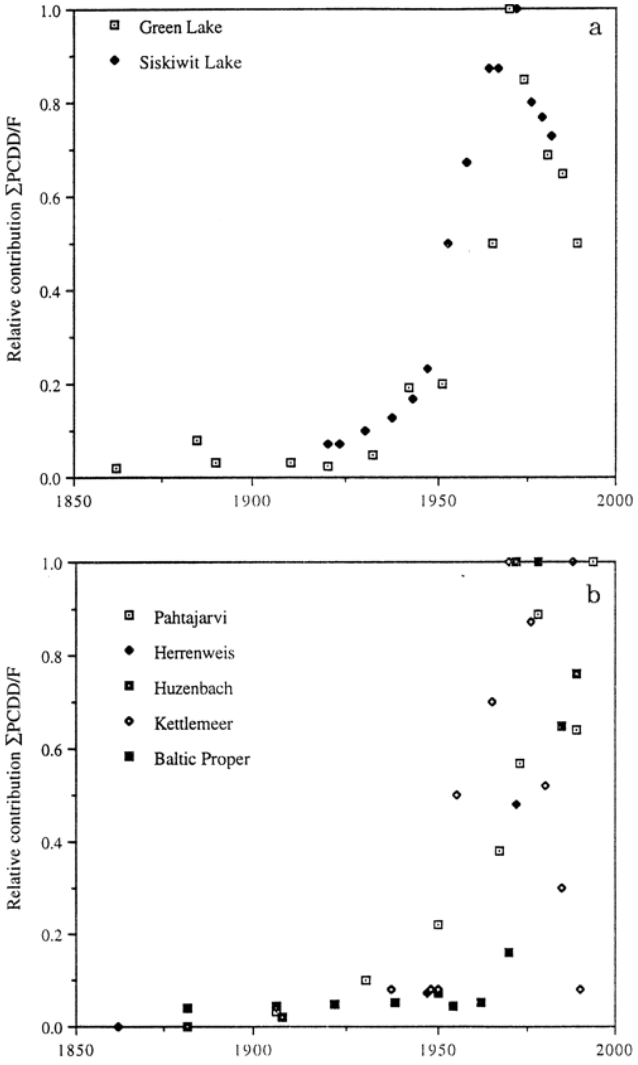

Figure 2.1(a) Generalized plot of PCDD/F trends from Green Lake and Siskiwit Lake. Data scaled relative to the peak year (set at 1.0) in each study. (b) PCDD/F trends from European studies. Adopted the figure from Alcock et al. *(15)*.

The congener profile of the 17 dioxins and furans contributing to the total TEQ is fairly stable over the years (Figure 5). High hexa- to octachlorinated dioxins and furans are dominant contributors, with OCDD accounts for 65% of total emission *(7)*.

2.1.4. Dioxin environmental fate and transport from incineration

Although the reduction of dioxin emissions was successful over the last decades, the complexity of dioxin behavior once released from sources is not well characterized. The dioxin behavior involves a number of processes such as dispersion, particle deposition, partitioning, transformation and transport in the environment *(16)*.Level of PCDDs in ambient air, for example, is ranging from less than 0.5 pg/m3 fore remote site; 0.5-4 pg/m3 for rural sites, and from 10-1000 og.me3 for industrial sites *(16)*

A study team of the US EPA recently reported the results from the National Dioxin Air Monitoring Network (NDAMN) in determining the temporal and spatial distribution of dioxins, furans and PCBs in the ambient air at rural and remote areas throughout the United States *(17)*. The NDAMN intensive monitoring during 1999-2002 showed that levels of PCDDs, PCDFs at rural and remote areas are fairly stable throughout this period. The dioxin congener profiles were found to be identical between rural and nearby urban sources inferring that the main pollution source for the rural background is due to anthropogenic activities in urban areas. The dioxin profile from an incinerator stack include dominant congeners such as OCDD, OCDF, followed by HpCDD and HpCDF*(18, 19)*. The traveling distance of these chemicals from point source to the rural land is in the order of hundred of kilometers. An interesting study by Lohman et al. *(20)* suggested that the local impact of deposition from an incinerator stack accounts for only 10% of the total release. The remainder transports beyond 100 km from the

source. A US EPA study lead by Cleverly *(17)*on the levels of PCDDs/PCDFs in ambient air of remote and rural areas also introduced an hypothesis that the seasonal variation (higher levels of dioxin compounds in winter relative to summer), may be inversely related to the change of hydroxyl radicals in the atmosphere. There is less evidence in the Cleverly study to support that these pollutants are involved in long range transport processes, which is contradictory to the intensive effort of modeling and monitoring work *(21)*; *(22)*; *(23)*) It is possible that the duration of the Cleverly study was not long enough to track the temporal trend of these pollutants and also, the monitoring attempt was conducted at local and regional level only.

In the case study of the Dow Chemical Company's incinerator reported in the current work, we seek to investigate local impacts of the incinerator emission, therefore air dispersion modeling domain covers a 13x13 km^2 area surrounding the plant. The spatial variability of dioxin deposition is based on the coupling of geostatistical and air dispersion models*(24)*. Dioxin emission profiles are collected from the Dow Chemical Company, Michigan Department of Environmental Quality (MDEQ), and the US Environmental Protection Agency (US EPA) in 1983 for bulk emissions and in 1992 for specific congeners' emissions*(25, 26)*. This information will be further elaborated on in the methodology section.

2.1.5. Dow Chemical Company's hazardous waste incineration

The Dow Chemical Plant located south of the city of Midland, Michigan was founded in 1897, and manufactured a wide range of chemicals *(14)*. Hazardous waste incinerator complexes were built on-site to treat all kinds of waste from liquid, tars and solid waste *(14)*. There are two on-site incinerators, officially documented by Dow: building 703 (rotary kiln) and building 830 (stationary burner, later converted into rotary kiln) operated since 1958 and 1968, respectively until 2004. Building 703, illustrated in Figure 2.4 was reported to have a daily burning capacity of 200 tons of waste. These two incinerators were presumed to be the point sources of dioxin contamination in surface soil in the vicinity of the Dow Chemical company at least prior to 1983 before the corrective actions for dioxin reductions had been implemented *(27)*. As of 2002, the two incinerator complexes had been replaced by incinerator building 32, which has dioxin destruction capacity of 99.9999%.

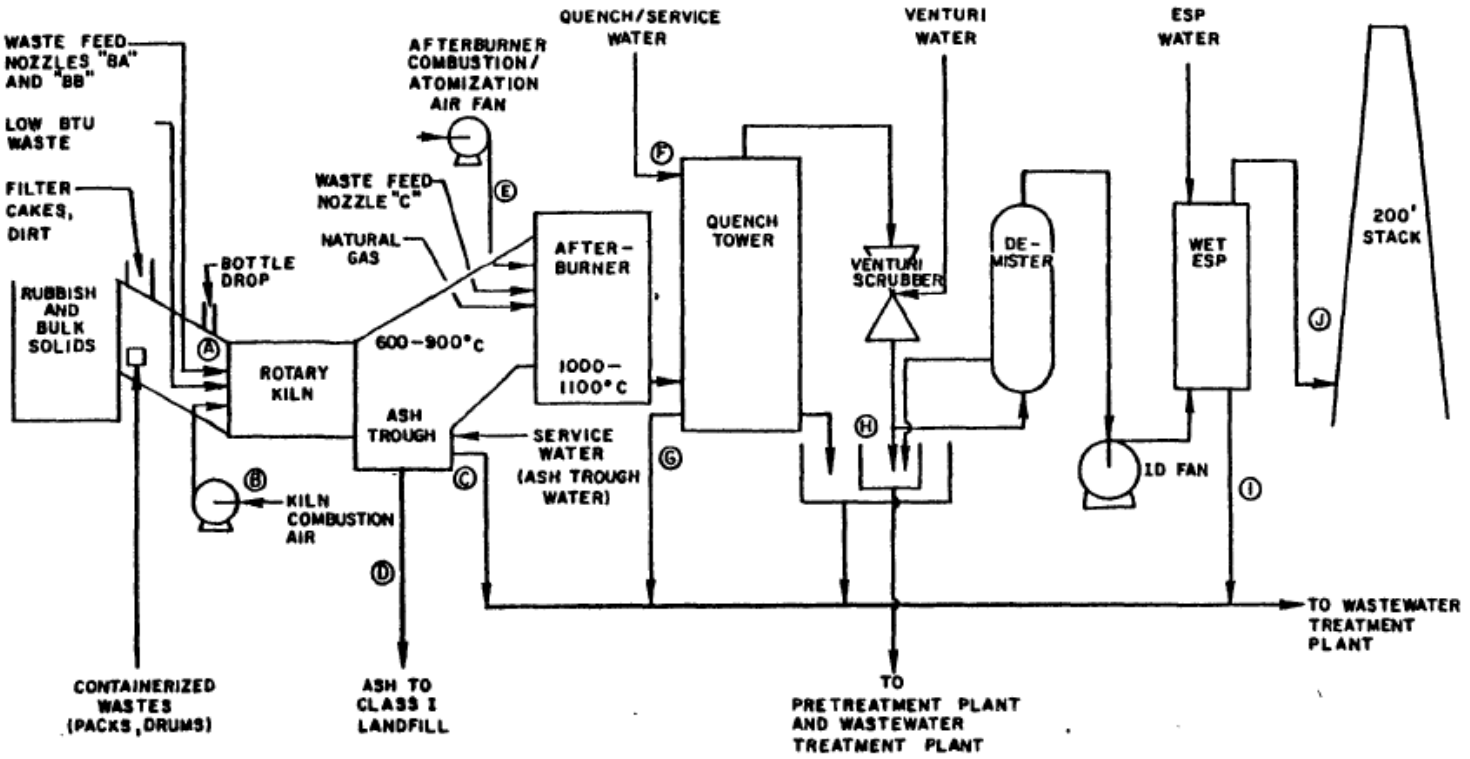

Figure 2.1 Schematic diagram of building 703 incinerator complex *(14)*.

2.2. Modeling spatial distribution of dioxins and furans

2.2.1. Air dispersion and geostatistical model

The Industrial Source Complex (ISC) model was developed by the US EPA in 1995 *(28)* as a regulatory application for air dispersion modeling work. It models the dispersion plume as Gaussian distribution and can handle various emission input types such as point sources and open pit sources. The modeled chemicals are treated as non-reactive agents that partition into the vapor and particle phases in the atmosphere at ambient temperature. The ISCST3 input files include information on stack emission, particle size distribution and meteorological data. Data are reported at receptor grid network in either Cartesian or polar coordinates. Dry and wet particle deposition are obtained according to the chosen algorithm (see also Methods and Chapter 6) with additional requirements for meteorological data such as Monin-Obukhov length and surface friction velocity for dry deposition and precipitation data for the wet deposition output *(28)*. The model needs a comprehensive source of information, which is not always available on-site (e.g. emission profile or meteorological data over long period of time).

Users of the ISCST3 model often run the model on a “unitized” basis at a deposition rate of 1 gram/second for contaminant-bound particles *(29)* due to the fact that information on particles is rarely available, as is stack emission. The model predictions therefore are theoretical, and ground level estimates tend to equal the plume depletion as a function of distance. In fact, however the dioxin level in soil concentration greatly varies, up to 2 or 3 orders of magnitude*(30)* due to the landscape heterogeneity, weather conditions, and uncertainties in point source, among others. Elevation information is required for each receptor.

2.2.2. Geostatistical models

Having been aware of the local uncertainties in the dispersion model, Goovaerts et al. *(24, 30)* introduced a geostatistical approach to utilize the outputs of the air dispersion model (dry and wet deposition fluxes) and the available soil data at the modeling site to better characterize the spatial distributions of dioxin concentrations in soil. The set of soil data included 53 measurements collected by the Michigan Department of Environmental Quality (MDEQ) and the US Environmental Protection Agency (US EPA) during the 1987 to 1991 soil sampling campaigns, ranging from less than 1 ppt to 450 part per trillions (ppt). The derived regression function between deposition fluxes predicted by air dispersion model and available soil measurements was then applied on to the modeling grid nodes or receptors to extract residual trends by comparing the regressed data with observed values. Residual trend helps in constructing the data's spatial structure, which is attributed to the sequential Gaussian simulations*(31, 32)* to get point-simulated values at grid nodes. The Sequential Gaussian Simulation (GSIM) generates 100 point simulated values at each grid node providing a probability framework to capture the real measurements.

Simulated point values are later aggregated onto the census block level to aid decision making for locating new UMDES samples in the expected plume area in the city of Midland. Census blocks where the soil concentration might exceed 75 part per trillion (ng/kg soil) were mapped. The predicted map showed 196 census blocks where the probability of exceeding 75 ppt is greater than 40%. The selection criteria follow

randomly population-based method as described in the UMDES study design *(33)*. Details of soil sampling techniques and analytical methods can be found elsewhere*(34)*.

The UMDES soil sampling was conducted downwind of the Dow Chemical Plant's incinerator (building 830). 51 new soil samples were collected, ranging from 5 to 922 ppt. in total TEQ. Total TEQ was calculated based on $TEF_{WHO\text{-}2005}$ scheme and contributions of PCBs were omitted as for the 53 EPA/MDEQ samples used in the geostatistical model. To evaluate the accuracy of the geostatistical model, we used the newly collected 51 UMDES soil data.

In an extended modeling work, AERMOD coupled with geostatistical model was applied to ten dioxin and furan congeners, which are 2,3,7,8-Tetrachlorodibenzo-p-dioxin (TCDD); 1,2,3,4,7-Pentachlorodibenzo-p-dioxin (PCDD); 1,2,3,4,7,8-Hexachlorodibenzo-p-dioxin (1,2,3,4,7,8-HxCDD); 1,2,3,4,6,7,8-Heptachlorodibenzo-p-dioxin (1,2,3,4,67,8-HpCDD); Octachlorodibenzo-p-dioxin (OCDD); 2,3,7,8-Tetrachlorodibenzofuran (TeCDF); 2,3,4,7,8-Pentachlorodibenzofuran (PeCDF); 1,2,3,4,7,8-Hexachlorodibenzofuran (1,2,3,4,7,8-HxCDF); 1,2,3,4,6,7,8-Heptachlorodibenzofuran (1,2,3,4,6,7,8-HpCDF) and Octachlorodibenzofuran (OCDF). Model validation was also conducted for dioxin and furan congeners using 51 UMDES available measurements.

2.2.3. Validation of air dispersion models

A limited numbers of validation or verification studies of air dispersion models are available, yet they are constrained by (i) numbers of samples, or (2) sampling locations that are biased towards the local, downwind locations expected to exhibit high concentration values. For example, Lorber et al. (2000) used five ambient air sites and 34

soil samples taken at a distance of about 8 km away from the incinerator over the two reference years of 1995-1996 in a study of a municipal waste incinerator in Columbus, Ohio to validate their prediction model. They observed that both soil- and air-predicted concentrations were within a factor of 10 of observations. The major uncertainties affecting predictions were: source characterization (stack emission rates of dioxins), meteorological data, and atmospheric and soil fate and transformation processes of the dioxins. An extensive soil sampling conducted in France *(35)* included 75 soil samples. It was observed that, in simple terrain, there was a significant association between modeled dioxin ground-level air concentrations and log-transformed measured dioxin soil concentrations. Conversely, in a complex topography situation, the model over-predicted ground-level air concentrations. Other validation studies often have less than ten samples each for air and soil media *(36-38)*; and predictions are again in the order of magnitude range.

It is not common for models to be updated or further modified to incorporate the results from validation studies. Several studies have modified the ISCST3 model to account for partitioning of the contaminant between vapor and particle phase *(39)* or included a simple soil mixing model considering the decay of dioxins in the soil reservoir *(29)* The former modification improved predicted soil concentration in case of simple and flat terrain, but over predicted in case of a complex terrain. Predictions in the latter case were within a factor of ten with the soil dioxin congener concentrations, and were within a factor of 2 for total soil TEQ.

Although, the previously regulatory ISCST3 and the current air dispersion AERMOD model have been used extensively, the validation process is rather less

sophisticated. For the studies that have limited observations, the validation work was in form of a direct comparison between model predictions and the available air sampling data *(36-38).* When more extensive observations are available, iso-concentration maps *(29)* or contour maps were generated to reflect the spatial distribution of the contaminants *(35)*. However, not much attention has been paid to evaluate the local uncertainties of the model predictions. ISCST3, or AERMOD in particular requires substantial data inputs (e.g. long-term average meteorological data, stack emission profile, landscape characterization, and particle size distribution), which might not be all available on every site, creating uncertainties to the model. To assess the propagation of uncertainty associated with selected input data, probabilistic approaches have been considered*(24)*. Among these approaches, sequential Gaussian simulation allows to assess the accuracy and precision of model predictions*(31, 40, 41).*

2.3. Identification of Literature Gap

Although research has shown that emission from hazardous waste incineration can contaminate the soil in the vicinity of the point source, limited investigations have considered the impacts of local uncertainties about the model predictions, region heterogeneity, and variable deposition modes on the soil contamination level. Local uncertainties play an important role in spatial interpolation modeling while environmental heterogeneity and chemical's persistence are essential for the fate and transport modeling. Second gap is the previous work have been conducted with total TEQ, not with individual dioxin compounds and or dioxin congeners. Dioxin congeners are emitted from the incinerator stack at different emission rates. Difference in emission rate, and in physico- chemical properties of each congeners might lead to different plume modeling of dioxin congeners. We expect that predictions of TEQ deposition plume which resulted from the congeners' predictions would be improved, better capturing the high-end concentrations of TEQs in the vicinity of an incinerator.

2.4. Goal and Objectives

The overall goal of the research is to improve the dioxin deposition modeling for dioxin congener specifics. As such, the governing hypothesis of the research is that probabilistic models, using an air dispersion coupled geostatistical approach can capture the spatial distributions of dioxin plumes from hazardous waste incineration.

Hypothesis:

The AERMOD air dispersion model is considered an improvement to the prediction of dispersion and deposition fluxes of dioxin plumes due to updates of model algorithms and meteorological process details of model inputs. The improved AERMOD deposition fluxes are then coupled with the geostatistical model to derive spatial distributions of dioxin contaminations. Cross-validation of the model predictions with the available soil measurements adds to the last step of the dioxin plume modeling.

Rationale:

The air dispersion model, ISCST3 and its replacement, AERMOD developed by the US Environmental Protection Agency in 1995 and in 2006, respectively have been widely applied as a screening step for soil sampling decisions. The model validation work so far has been based on very few samples and suggested the gap between actual measurements and model predictions can be within 10 fold (Lorber M., 1998; Bisham 1999, Oh, 2006). The geostatistical approach that combines air dispersion outputs with available field data (soil concentrations) provides probability ranges of predictions as a base to facilitate a number of probabilistic validation techniques. By way of an accuracy plot and a precision

plot (see methods section), the local uncertainties of the geostatistical model can be quantified.

References

(1) Fiedler, H., National PCDD/PCDF release inventories under the Stockholm Convention on Persistent Organic Pollutants. *Chemosphere* **2007,** 67, (9), S96-S108.

(2) EPA Available: Exposure and Human Health Reassessment of 2,3,7,8-Tetrachlorodibenzo-p-Dioxin (TCDD) and Related Compounds National Academy Sciences (NAS) Review Draft. http://www.epa.gov/ncea/pdfs/dioxin/nas-review/pdfs/part1_vol1/dioxin_pt1_vol1_ch02_dec2003.pdf Accessed June 16, 2009,

(3) Van den Berg, M.; Birnbaum, L. S.; Denison, M.; De Vito, M.; Farland, W.; Feeley, M.; Fiedler, H.; Hakansson, H.; Hanberg, A.; Haws, L.; Rose, M.; Safe, S.; Schrenk, D.; Tohyama, C.; Tritscher, A.; Tuomisto, J.; Tysklind, M.; Walker, N.; Peterson, R. E., The 2005 World Health Organization reevaluation of human and mammalian toxic equivalency factors for dioxins and dioxin-like compounds. *Toxicological Sciences* **2006,** 93, (2), 223-241.

(4) Fiedler, H., Dioxins and Furans (PCDD/PCDF). In *The Handbook of Environmental Chemistry*, Fiedler, H., Ed. Springer-Verlag 2003; Vol. Vol. 3, Part O.

(5) Dyke, P. H.; Foan, C.; Fiedler, H., PCB and PAH releases from power stations and waste incineration processes in the UK. *Chemosphere* **2003,** 50, (4), 469-480.

(6) The US Environmental Protection Agency *A report on Polychlorinated dibenzo-p-dioxins (PCDDs) and polychlorinated dibenzo furans (PCDFs): A summary of studies conducted in the Great Lakes area*; 905R81119; Region V, Chicago, Illinois: 1981.

(7) The US Environmental Protection Agency *EPA Dioxin Reassessment (NAS Draft Review)*; 2003.

(8) Winter, D.

(9) Dyke, P. H.; Amendola, G., Dioxin releases from US chemical industry sites manufacturing or using chlorine. *Chemosphere* **2007,** 67, (9), S125-S134.

(10) Bumb, R. R.; Crummett, W. B.; Cutie, S. S.; Gledhill, J. R.; Hummel, R. H.; Kagel, R. O.; Lamparski, L. L.; Luoma, E. V.; Miller, D. L.; Nestrick, T. J.; Shadoff, L. A.; Stehl, R. H.; Woods, J. S., Trace Chemistries of Fire: A Source of Chlorinated Dioxins. *Science* **1980,** 210, (4468), 385-390.

(11) Czuczwa, J. M.; Hites, R. A., Airborne dioxins and dibenzofurans: sources and fates. *Environ. Sci. Technol.* **1986,** 20, (2), 195-200.

(12) Smith, R. M.; O'Keefe, P.; Aldous, K.; Briggs, R.; Hilker, D.; Connor, S., Measurement of PCDFs and PCDDs in air samples and lake sediments at several locations in upstate New York. *Chemosphere* **1992,** 25, (1-2), 95-98.

(13) Alcock R. E., J. K. C., Dioxins in the environment: A review of trend data. *Environmental Science and Technology* **1996,** 30, (11), 3133-3143.

(14) Trembly, M. G.; Amendola, G. A., Dow Chemical Building 703 incinerator exhaust and ambient air study. Final report. In 1987; p Pages: 308.

(15) Alcock, R. E.; Jones, K. C., Dioxins in the Environment: A Review of Trend Data. *Environ. Sci. Technol.* **1996,** 30, (11), 3133-3143.

(16) Lohmann, R.; Jones, K. C., Dioxins and furans in air and deposition: A review of levels, behaviour and processes. *The Science of The Total Environment* **1998,** 219, (1), 53-81.

(17) Cleverly, D.; Ferrario, J.; Byrne, C.; Riggs, K.; Joseph, D.; Hartford, P., A General Indication of the Contemporary Background Levels of PCDDs, PCDFs, and Coplanar PCBs in the

Ambient Air over Rural and Remote Areas of the United States. *Environ. Sci. Technol.* **2007,** 41, (5), 1537-1544.

(18) Lee, C. C.; Chen, H. L.; Su, H. J.; Guo, Y. L.; Liao, P. C., Evaluation of PCDD/Fs patterns emitted from incinerator via direct ambient sampling and indirect serum levels assessment of Taiwanese. *Chemosphere* **2005,** 59, (10), 1465-1474.

(19) Vizard, C. G.; Rimmer, D. L.; Pless-Mulloli, T.; Singleton, I.; Air, V. S., Identifying contemporary and historic sources of soil polychlorinated dibenzo-p-dioxins and polychlorinated dibenzofurans in an industrial urban setting. *Science of The Total Environment* **2006,** 370, (1), 61-69.

(20) Lohman, K.; Seigneur, C., Atmospheric fate and transport of dioxins: local impacts. *Chemosphere* **2001,** 45, (2), 161-171.

(21) Wania, F.; Mackay, D., Global Fractionation and Cold Condensation of Low Volatility Organochlorine Compounds in Polar-Regions. *Ambio* **1993,** 22, (1), 10-18.

(22) Bennett, D. H.; Scheringer, M.; McKone, T. E.; Hungerbuhler, K., Predicting long range transport: A systematic evaluation of two multimedia transport models. *Environmental Science & Technology* **2001,** 35, (6), 1181-1189.

(23) Lohmann, R.; Ockenden, W. A.; Shears, J.; Jones, K. C., Atmospheric distribution of polychlorinated dibenzo-p-dioxins, dibenzofurans (PCDD/Fs), and non-ortho biphenyls (PCBs) along a North-South Atlantic transect. *Environmental Science & Technology* **2001,** 35, (20), 4046-4053.

(24) Goovaerts, P.; Trinh, H. T.; Demond, A.; Franzblau, A.; Garabrant, D.; Gillespie, B.; Lepkowski, J.; Adriaens, P., Geostatistical modeling of the spatial distribution of soil dioxins in the vicinity of an incinerator. 1. Theory and application to Midland, Michigan. *Environmental Science & Technology* **2008,** 42, (10), 3648-3654.

(25) EPA *Michigan Dioxin Studies Atmospheric Sampling Fact Sheet*; 1983.

(26) EPA/OSW, 1996 National Dioxin Database. **1996**.

(27) EPA, Soil Screening Survey At Four Midwestern Sites **1985**, 163.

(28) The US Environmental Protection Agency, User's Guide for the Industrial Source Complex (ISC 3) Dispersion Models **1995,** Vol. 1

(29) Lorber, M.; Eschenroeder, A.; Robinson, R., Testing the USA EPA's ISCST-Version 3 model on dioxins: a comparison of predicted and observed air and soil concentrations. *Atmospheric Environment* **2000,** 34, (23), 3995-4010.

(30) Goovaerts, P.; Trinh, H. T.; Demond, A. H.; Towey, T.; Chang, S. C.; Gwinn, D.; Hong, B.; Franzblau, A.; Garabrant, D.; Gillespie, B. W.; Lepkowski, J.; Adriaens, P., Geostatistical modeling of the spatial distribution of soil dioxin in the vicinity of an incinerator. 2. Verification and calibration study. *Environmental Science & Technology* **2008,** 42, (10), 3655-3661.

(31) Deutsch, C. V., Journel A.G., *GSLIB Geostatistical Software Library and User's Guide*. Second edition ed.; Oxford University Press 1992.

(32) Goovaerts, P., *Geostatistics for Natural Resources Evaluation*. Oxford University Press 1997.

(33) The University of Michigan Dioxin Exposure Study Available: http://www.sph.umich.edu/dioxin/ Accessed September 2, 2007,

(34) Demond, A.; Adriaens, P.; Towey, T.; Chang, S. C.; Hong, B.; Chen, Q.; Chang, C. W.; Franzblau, A.; Garabrant, D.; Gillespie, B.; Hedgeman, E.; Knutson, K.; Lee, C. Y.; Lepkowski, J.; Olson, K.; Ward, B.; Zwica, L.; Luksemburg, W.; Maier, M., Statistical Comparison of Residential Soil Concentrations of PCDDs, PCDFs, and PCBs from Two

Communities in Michigan. *Environmental Science & Technology* **2008,** 42, (15), 5441-5448.

(35) Floret, N.; Viel, J. F.; Lucot, E.; Dudermel, P. M.; Cahn, J. Y.; Badot, P. M.; Mauny, F., Dispersion modeling as a dioxin exposure indicator in the vicinity of a municipal solid waste incinerator: A validation study. *Environmental Science & Technology* **2006,** 40, (7), 2149-2155.

(36) Chao, M.-R.; Hu, C.-W.; Chen, Y.-L.; Chang-Chien, G.-P.; Lee, W.-J.; Chang, L. W.; Lee, W.-S.; Wu, K.-Y., Approaching gas-particle partitioning equilibrium of atmospheric PCDD/Fs with increasing distance from an incinerator: measurements and observations on modeling. *Atmospheric Environment* **2004,** 38, (10), 1501-1510.

(37) Yoshida, K.; Ikeda, S.; Nakanishi, J.; Tsuzuki, N., Validation of modeling approach to evaluate congener-specific concentrations of polychlorinated dibenzo-p-dioxins and dibenzofurans in air and soil near a solid waste incinerator. *Chemosphere* **2001,** 45, (8), 1209-1217.

(38) Oh, J.-E.; Choi, S.-D.; Lee, S.-J.; Chang, Y.-S., Influence of a municipal solid waste incinerator on ambient air and soil PCDD/Fs levels. *Chemosphere* **2006,** 64, (4), 579-587.

(39) Basham, J. P.; Whitwell, I., Dispersion modelling of dioxin releases from the waste incinerator at Avonmouth, Bristol, UK. *Atmospheric Environment* **1999,** 33, (20), 3405-3416.

(40) Deutsch, C. V., *Direct assessment of local accuracy and precision.* Kluwer Academic Publishing: Dordrecht, 1997; p 115–125.

(41) Goovaerts, P., Geostatistical modelling of uncertainty in soil science. *Geoderma* **2001,** 103, (1-2), 3-26.

Chapter 3

Methodology

3.1. Air dispersion model

3.1.1. Industrial Source Complex Sort Term Model (ISCST3)

Air concentrations values, as well as total deposition flux values (both dry and wet), will be predicted at the nodes of a receptor grid using EPA Industrial Source Complex (ICS3) dispersion model*(1)*. The format for the output files will be selected such that predicted values can be easily imported into GIS software for visualization. The following input information is available for the Dow Chemical Plant incinerator:

Hourly meteorological data

The available data set during 1987-1991 includes flow vectors, wind speed, ambient temperature, stability class, rural and urban mixing heights, parameters for calculation of dry deposition (friction velocity, Monin-Obukhov length, and surface roughness length) and wet deposition (precipitation code and rate). The surface station is located in Midland, while the upper air station is located in Flint (for mixing height data).

Characteristics of the source (Dow Chemical Plant incinerator)

• Single source: STK830U

• UTM coordinates (m): X=724110.6 Y=4830384.0

• Emission rate: 0.126 g/s

• Stack height: 61 m

• Stack diameter: 1.37 m

• Stack temperature: 326 K

• Stack exit velocity: 18.3 m/s

Variables for settling, removal and deposition calculation

Table 3.1. Particle size distribution and scavenging ratio for TEQ

Particle size category	Particle diameter (micron)	Mass fractions (%)	Particle density (g/cm^2)	Scavenging coefficient for liquid precipitation $(s\text{-}mm/hr)^{-1}$	Scavenging coefficient for frozen precipitation $(s\text{-}mmhr)^{-1}$
I	1.26	99	1.0	6.5E-5	2.2E-5
II	6.78	0.5	1.0	4.5E-4	1.5E-4
3	21.5	0.5	1.0	6.7E-4	2.2E-4

Dispersion option

All regulatory default options will be used in the calculations, including plume depletion due to dry and wet removal mechanisms.

3.1.2. AERMOD Air dispersion model

Air Dispersion Model

Air dispersion concentration:

A detailed description of AERMOD and its modeling formulations are found elsewhere*(1-5)*. The features of AERMOD that render this model superior to other regulatory air dispersion models include up-to-date understanding of air dispersion and deposition processes. For example, a two layer-structure of the plume is described with respect to terrain features, where the plume in considered a combination of the horizontal flow and the vertical flow (rising with elevated terrain). Concentration at each receptor at each hour of meteorological data is a weighted sum of these two scenarios:

$$C_T\{x_r, y_r, z_r\} = f \cdot C_{c,s}\{x_r, y_r, z_r\} + (1-f) C_{c,s}\{x_r, y_r, z_p\} \quad (3.1)$$

where, $C_T\{x_r, y_r, z_r\}$ is the total concentration at each receptor; $C_{c,s}\{x_r, y_r, z_r\}$ is a portion of concentration contributed by the horizontal flow and $C_{c,s}\{x_r, y_r, z_p\}$ is a portion of concentration contributed from the terrain-following plume; also, z_p is the height above the local ground of a receptor; z_r is receptor height and z_t is the terrain height ($z_p = z_r - z_t$). Lower case c,s associated with C are notations for convective and stable scenarios. Lower case f is a weighted plume state function. In the two layer plume structure, H_c, a dividing stream height is introduced as a critical parameter calculated from the model

based on wind speed at height H_c and other site characteristics. For a height larger than H_c, the plume would rise following the terrain, while below H_c, the flow is fully horizontal (f = 1) *(6)*.

Apart from inclusion of terrain features, AERMOD considered two scenarios in which (1) under stable conditions (night time), the plume follows a Gaussian distribution in both vertical and lateral direction, but (2) in unstable conditions (day time) when the heat strongly affects mixing in the convective layer, the plume is treated as a non-Gaussian probability distribution function in vertical direction. This is a different from the Industrial Source Complex (ISCST3) model, which treats the dispersion plume only as a steady state Gaussian plume both in vertical and lateral direction *(7)*. The above equation can also be described with respect to concentration in stable and convective conditions using the following expression:

$$C\{x,y,z\} = \left(Q/\tilde{u}\right) P_y\{y;x\}\, P_z\{z;x\} \quad (3.2)$$

where Q is the source emission rate, *u* tilde is the effective wind speed, and p_y and p_z are probability density functions (pdf) which describe the lateral and vertical concentration distributions, respectively *(6)*.

In the convective boundary layer (CBL), the pdf function comprises three different plumes, respectively a direct plume, an indirect plume and a penetrated plume, following the dispersion concept proposed by Weil (1997) (cited from *(6)*):

$$C_c\{x_r, y_r, z_r\} = C_d\{x_r, y_r, z_r\} + C_r\{x_r, y_r, z_r\} + C_p\{x_r, y_r, z_r\} \quad (3.3)$$

The direct plume, C_d describes the source of the incinerator stack and the dispersion mass reaching the ground directly following a downdraft:

$$C_d\{x_r, y_r, z\} = \frac{Qf_p}{\sqrt{2\pi}\bar{u}} F_y \cdot \sum_{j=1}^{2} \sum_{m=0}^{\infty} \frac{\lambda_j}{\sigma_{zj}} \left[\exp\left(-\frac{\left(z - \Psi_{dj} - 2mz_i\right)^2}{2\sigma_{zj}^2} \right) + \exp\left(-\frac{\left(z + \Psi_{dj} + 2mz_i\right)^2}{2\sigma_{zj}^2} \right) \right] \quad (3.4)$$

The indirect plume, C_r describes a portion of the plume mass that rises to the top of the CBL (updraft) followed by a downdraft:

$$C_r\{x_r, y_r, z\} = \frac{Qf_p}{\sqrt{2\pi}\bar{u}} F_y \cdot \sum_{j=1}^{2} \sum_{m=1}^{\infty} \frac{\lambda_j}{\sigma_{zj}} \left[\exp\left(-\frac{\left(z + \Psi_{rj} - 2mz_i\right)^2}{2\sigma_{zj}^2} \right) + \exp\left(-\frac{\left(z - \Psi_{rj} + 2mz_i\right)^2}{2\sigma_{zj}^2} \right) \right] \quad (3.5)$$

The penetrated plume, C_p describes the portion of plume that rises to the top of the CBL and deposits via turbulence of the mixing layer:

$$C_p\{x_r, y_r, z\} = \frac{Q\left(1 - f_p\right)}{\sqrt{2\pi}\bar{u}\sigma_{zp}} F_y \cdot \sum_{m=-\infty}^{\infty} \left[\exp\left(-\frac{\left(z - h_{ep} + 2mz_{ieff}\right)^2}{2\sigma_{zp}^2} \right) + \exp\left(-\frac{\left(z + h_{ep} + 2mz_{ieff}\right)^2}{2\sigma_{zp}^2} \right) \right] \quad (3.6)$$

In a stable boundary layer (SBL), the dispersion plume is treated as Gaussian distribution as in ISCST3 and other regulatory dispersion models (Hanna and Paine (1989) cited from *(6)*).

$$C_s\{x_r, y_r, z\} = \frac{Q}{\sqrt{2\pi}\bar{u}\sigma_{zs}} F_y \cdot \sum_{m=-\infty}^{\infty} \left[\exp\left(-\frac{\left(z - h_{es} - 2mz_{ieff}\right)^2}{2\sigma_{zs}^2} \right) + \exp\left(-\frac{\left(z + h_{es} + 2mz_{ieff}\right)^2}{2\sigma_{zs}^2} \right) \right] \quad (3.7)$$

where, z_{ieff} is the effective mechanical mixed layer height, σ_{zs} is the total vertical dispersion in the

SBL, and h_{es} is the plume height (stack height plus the plume rise) *(6)*.

AERMOD Deposition Algorithms:

The deposition algorithms in AERMOD include formulations for dry and wet depositions following distribution between particulate and gaseous phases. For dry deposition, the process is a function of deposition velocity as follows *(8)*:

$$F_d = \chi_d \cdot V_d \quad (3.8)$$

where, F_d is dry deposition flux (μg/m^2/s)*;* χ_d is concentration (μg/m^3), calculated at reference height, *zr;* V_d is deposition velocity (m/s)*;* z_r is deposition reference height (m) = *zo*+1, and

z_o is surface roughness length for the application site (m), from the meteorological file.

The dry deposition flux is also calculated on an hourly basis and summed up to a yearly or a 5 year meteorological data period. The default output units for dry deposition flux are μg/m^2 *(8).* The deposition velocity is a function of particle size distribution and sub-layer resistances in particle dry deposition and of surface and bulk resistances in gaseous dry deposition.

For wet deposition, the flux depends on a washout coefficient which describes the mass of pollutant removed by rain. The particle wet deposition algorithm is as follows *(8)*:

$$F_{wp} = 10^{-3} \rho_p W_p r \quad (3.9)$$

where F_{wp} = flux of particulate matter by wet deposition (μg/m2/hr); ρ_p = column average concentration of particulate in air (μg/m3); W_p = particle washout coefficient (dimensionless); and r is water or water equivalent precipitation rate (mm/hr), from the meteorological file.

The gaseous wet deposition, in turn, is described as follows *(8)*:

$$F_{wg} = 10^{6} C_l M_w r \quad (3.10)$$

where, F_{wg} = flux of gaseous pollutants by wet deposition (μg/m2/hr); C_l = concentration of pollutant in the liquid phase (moles/liter), and M_w = molecular weight of pollutant (grams/mole).

Wet deposition flux is also calculated per hourly basis and summed up to the yearly basis or to 5 years of meteorological data period.

The AERMOD model described here indicates the complexity of the dispersion and deposition processes. To support the application of AERMOD, meteorological data prepared by the meteorological pre-processor AERMET are crucial. The meteorological data used in this work were prepared by Michigan Department of Environmental Quality (MDEQ) from 2001-2005, the period that UMDES study was conducted. The surface and upper air meteorological data obtained from Midland-Bay-Saginaw airport and from White Lake in Detroit *(9)* for each year are surface data and profiling data. Five year meteorological data files were then compiled as a 5 year surface file and a 5 year profiling file. The former file contained hourly surface parameters such as sensible heat

flux, heights of convective layer and of mechanical mixing layer, Monin-Obukhov length, and precipitation amount among others. The latter profiling data file included vertical gradients of temperature, wind speed and turbulence computed from the radiosonde data. The details of AERMET data files are described elsewhere *(10)*.

The modeling conditions for AERMOD were based on a unitary emission rate of 1gram/second for 10 dioxin congeners using both gaseous and particulate algorithms. The outputs included air concentrations and dioxin deposition fluxes (calculated separately for gaseous and particulate forms, were multiplied by conversion factor derived from the 1992 emission profile and 1983 emission level).

3.2. Geostatistical model

3.2.1 Study area

The study area is the vicinity of the Dow Chemical Company facility in Midland, Michigan. Accounting for 53 field data and the output of the EPA Industrial Source Complex (ISC) dispersion model, the spatial distribution of dioxin around the Dow facility incinerator was modeled using geostatistical simulation in the companion paper. The set of simulated maps were used to compute, for each census block, the probability that the average TEQ value within that block exceeds a threshold of 90 ppt, which is the soil generic residential Direct Contact Criterion (DCC) used by the Department of Environmental Quality for Midland, Michigan*(11)*. Census blocks that were the most likely to exceed the DCC threshold and have the largest population at risk were targeted for a recent soil sampling campaign. This estimation was based on using a conservative threshold of 75 ppt TEQ (Figure 2, bottom), which yielded 196 census blocks with a probability greater or equal to 0.4. This campaign was conducted within the framework

of the University of Michigan Dioxin Exposure Study (UMDES) that focuses on quantifying exposure pathways to dioxins from industrial sources, relative to background exposures.

3.2.2. Soil sampling and measurement

The UMDES soil sampling campaign was carried out at 51 locations in the vicinity of the Dow Chemical's incinerator complex. Due to binding with confidentiality agreements, the sampling locations can not be disclosed. Analytical results of the 1-inch depth UMDES soil samples provide concentrations of 29 dioxins, furans and PCB congeners. Total TEQs excluding PCBs' contributions of these 51 UMDES samples were used to validate the deposition model. The soil sampling and analysis is described in Demond et al. *(12).* Up to four sampling stations were located around the perimeter of the house. If responses to interview questions indicated soil contact activities, samples were also taken at those locations (maximum of two), usually a vegetable garden and/or a flower garden. Each sampling station was defined by laying out a 3-foot diameter sampling ring. Three equally spaced cores around the ring were collected using custom-made, single-use, 2 inch I.D., and polycarbonate sample tubes. This procedure allowed for direct sample collection in the tube, sealing of the tube, and the minimization of cross-contamination between samples. The sealed sample cores were stored at 4°C until they were composited.

The soil cores were pushed out of the polycarbonate tubes using a Geotest core extruder (Model E-267, Evanston, Illinois). The extruded cores from the house perimeter stations were then separated into two strata: 0-1 inch and 1-6 inch. The cores from the

soil contact stations were not separated into strata. Vegetation, if present, was separated from the 0-1 inch stratum. The respective strata from each station were first combined and homogenized and then the stratum composites from the same station type were combined and homogenized. Ultimately, each residence yielded some or all of the following composite samples for analysis: (i) House perimeter set 0-1 inch composite (HP 0-1 inch); (ii) House perimeter set 1-6 inch composite (HP 1-6 inch); (3) Soil contact set 0-6 inch composite (Garden). The soil samples were archived in dioxin-grade amber glass jars to avoid photolytic degradation, and stored in dedicated 4° C cold rooms prior to analysis.

The HP 0-1 inch composite sample was analyzed for all residences. In addition, if the respondent had a vegetable garden or worked in a flower garden, the garden composite was analyzed. The HP 1-6 inch composite was only analyzed if the TEQ_{DFP}-WHO_{98} (the subscript p refers to the 12 PCBs listed by the WHO) (EPA, 2003) of the HP 0-1 inch composite was > 8 pg/g. The trigger value of 8 pg/g TEQ_{DFP}-WHO_{98} represents the 75^{th} percentile of the background distribution for the lower peninsula of Michigan based on MDEQ sampling (TEQ_{DF}-WHO_{98}) *(13)* (i.e., 25% of background soil samples were expected to be above 8 pg/g). All samples that were subjected to analysis were shipped to Vista Analytical Laboratory (El Dorado Hills, California), where they were analyzed by high-resolution gas chromatography/high resolution mass spectrometry (HRGC/HRMS) for the WHO 29 congeners using internal modifications of EPA methods 8290 *(14)* and 1668 *(15)*.

3.2.3. Air dispersion model coupled with geostatistical model

The procedure of geostatistical modeling was detailed in *(16, 17)* using a set of 51 dioxin soil congener data and Total Equivaent TEQ as follows:

1. The dioxin concentrations were normal score transformed to correct for the strongly positively skewed sample. Because the UMDES samples were preferentially located in census blocks with expected high concentrations of dioxins (based on the prior ISCT3 model predictions), sample statistics likely overestimate the magnitude of the contamination over the entire modeled area.
2. The 51 transformed data were regressed against the deposition (wet and dry) values predicted by air dispersion model (ISCST3 or AERMOD) using the emission profile of 1992 and the bulk emission of 1983. Meteorological data and site information were collected from the local area in Alpena and Flint (in case of ISCST3 model) and in Midland and Detroit (in case of AERMOD model) . This resulting regression model was used to predict the dioxin concentration and standard error at the nodes of the 261×261 simulation grid centered on the incinerator. The grid, which has a 50 m spacing, does not include any node within the boundary of the plant.
3. The spatial variability of regression residuals was modeled using a variogram based on the 51 measured data.
4. Sequential Gaussian simulation was used to simulate the spatial distribution of dioxin values conditionally to the 51 UMDES soil observations, the trend model inferred from the calibration of the deposition data (step 2) and the pattern of correlation modeled in step 3. One hundred realizations were generated over the 261×261 simulation grid.

5. Point simulated values were averaged within each census block to yield a simulated block value (upscaling). This averaging was repeated for each realization, yielding a set of 100 simulated values for each census block. E-type mean over100 realizations were derived.

The procedure SAS GLM*(18)* was used for the regression, while normal score transform was conducted using the program *nscore* in the public domain software library, GSLIB*(19)*. Sequential Gaussian simulation with local means was implemented by modifying the FORTRAN source code Sgsim in GSLIB. Semivariogram models, aggregation within census blocks and mapping were accomplished using TerraSeer STIS (Space-Time Intelligence System)*(20)*, a commercially available product.

3.2.4. Validation of the Geostatistical Model of Uncertainty

The geostatistical model consists of 100 maps of TEQ values simulated on a 261×261 grid with a 50 m grid spacing. The set of simulated values is denoted $\{z^{(l)}(\boldsymbol{u}_j);\ l=1,\ldots,L\ ;\ j=1,\ldots,N\}$, with L=100 and $N=(261)^2$. Each of the 51 new observations, $\{z(u_\alpha),\ \alpha=1,\ldots,n\}$, was compared to the distribution of 100 TEQ values simulated at the closest grid node $\boldsymbol{u}_i$, with $\|\boldsymbol{u}_i - \boldsymbol{u}_\alpha\| < \|\boldsymbol{u}_i - \boldsymbol{u}_\alpha\|\ \forall$ j. The validation stage proceeded as follows:

1. Boxplots were used to visualize where the measured value $z(\boldsymbol{u}_\alpha)$ falls within the distribution of 100 simulated values, $\{z^{(l)}(\boldsymbol{u}_i);\ l=1,\ldots,100\}$.

2. From the distribution of 100 simulated values we computed, for each of the 51 new sampled locations, a series of symmetric *p*-probability intervals (PI) bounded by the (1-*p*)/2 and (1+*p*)/2 quantiles of that distribution. For example, the 0.5-PI is bounded by the lower and upper quartiles. A correct modeling of local uncertainty would entail

that there is a 0.5 probability that the actual TEQ value at that location falls into that interval or, equivalently, that over the study area 50% of the 0.5-PI include the true value. The fraction of true values falling into the symmetric *p*-PI is estimated as:

$$\bar{\zeta}(p) = \frac{1}{n}\sum_{\alpha=1}^{n}\zeta(\mathbf{u}_\alpha; p) \qquad (3.11)$$

where $\zeta(\mathbf{u}_\alpha; p)$ equals 1 if $z(\boldsymbol{u}_\alpha)$ lies between the (1-*p*)/2 and (1+*p*)/2 quantiles, and zero otherwise. The scattergram of the estimated, $\bar{\zeta}(p)$, versus expected, *p*, fractions is called the "accuracy plot" and quantifies the accuracy of the model of uncertainty. The average width of the PIs that include the new observations informs on the precision of the models of local uncertainty.

3. The correlation was computed between each measured TEQ or congener value $z(\boldsymbol{u}_\alpha)$ and the average simulated value $\bar{z}(\mathbf{u}_i)$ calculated as:

$$\bar{z}(\mathbf{u}_i) = \sum_{l=1}^{100} z^{(l)}(\mathbf{u}_i) \quad (3.12)$$

4. Prediction errors, $\bar{z}(\mathbf{u}_i) - z(\boldsymbol{u}_\alpha)$, were mapped to identify any spatial pattern for the over and under-estimation of TEQ/congener values.

3.2.5. Updating of the Geostatistical model

The procedure used to derive the first model of uncertainty and described in *(21)* was applied to the combined set of 53 data collected during 1983-1998 sampling campaigns and the new 51 observations from the UMDES sampling. The methodology is as follows:

1. The 104 soil TEQ concentrations were normal score transformed to correct for the strongly positively skewed sample histogram. Because the UMDES samples were preferentially located in census blocks with expected high level of dioxin, sample statistics likely overestimate the magnitude of the contamination over the entire modeled area. In order to reduce the weight assigned to these redundant observations and obtain statistics (e.g. mean, variance) that are more representative of the distribution of TEQ values within the modeled area, declustering weights were computed and used in the normal score transform; recall equation (1) in companion paper. A cell-declustering method, with cell sizes ranging from 50 to 350 meters, was applied and the cell size of 218 meters leading to the smallest declustered mean was retained since high values were preferentially sampled.
2. The 104 transformed data were regressed against the deposition (wet and dry) values predicted using the numerical dispersion model (base case scenario). This regression model was used to predict the TEQ concentration and standard error at the nodes of the 261×261 simulation grid centered on the incinerator. The grid, which has a 50 m spacing, does not include any node within the boundary of the plant.
3. The spatial variability of regression residuals was modeled using the semivariogram.
4. Sequential Gaussian simulation was used to simulate the spatial distribution of TEQ values conditionally to the 104 soil TEQ data, the trend model inferred from the calibration of the deposition data (step 2) and the pattern of correlation modeled in step 3. One hundred realizations were generated over the 261×261 simulation grid.
5. Point simulated values were averaged within each census block to yield a simulated block value (upscaling). This averaging is repeated for each realization, yielding a set

of 100 simulated values for each census block. The following three statistics were derived from the distribution of 100 simulated block TEQ values: mean, variance and proportion of block values that exceeds a threshold of 90 ppt which is the soil generic residential Direct Contact Criterion (DCC) used by the Department of Environmental Quality for Midland, Michigan *(22)*.

The procedure SAS GLM*(18)* was used for the regression, while the declustering and normal score transform were conducted using the programs declus and nscore in the public domain software library, GSLIB*(19)*. Sequential Gaussian simulation with local means was implemented by modifying the FORTRAN source code Sgsim in GSLIB. Aggregation within census blocks and mapping were accomplished using the commercial product, TerraSeer STIS (Space-Time Intelligence System)*(20)*.

References

(1) EPA, U., User's Guide for the Industrial Source Complex (ISC 3) Dispersion Models **1995,** Vol. 1

(2) Cimorelli, A. J.; Perry, S. G.; Venkatram, A.; Weil, J. C.; Paine, R. J.; Wilson, R. B.; Lee, R. F.; Peters, W. D.; Brode, R. W., AERMOD: A dispersion model for industrial source applications. Part I: General model formulation and boundary layer characterization. *Journal of Applied Meteorology* **2005,** 44, (5), 682-693.

(3) EPA, U., The American Meteorological Society/Environmental Protection Agency Regulatory Model Improvement Committee (AERMIC) *AERMOD* **2006**.

(4) EPA, U., User's Guide for the AMS/EPA Regulatory Model - AERMOD. **2006**

(5) Wesely, M. L. D. P. V. S. J. D. *Deposition Parameterizations for the Industrial Source Cmplex (ISC3) Model*; Argonne National Laboratory: 2002.

(6) Cimorelli, A. P. G. V. A. e. a. *AERMOD: Description of Model formulation* 2004; p 91.

(7) EPA, U. *Comparison of regulatory design concentrations AERMOD vs ISCST3, CTDMPLUS, ISC-PRIME*; 2003.

(8) EPA *AERMOD Deposition Algorithms – Science Document (Revised Draft)*; 2004; p 22.

(9) MDEQ, Meteorological Data Support Document. In Michigan Department of Environmental Quality: 2009.

(10) EPA *Addendum to the User's Guide for the AERMOD Meteorological Data Preprocessor, AERMET*; 2004; p 19.

(11) MDEQ *Part 201 Generic Soil Direct Contact Criteria* Michigan Department of Environmental Quality Environmental Response Division: 1998.

(12) Demond, A.; Adriaens, P.; Towey, T.; Chang, S.-C.; B, H.; Chen, Q.; Chang, C.-W.; Franzblau, A.; D, G.; Gillespie, B.; E, H.; Knutson, K.; Lee, C.; Lepkowski, J.; Olson, K.; Ward, B.; Zwica, L.; Luksemburg, W.; Maier, M., Residential Soil Concentrations of PCDDS/PCDFS/PCBS in a Community in Michigan. *Environ. Sci. Technol.* **2007,** In Review.

(13) Michigan Department of Environmental Quality, *Michigan Soil Background Dioxin Data*. Available at http://www.deq.state.mi.us/documents/deq-whm-hwp-mi_soil_bkgd_dioxin_data.pdf Accessed July 2nd, 2007: Lansing, MI, 1999.

(14) U.S. Environmental Protection Agency *Method 8290: Polychlorinated dibenzodioxins (PCDDs) and polychlorinated dibenzofurans (PCDFs) by high-resolution gas chromatography/high-resolution mass spectrometry (HRGC/HRMS)*; Washington, DC, 1994: 1994.

(15) U.S. Environmental Protection Agency *Method 1668, Revision A: Chlorinated biphenyl congeners in water, soil, sediment, and tissue by high-resolution gas chromatography/high-resolution mass spectrometry (HRGC/HRMS).* Washington, DC: 1999.

(16) Goovaerts, P., Geostatistical modelling of uncertainty in soil science. *Geoderma* **2001,** 103, (1-2), 3-26.

(17) Goovaerts, P.; Trinh, H. T.; Demond, A.; Franzblau, A.; Garabrant, D.; Gillespie, B.; Lepkowski, J.; Adriaens, P., Geostatistical modeling of the spatial distribution of soil dioxins in the vicinity of an incinerator. 1. Theory and application to Midland, Michigan. *Environmental Science & Technology* **2008,** 42, (10), 3648-3654.
(18) Inc., S. I. *SAS/STAT User's Guide* Fourth Edition, Vol. 2; SAS Institute Inc.: Cary, NC, 1989.
(19) Deutsch, C. V., Journel A.G., *GSLIB Geostatistical Software Library and User's Guide*. Second edition ed.; Oxford University Press 1992.
(20) TerraSeer *STIS (Space-Time Intelligence System)*, 1.6.002.
(21) Goovaerts, P.; Trinh, H. T.; Demond, A. H.; Towey, T.; Chang, S. C.; Gwinn, D.; Hong, B.; Franzblau, A.; Garabrant, D.; Gillespie, B. W.; Lepkowski, J.; Adriaens, P., Geostatistical modeling of the spatial distribution of soil dioxin in the vicinity of an incinerator. 2. Verification and calibration study. *Environmental Science & Technology* **2008,** 42, (10), 3655-3661.
(22) Michigan Department of Environmental Quality, *Dioxin Contamination in the Midland Area*. Availabel at http://www.deq.state.mi.us/documents/deq-whm-hwrp-dowfactsfinal.pdf, Accessed July 2nd, 2007, U.S. EPA: Research Triangle, NC: 2004.

Chapter 4

Geostatistical Model's Validation and Update Results

From *Geostatistical modeling of the spatial distribution of soil dioxin in the vicinity of an incinerator. 2. Verification and calibration study.*

Environmental Science & Technology 2008, 42, (10), 3655-3661.

4.1. Previously-available versus UMDES TEQ data

Figure 4.1 (a, b) shows the histograms of the 53 TEQ data used to build the geostatistical model described in Goovaerts et al. *(1)*and the 51 TEQ data collected within the framework of the University of Michigan Dioxin Exposure Study (UMDES). UMDES data exhibit larger mean and median values, while their maximum (923 ppt) is more than twice the maximum of 450 ppt observed in the dataset used for the original model. This observation underscores the spatial heterogeneity of dioxin deposition, considering that the first dataset *(2)* was collected in areas near the plant with expected high values, while the 51 new UMDES data were preferentially located in census blocks with TEQ values in excess of 75 ppt. The geographic distribution of the sampled census blocks includes locations North, East and South-East of the incinerator complex. The data statistics may further indicate the contribution of multiple sources of dioxins in soil, aside from incinerator deposition; preliminary fingerprinting analysis of the deposition patterns

indeed indicates a divergence of some samples based on their congener contributions to the TEQ (data not shown;*(3)*).

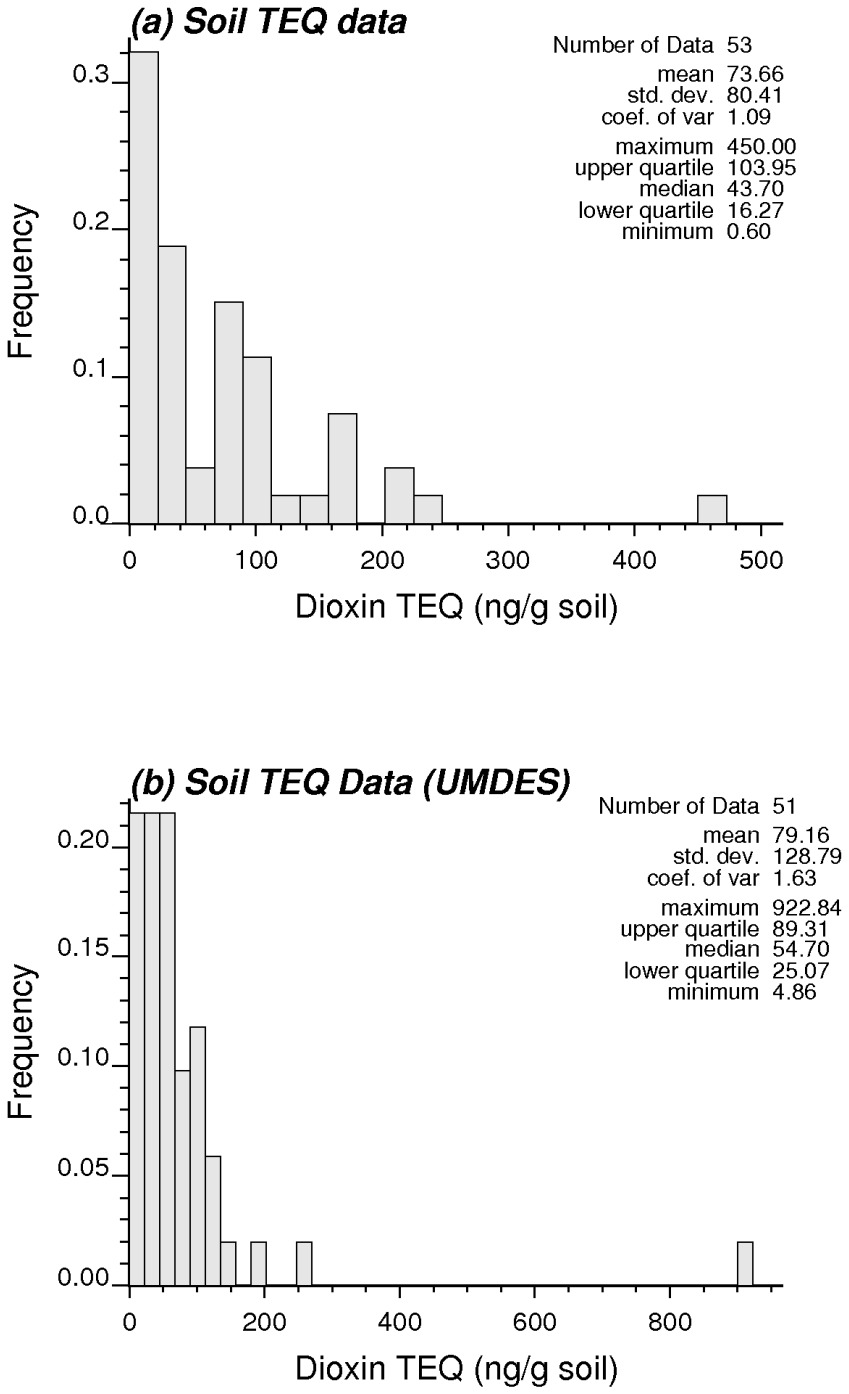

Figure 4.1. Histograms of: (a) 53 TEQ data used to construct the original geostatistical model and (b) the 51 new samples collected during the UMDES campaign.

In addition to the differences in summary statistics, the two normal score transformed datasets correlate differently with the five-year dry and wet deposition values predicted by the dispersion model. While the 53 old data were better correlated with dry deposition (r=0.641) than wet deposition (r=0.344)*(1)*, the opposite pattern is displayed by the 51 UMDES data. The strongest correlation (r=0.691) is observed for wet deposition, while dry deposition has a smaller correlation (r=0.513) with the data (Figure 4.2). The two correlation coefficients are significantly different for wet deposition (p=0.015) but non-significant for dry deposition (p=0.339). This change in the pattern of correlation can be explained by the fact that the South-western side of the plant, where most of wet deposition occurred according to the numerical model, was not sampled during the UMDES campaign because of its low population density (and thus decreasing likelihood to be included in a random sampling). Previous studies, which did not employ the ISCST3 model, indicated the importance of a regional component in designating whether wet or dry deposition were dominant for dioxin deposition (e.g. *(4-6))*. Dry deposition tended to dominate in the Midwest; wet deposition was most important in Western Europe and the Houston area.

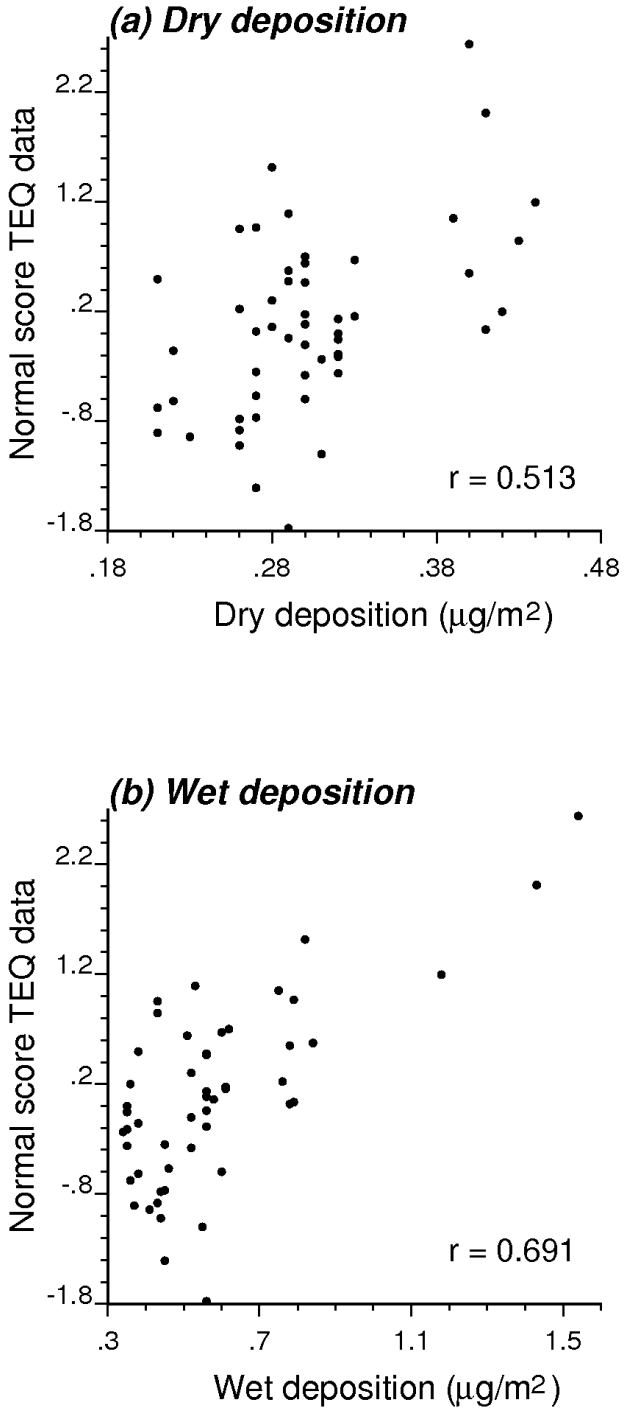

Figure 4.2. Scatterplots of soil TEQ normal scores versus 5-year dry (a) and wet deposition (b) values predicted by the dispersion model (units= $\mu g/m^2$).

4.2. Validation study

Each of the 51 UMDES data was compared to the distribution of 100 TEQ values simulated at the closest grid node. Box plots in Figure 4.3 summarize the results for all 51 sampled locations. The UMDES-sampled TEQ values tend to fall within the upper tail of the simulated local distributions (based on EPA/DEQ data,*(2)*: 42 observations out of 51 are above the median, with 7 data exceeding the 95 percentile.

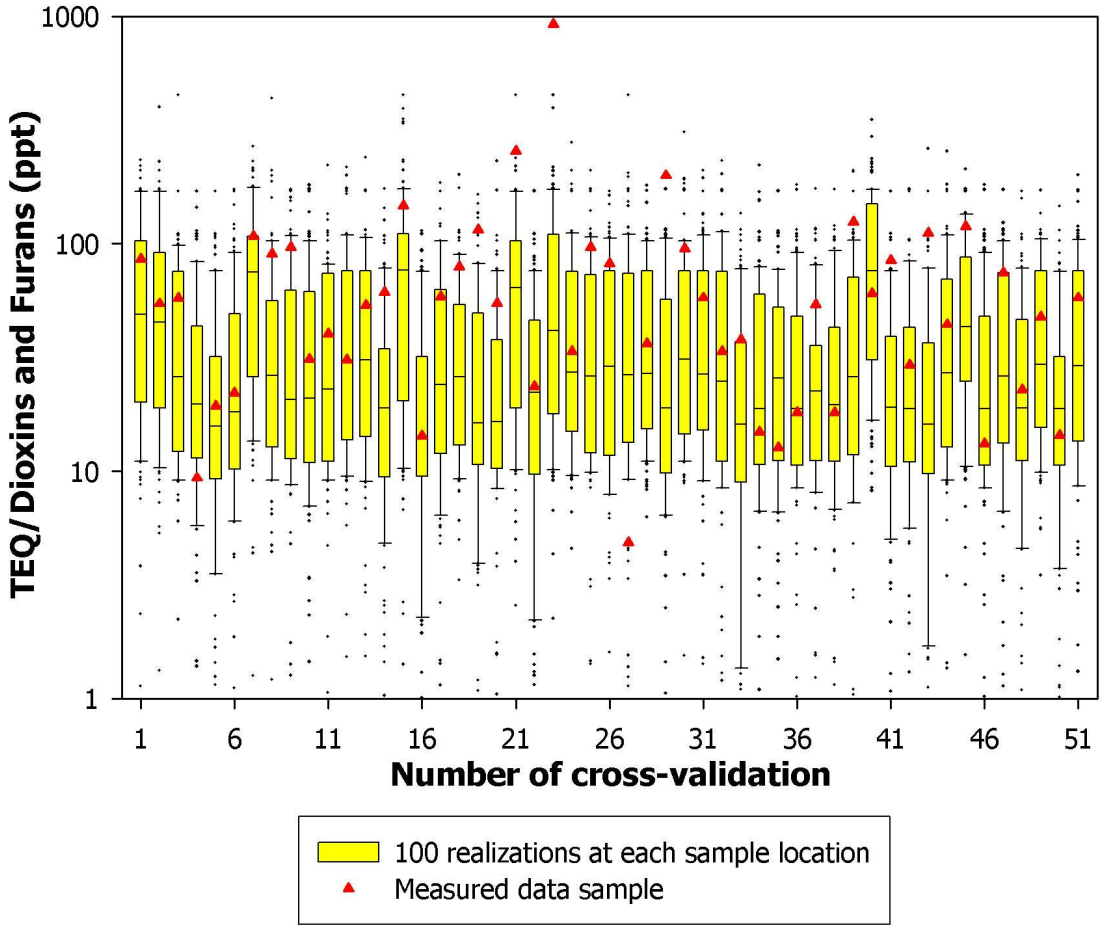

Figure 4.3. Box plots of the distributions of 100 simulated TEQ values corresponding to the grid nodes the closest to the location of the 51 UMDES samples (values denoted by red triangles).

This underestimation by the geostatistical model is confirmed by the scatter plot of observed concentrations versus averaged simulated values (Figure 4.4a). Although predicted values are on average lower than observed values (44.24 versus 62.29 ppt), there is a reasonably good agreement between the two datasets (correlation=0.44). Note that these statistics are computed after discarding the extreme observation of 923 ppt. The difference in summary statistics between the dataset used for the prediction model and those collected for UMDES explains this underestimation of concentrations. The map of prediction errors (not shown for confidentiality reasons) indicates that the underestimation occurs mainly in the vicinity of the plant property line.

Lognormal kriging displays a similar underestimation (Figure 4.4b), although the use of 8 neighbors instead of 32 for the simulation procedure (Supporting Information in companion paper) reduces the smoothing effect. Figure 4.4c indicates that both average simulated and estimated values are fairly similar. Indeed, discrepancies between the two approaches are observed farther away from the incinerator, where UMDES data were not collected. Differences between approaches are larger in terms of uncertainty assessment: the average kriging standard error (51.1) exceeds the average standard deviation of the local distribution of 100 simulated values (44.4). Yet, the confined and well-sampled area analyzed in the UMDES study does not allow a realistic assessment of the benefit of the air dispersion model which is expected to increase away from the incinerator (e.g. SE corner) where no field data are available.

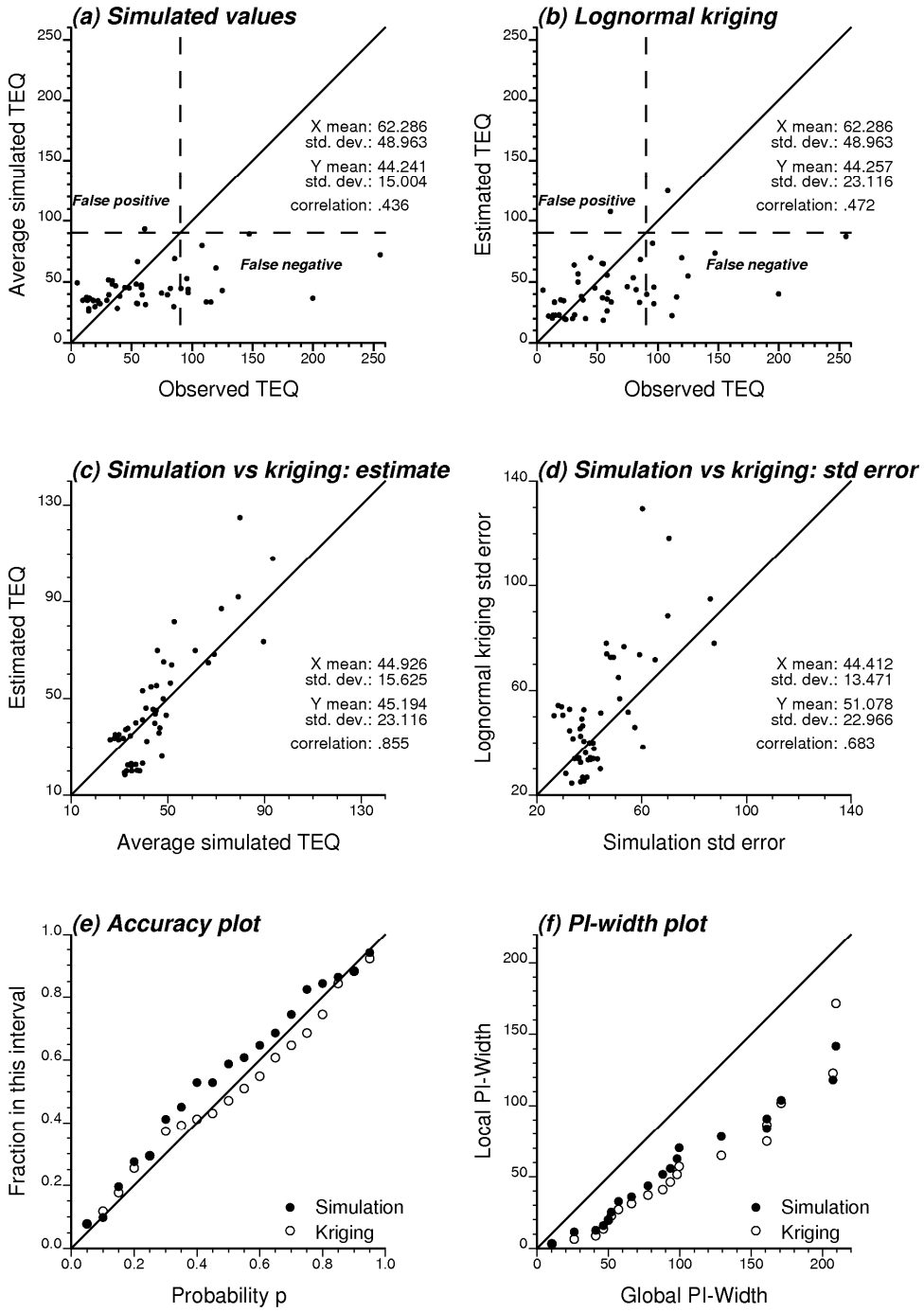

Figure 4.4. Scatterplot of UMDES observations versus the mean of the 100 simulated TEQ values (a) or the lognormal kriging estimate (b) (the maximum observation of 923 ppt is not included for graph clarity). Scatterplots of simulation versus lognormal kriging results (c,d). Plot of the proportion of observed TEQ values falling into probability intervals (PI) of increasing size (accuracy plot, e). The width of these local PIs is plotted against the width of the global PIs that are derived from the sample histogram (f).

One consequence of the underestimation of TEQ concentrations is that only one averaged simulated value or two kriged values exceed the residential Direct Contact Criterion (DCC) of 90 ppt, see Figure 4.4a (upper left quadrant). Furthermore, only one of the 13 UMDES data exceeding 90 ppt is actually reflected in the geostatistical model (Figure 4.4b, upper right quadrant). This is due to the fact that all least-square interpolation algorithms tend to underestimate the high values while the low values are overestimated (e.g.*(6)*. Considering that this study attempts to provide a probabilistic interpretation of spatially differentiated data, the interpretation needs to be supplemented by a measure of the likelihood that the soil generic residential Direct Contact Criterion (DCC) of 90 ppt is exceeded. This likelihood was computed, for each simulation grid node, as the proportion of 100 simulated TEQ values that are larger than 90 ppt (Figure 4.4e in *(1)*. The average likelihood is 0.12 for the 38 UMDES data below 90 ppt and 0.21 for the 13 UMDES data above 90 ppt. The analysis of lognormal kriging results yields similar probabilities of 0.1 and 0.2, respectively. Despite the low average probability of exceedence resulting from the underestimation of TEQ concentrations, the geostatistical measure of uncertainty allows discrimination between locations with potentially high and low dioxin levels. This result also illustrates the potential hazard of ignoring the uncertainty attached to estimates in the decision-making process *(7-9)*.

Figure 4.4e shows that the simulation-based model of uncertainty is accurate: the proportion of observations that fall within probability intervals (PI) exceeds what is expected from the model. For example, the observed TEQ value is included in the 0.5-PI for 59% of the 51 new samples (expected proportion=50%). The accuracy of the kriging-based model fluctuates with the probability p; the PIs contain a smaller than expected

fractions of true values for probabilities larger than 0.45. Not only should the true TEQ value fall into the PI according to the expected probability p, but this interval should be as narrow as possible to reduce the uncertainty about that value. The average width of these local PIs should also be smaller than the global PI inferred from the sample histogram. The scatter plot in Figure 4.4f indicates that, for both approaches and all probabilities p, the local PIs are narrower than the corresponding global PIs, which means that the geostatistical model of uncertainty is more precise than an aspatial model that ignores the location of soil samples.

4.3. Updated geostatistical model

The creation of an updated geostatistical model started with the regression of the output of the air dispersion model ISCST3 (dry and wet depositions plus their interaction) against the set of 104 normal score transformed TEQ data (to include both the previously collected EPA/DEQ data and the UMDES data). As for the 53 old data, TEQ values are better correlated with dry deposition (r=0.511) than wet deposition (r=0.361), although the difference is non significant (p=0.181). Application of the regression model to the 261×261 exposure assessment grid yields the trend model displayed in Figure 4.5a. The joint contribution of dry and wet depositions generates a continuous ring of high trend values around the plant. Comparison of the old and updated trend models in Figure 4.5b shows a decline in regression estimates on the southwestern side of the plant where wet deposition is the predominant mechanism, while the regression leads to larger estimates downwind of the plant where dry deposition prevails. These differences reflect changes in the calibration of the trend model which likely result from the more geographically

distributed census-block based sampling of UMDES data: none of the 51 additional samples was collected South of the plant because of the low population density.

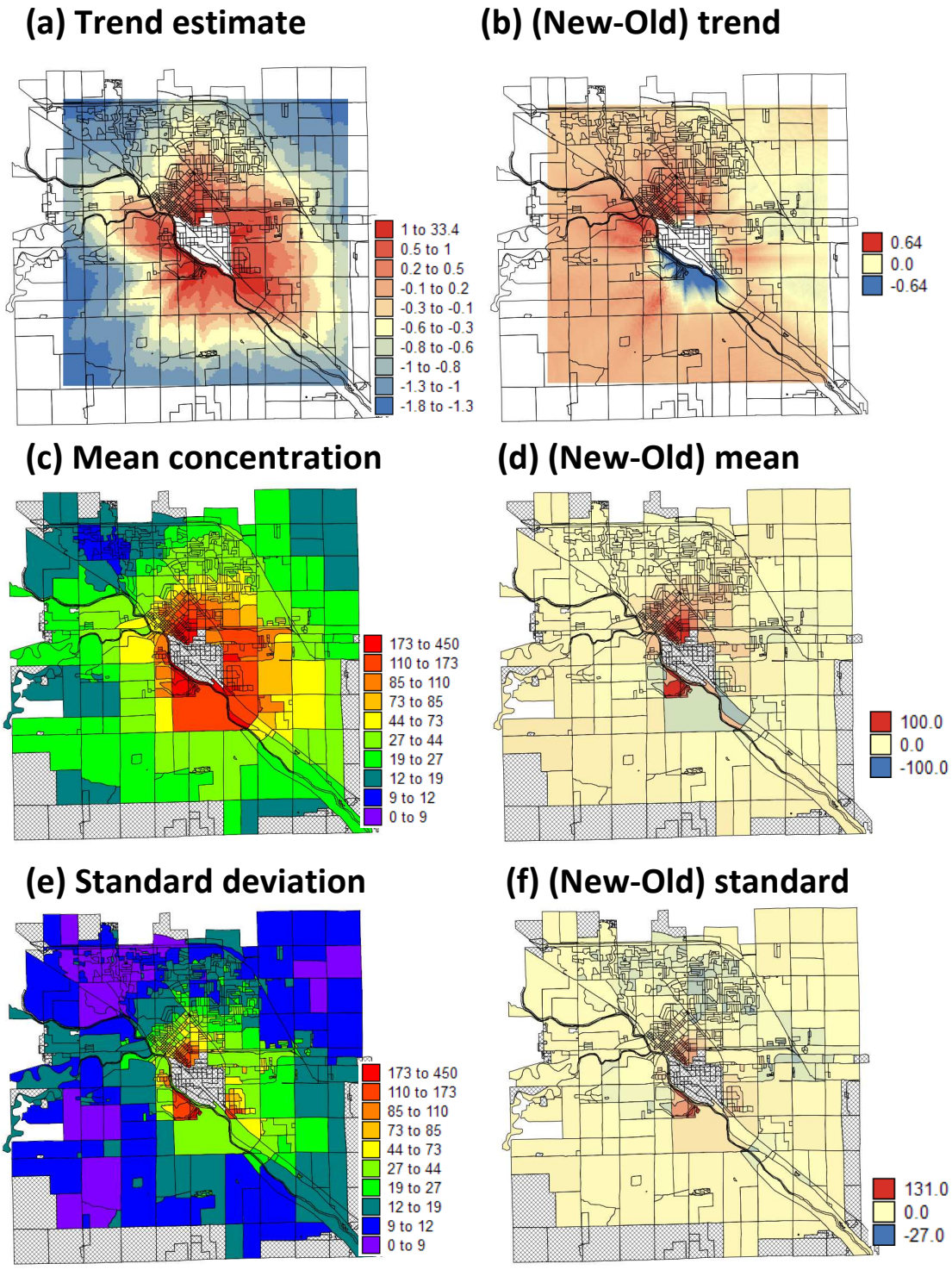

Figure 4.5. Impact of UMDES data on the definition of the trend component (a,b), and the mean (c,d) and standard deviation (e,f) of the distribution of 100 TEQ values simulated at the level of census blocks. Left column shows the results for the updated geostatistical model, while the right column illustrates differences with the old model. Hatched polygons denote census blocks outside the simulation area.

The incorporation of 51 new data changed the shape of the experimental semivariogram of normal score TEQ values that is now clearly bounded, with a range of autocorrelation of around 4 km (Figure 4.6a). The trend component and semivariogram model were used in sequential Gaussian simulation to generate 100 realizations of the spatial distribution of TEQ values. Figure 4.5c-e shows the maps of the mean and standard deviation of the distribution of 100 TEQ values simulated at the level of census blocks. The difference map of Figure 4.5d indicates that, except for a slight decline on the South-Eastern side of the plant, the new model displays larger TEQ values close to the plant, in particular in the North and South. This trend is consistent with the results of the validation procedure that revealed an underestimation by the old geostatistical model that occurred mainly in the vicinity of the plant property line. While the larger predicted values North of the plant reflect the influence of UMDES samples, smaller estimates on the Southern side are caused by the new calibration of the air dispersion model (recall Figure 4.5b).

The proportional effect is a particular form of heteroscedasticity where the local variance of data is related to their local mean *(9, 10)*. This effect explains the similarity between the spatial pattern of the maps of mean and standard deviation (Figure 4.5c-e): the rank correlation coefficient between the two sets of block-level values is 0.97. A decline in standard deviation, which translates into smaller uncertainty about block-level TEQ values, is also observed in the Northern and Eastern parts of the study area where most of the UMDES samples were collected (Figure 4.5f). Further calibration of the model requires incorporation of topographical changes (e.g. 5), temporal information on the climate and particle density variability that impacts local vs. distal deposition *(11)*,

and exclusion of samples whose homolog or congener profile does not support their origin as incinerator point sources (e.g. *(12)*).

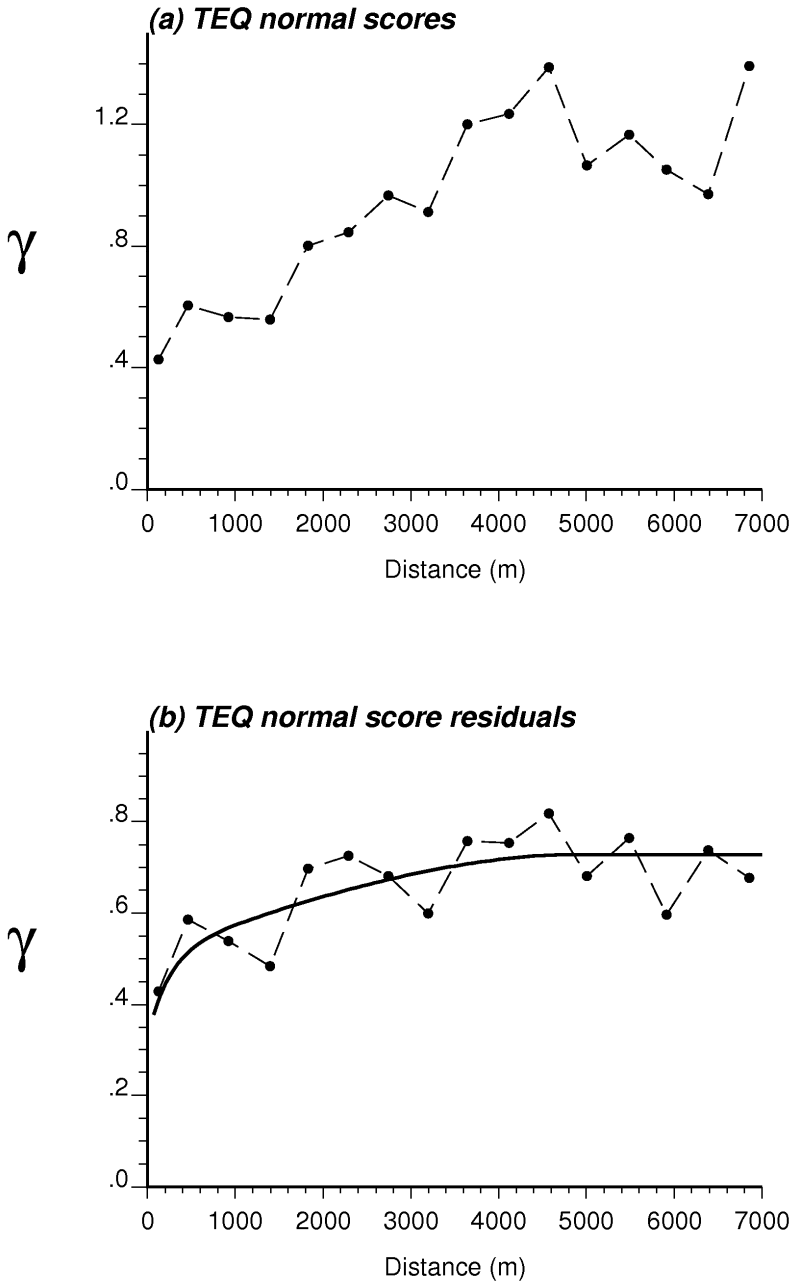

Figure 4.6. Omnidirectional semivariograms of soil TEQ normal scores before (a) and after (b) subtracting the trend modeled from deposition data.

References

(1) Goovaerts, P.; Trinh, H. T.; Demond, A.; Franzblau, A.; Garabrant, D.; Gillespie, B.; Lepkowski, J.; Adriaens, P., Geostatistical modeling of the spatial distribution of soil dioxins in the vicinity of an incinerator. 1. Theory and application to Midland, Michigan. *Environmental Science & Technology* **2008,** 42, (10), 3648-3654.

(2) MDEQ Available: http://www.deq.state.mi.us/documents/deq-whm-hw-dow-2005-06-10-midland-summary-map.pdf. Accessed July 2, 2008,

(3) Trinh, H. T.; Adriaens, P., Congener-Specific Differentiation of Soil Samples in the City of Midland, Michigan Using Multidimensional Scaling. *Organohalogen Compounds* **2007**.

(4) Eitzer, B. D.; Hites, R. A., Atmospheric transport and deposition of polychlorinated dibenzo-p-dioxins and dibenzofurans. *Environ. Sci. Technol.* **1989,** 23, (11), 1396-1401.

(5) Koester, C. J.; Hites, R. A., Wet and Dry Deposition of Chlorinated Dioxins and Furans. *Environmental Science & Technology* **1992,** 26, (7), 1375-1382.

(6) Schroder, J.; WelschPausch, K.; McLachlan, M. S., Measurement of atmospheric deposition of polychlorinated dibenzo-p-dioxins (PCDDs) and dibenzofurans (PCDFs) to a soil. *Atmospheric Environment* **1997,** 31, (18), 2983-2989.

(7) Barabas, N.; Goovaerts, P.; Adriaens, P., Geostatistical assessment and validation of uncertainty for three-dimensional dioxin data from sediments in an estuarine river. *Environmental Science & Technology* **2001,** 35, (16), 3294-3301.

(8) Goovaerts, P., *Geostatistics for Natural Resources Evaluation*. Oxford University Press 1997.

(9) Saisana, M.; Dubois, G.; Chaloulakou, A.; Spyrellis, N., Classification criteria and probability risk maps: Limitations and perspectives. *Environmental Science & Technology* **2004,** 38, (5), 1275-1281.

(10) Journel, A. G.; Huijbregts, C. J., *Mining Geostatistics*. Academic Press: London: 1978.

(11) Lohmann, R.; Jones, K. C., Dioxins and furans in air and deposition: A review of levels, behaviour and processes. *Science of the Total Environment* **1998,** 219, (1), 53-81.

(12) Trinh, H.; Adriaens, P., Congener-Specific Differentiation of Soil Samples in the City of Midland, Michigan Using Multidimensional Scaling. *Organohalogen Compounds* **2007**.

Chapter 5

Comparison of ISCST3 and AERMOD Models to Predict Dioxin Deposition from Industrial Incinerators

5.1. Introduction

The Industrial Source Complex-Short Term 3 (ISCST3) was developed in 1995 and since then it has been used as an air dispersion model in support of regulatory enforcement by the United States Environmental Protection Agency (US EPA) *(1)*. In December 2006, in cooperation with the American Meteorological Society (AMS), USEPA introduced a new air dispersion model, AERMOD to be fully promulgated to replace the ISCST3 model *(2-4)*. As described in detail in the Chapter 3, AERMOD is formulated with updated knowledge about the planetary boundary layers, vertical profiling of meteorological parameters such as wind, temperature as well as turbulence. The model also incorporates treatments of complex terrain features*(5)*. Since then, new atmospheric models such as CalPuf (http://www.src.com/calpuff/calpuff1.htm) are being developed and in various stages of regulatory review.

In support of AERMOD, a numbers of data processors were designed to help modelers prepare the required AERMOD input data formats. These data processors include (i) AERMET as a meteorological data processor, which is similar to PCRAMMET of the ISCST3 model; (ii) AERMAP as a terrain data processor, and (iii) AERSURFACE as a surface characterization processor among others*(2)*.

To convince the modeling community that AERMOD is a superior air dispersion model, EPA conducted a validation study in which 17 field site databases were set up to validate model predictions of air concentration of pollutants against field observations *(6)*. The study characterized 17 different field sites, ranging from rural areas (various locations of Illinois) to urban areas (Indiana); from simple terrain (very flat and rural area of Illinois or of Nebraska); to moderate terrain (hilly and rural areas of New York, Indiana and Maryland); and to complex terrain such in the mountainous area of Nevada. This validation of AERMOD was conducted with different tracers and air pollutants such as SO_2 and SF_6. The authors of the study paid special attention to the high end of the prediction distributions where regulatory thresholds of contaminants are enforced. The air concentrations of these tracers were measured under stable conditions between sunset and sunrise, in convective conditions at day time when the turbulence caused by heat fluxes are observed. Sampled data were also collected at a relative short and long distances to the emitted sources to meet the purposes of the validation. In addition, the model inputs (meteorological data) were made available to meet the needs of the model *(6)*.

The study showed that AERMOD outperformed the ISCST3 model on a number of accounts. Among the superior performances, AERMOD is better than ISCST3 in capturing the high end concentrations for cases with complex terrain. In one publication,

AERMOD was reported to predict air concentration of tracer SO_2 to be within a factor of 2 of site observations, in comparison to a factor of 7 for ISCST3 *(7)*. Other non-validation studies compared the performances of AERMOD to the current ISCST3 model or other available regulatory air dispersion model based on the available archives of data inputs and other necessary conditions for those models' implementation *(8)*. Not only was the comparison of model performance between ISCST3 and AERMOD conducted, but the comparison of the uses of model attributes such as meteorological data, and types of pollutant emission sources were also analyzed *(9-13)*. Various types of air pollutants were assessed through the application of AERMOD such as SO_2 and SF_6 *(6)*, and kypton-85 *(14)* as they were available from the database prepared for AERMOD calibration; carbon dioxide and particulates as indicators for finding the best location for a new incinerator *(15)*; ammonia as in an area source of emission of the study *(11)*. Other pollutants (benzene, hexa-valent chromium) can also be found in health risk assessments *(13, 16)*. Dioxins and dioxin-like compounds, have to date not been common air pollutants subjected to either ISCST3 or AERMOD air dispersion applications *(17-22)*. These compounds are associated more with airborne particles and in order to describe the deposition of particles, deposition algorithms of ISCST3 and AERMOD are to be employed.

As described in Chapter 4, our previous work *(20, 21)* reported on the coupling of the outputs of the air dispersion model, Industrial Source Complex – Short Term 3 (ISCST3), with a geostatistical model to predict dioxin deposition in the vicinity of a hazardous waste incinerator in Midland, Michigan. This work utilized dry and wet deposition fluxes obtained from ISCST3 as inputs to the subsequent geostatistical

analysis. Deposition fluxes of total dioxin toxic equivalents (TEQs) predicted by ISCST3 were regressed against normal score transformations of the available dioxin soil data. Regression functions are then applied to the whole modeling domain, which is a rectangular grid of receptors out to 10 km from the incinerator. Spatial trends of regression residuals are incorporated in the geostatistical model (an interpolation approach of using sequential Gaussian simulations *(20, 21)* to simulate point values of TEQ concentrations in soil. The regression between the uniform deposition patterns and the biased soil sampling resulted in a low regression coefficient, and a variogram range of 4km*(21)*. The net result was that the spatial distribution of dioxin near the emission source displayed a complex pattern, which was further influenced by meteorological parameters such as wind speed, wind direction, and precipitation rates used in the air dispersion model.

Considering the algorithmic differences among the air dispersion models, there is a need to further explore the impact of model attributes on the deposition predictions of dioxins. This chapter describes the comparison of AERMOD-based depositions of dioxin TEQ with the ISCST3 predictions *(20, 21)*. Aside from the differences in the model algorithms (described in the Chapter 3), and different formatting requirements of the data to comply with AERMOD, there were changes in the locations of the meteorological stations. These data are of the Midland site (Tri City, Midland-Bay-Saginaw (MBS) and Detroit (DTX) instead of the weather stations (Alpena (APN) and Flint (FNT)) at further distance from Midland as used in our previous publication. The reason for this was at the time when ISCST3 model was employed, formatted meteorological data were available only for stations in Alpena and Flint as the closest weather stations to the modeling area.

A second modification of the model comparison is the use of both vapor- and particle-associated dioxin depositions. Prior validation studies of AERMOD *(2, 3)* modeled wet and dry deposition of pollutants separately in the vapor phase and the particulate phase. Mechanistically, highly hydrophobic and sorptive compounds such as dioxins are associated with airborne particles once emitted from the incinerator stack into the atmosphere *(23-25)*.

The analysis of three scenarios will be compared and discussed: (1) the original TEQ deposition results*(20, 21)* obtained from ISCST3 with meteorological data from Alpena (surface station) and Flint (upper air station) during 1987-1991*(2)*; (2) dioxin TEQ deposition predictions based on ISCST3 using surface weather data from Tri City (MBS) and upper air data from Detroit (DTX)*(26)*; and (3) dioxin TEQ deposition results predicted by AERMOD using data from the MBS and DTX weather stations during 2001-2006.

5.2. Materials and Methods

Study Site. The study area is the vicinity of the Dow Chemical Company facility in Midland, Michigan as described in detail elsewhere (Chapter 3). The dioxin contamination source in Midland is believed to have been impacted by the operation of hazardous waste incinerators since the 40s *(10)*. Halogenated materials were among the processed wastes, amounting to about 200 tons daily as reported in 1984 *(27)* and the burning of those materials produced dioxins as byproducts *(28, 29)*. Although currently a new incinerator complex with high dioxin removal efficiency (99.9999%) is in place *(30)* our modeling is based on the incinerator complex 830, which was demolished in 2002

prior to the operation of the current incinerator. This incinerator had been operated for decades and was a point source of dioxin contamination in Midland.

Field Data. Meteorological data were obtained from surface weather stations in the Tri City, Midland-Bay-Saginaw (MBS) and the upper air station, White Lake of Detroit Metropolitan (DTX) in the period from 2001 to 2006 *(26)*. The stations are located closer to the Midland site as compared to the Alpena and Flint weather stations, from which surface and upper air data were used in the earlier ISCST3 runs. The weather stations of Alpena, Flint, Tri City and Detroit are depicted on a map provided by the Michigan Department of Environmental Quality (Figure 5.1).

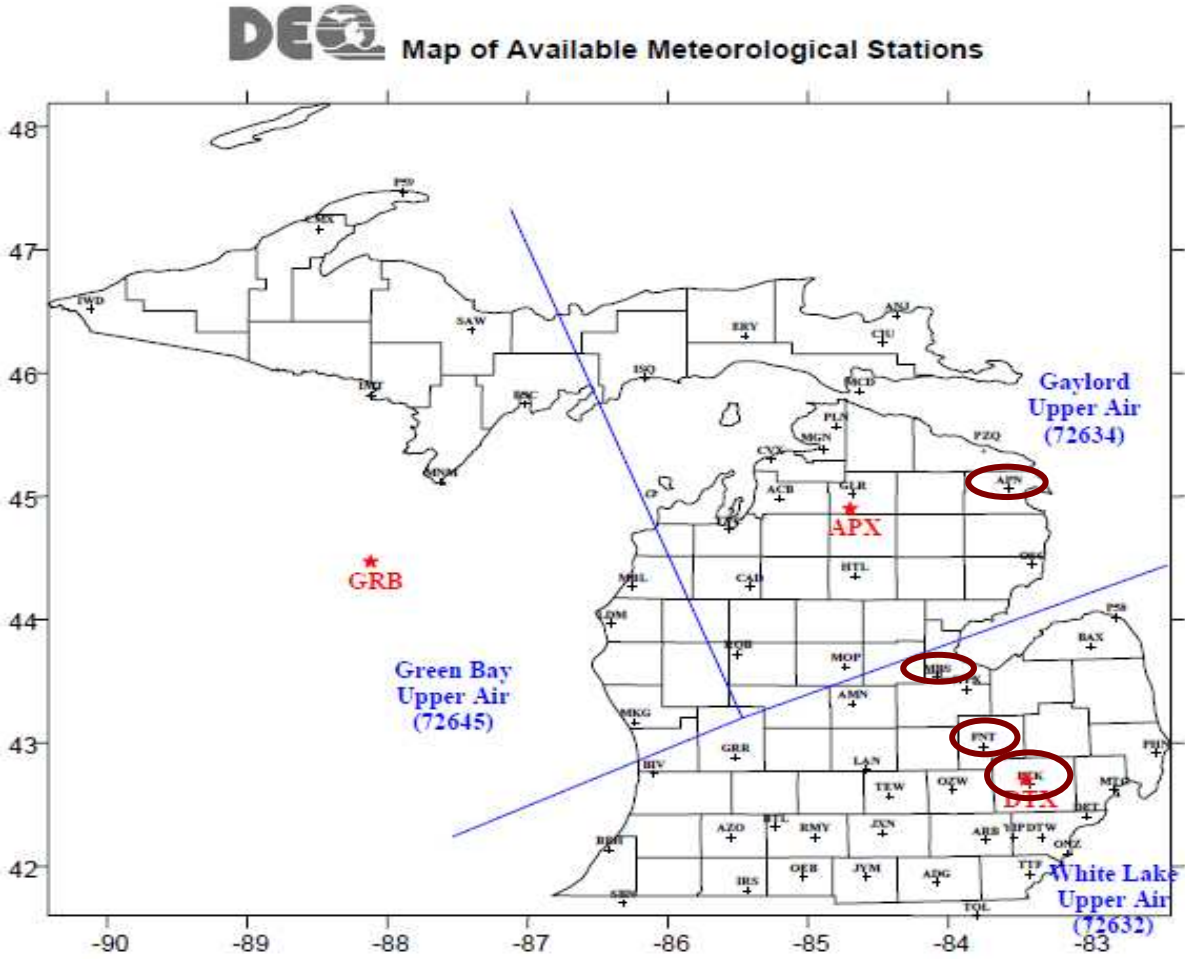

Figure 5.1. Meteorological data available at Michigan weather monitoring stations. All stations are denoted by their three letter abbreviated call sign. Stations in red are those for which upper meteorological data is available. Stations in brown circles are those used in the previous and current air dispersion models: Alpena (APN), Flint (FNT), Tri City (MBS) and Detroit (DTX).

Meteorological Data Preparation.

The meteorological data used in ISCST3 and AERMOD are largely different with respect to a number of input variables and formatting of meteorological data files. The AERMET meteorological data processor computed 25 variables, among which are friction velocity, Monin–Obukhov length, convective velocity scale, temperature scale, mixing height, and surface heat flux based on surface characteristics, cloud cover, an upper air sounding, and

a near-surface measurement of wind speed, wind direction, and temperature. Those attributes, together with the vertical profiling of temperature, wind and turbulence data are necessary to construct the depth of the planetary boundary layer (PBL) and to characterize the plume (5).

AERMOD's meteorological data processor AERMET generates two separate files describing surface and upper air while PCRAMMET, ISCST3's similar pre-processor creates a single meteorological data file. Common hourly surface variables between both models are: (i) wind direction, (ii) wind speed, (iii) temperature, (iv)surface roughness length, (v) Monin-Obukhov length, (vi) friction velocity and (vii) precipitation amount. Variables used only in ISC include hourly mixing height in rural and urban environments. Variables that are required for AERMOD include (i) height of convectively-generated boundary layer, (ii) height of mechanically-generated boundary layer, (iii) convective velocity scale, (iv) vertical potential temperature gradient, and (v) cloud cover, among others.

As ISCST3 is no longer used as a regulatory model, the data processed by PCRAMMET are no longer available from the Air Quality Department of MDEQ for the past three years*(26)*. In contrast, meteorological data processed by AERMET for AERMOD runs are provided by MDEQ on its website*(26)*. The department made these data available for all weather stations of Michigan (Figure 5.1) for a meteorological data set of 3 to 5 consecutive years, including the current year as for the purpose of air dispersion modeling. To model atmospheric deposition of incinerator emissions in the Midland region, the MDEQ recommends the use of weather data from MBS and DTX *(26)*.

Regarding the meteorological data collected at MBS and DTX during 2001-2006 for AERMOD run, which were different than the data we had at APN, FNT station during 1987-1991 for ISCST3 runs, the three following scenarios (1 to 3) were considered:

Scenario 1:

Scenario1 used meteorological data set of 1987-1991, which was in a compatible format for ISCST3 model from surface station in Alpena and upper air station in Flint. Surface meteorological data were from Alpena station, located at the north east side of Midland and the upper sounding data were of Flint station, located in the south of Midland. The timeframe encompassed 1987 to 1991 data availability from US.EPA and Lakes Environmental Software *(2, 31)*. The available data, however, were not in the required format for the wet and dry algorithm specifications in ISCST3, and had to be post-processed. Whereas surface air data files of some Michigan stations (including Alpena, but not Midland) were available for more than 5 consecutive years, mixing height data files derived from upper air soundings (Flint station) only for 1987-1991. The mixing height data of Flint station were compiled with the surface air data processed using PCRAMMET to generate inputs for the ISCST3 model. Since the upper air station in Flint stopped recording upper air soundings in 1999 (24), alternative station data needed to be considered. In Michigan, three upper air stations, Gaylord (APX), Detroit (DTX) and Sault Saint Marie (SSM) (red in Figure 5.1) currently record twice daily sounding data. Hourly mixing heights were interpolated from these recordings. We used the data

from the Gaylord station because of its geographic proximity to Midland and data availability during the period of choice for the modeling exercise (1987-1991).

Scenario 2 and 3:

Scenario 2 was implemented using ISCST3 model with meteorological data derived from MBS and DTX stations 5 consecutive years from 2002 to 2006. A five year meteorological data set is required for the regulatory air dispersion model *(2)*. The raw surface data and upper air data were processed using PCRAMMET to generate the inputs for the ISCST3 model. The ISCST3 model predictions using meteorological data from the MBS and DTX stations allow for a transition in comparing dioxin deposition estimates between scenarios following the change in weather stations and the change from the ISCST3 model to AERMOD model. The shift in the 5-year time frame (2002-2006) from scenario 2 to scenario 3 (2001-2005) was necessary because the raw sounding records are missing for the first three days in 2001. Missing data are not acceptable in the hourly mixing height interpolation specifications for the PCRAMMET processor. In order to ensure a complete dataset for 5 years, we collected raw meteorological data from the first day of the year 2002 to the last day of the year 2006.

Scenario 3 was conducted using the AERMOD air dispersion model with the meteorological data set available at MDEQ website from 2001-2005*(26)*. The weather data for this scenario are from 2001-2005, the time when the University of Michigan Dioxin Exposure Study (UMDES) was conducted in Midland, Saginaw and Jackson counties in Michigan. Meteorological data are processed by MDEQ using the surface air

data of the Midland-Saginaw-Bay airport's weather station (MBS) and the upper air soundings of White Lake station in Detroit (DTX).

In summary, meteorological data for scenario 1 and 3 were readily available, but not for scenario 2. The methodology to obtain meteorological inputs for PCRAMMET processing for the ISCST3 model in scenario 2 includes the following steps:

(1) Use data available from http://www.webmet.com and http://www.epa.gov/scram001 (as in scenario 1*(22, 23)*).

(2) Obtain raw surface data from the "Integrated Surface Database" of the National Climatic Data Center (NCDC) at http://lwf.ncdc.noaa.gov/oa/ncdc.html. Data are in GMT instead of Local Standard Time therefore we add an extra day accounting for this fact *(32)*.

(3) Use NCDC_CNV software developed by Russell Lee Consulting *(33)* to convert the raw surface air data into a readable format for ISC and AERMOD

(4) Surface air data files in the appropriate format (e.g. SAMSON) are provided by the MDEQ *(18)* for stations of Alpena and Midland-Saginaw-Bay (MBS). We used the SAMSON format of the MBS surface data as inputs for PCRAMMET.

(5) Download upper air data from the radiosonde database at http://www.raob.fsl.noaa.gov *(34)*.

(6) Upper air data are run through MIXHTR program *(25)* to obtain hourly mixing height data file for each year of the 5 year set.

(7) Run PCRAMMET processor using mixing height files and SAMSON surface files. Site-specific characteristics are required to produce output files for dry/wet deposition to be implemented in ISCST3.

Air dispersion modeling. The previous and current regulatory air dispersion models (ISCST3 and AERMOD) are used to predict air concentrations values, as well as total deposition flux values (both dry and wet) on a receptor grid for the period 2001-2006 (except for scenario 1). ISCST3 is a steady-state Gaussian dispersion model, which considers a Gaussian dispersion plume both in horizontal and vertical direction. AERMOD treats the plume similar to the ISCST3 model only under stable condition (at night, between sunset and sunrise when mixing is stable and not significant). Under unstable condition between sunrise and sunset, AERMOD regards the plume as bi-Gaussian, a probability distribution function in vertical direction *(35)*. All three scenarios employ the same receptor grid, comprising of four nested receptor grids that get coarser further away from the plant property line: 50 m (around the plant property and up to 1,000 m), 100 m (1,000 to 5,000 m range), and 500 m (5,000 to 10,000 m range) (Figure 5.2).

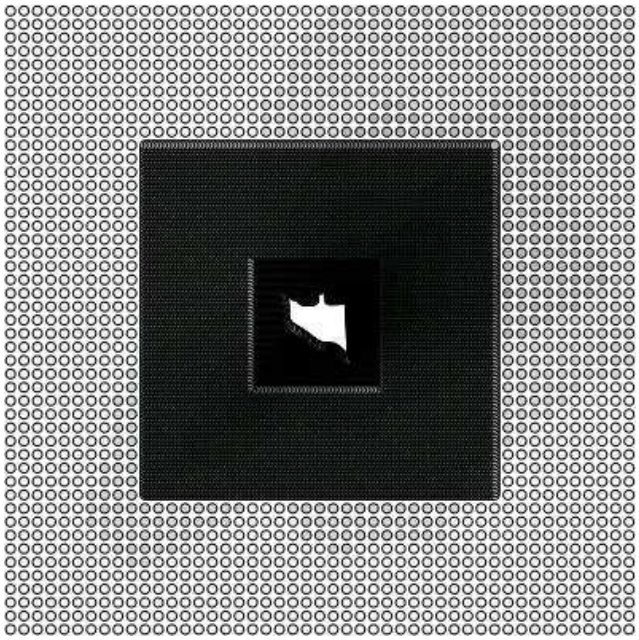

Figure 5.2. Three nested grids of receptors, including fine grid with spacing of 50 m out to 1 km; medium grid with spacing of 100 m out to 5 km and coarse grid with spacing of 500 m out to 10 km away from the plant incinerator. Plant boundary is in white at the centre of the receptor grid.

Aside from the differences in meteorological inputs discussed in the previous section, the other model inputs for each scenario are kept the same as that of scenario 1, assuming an emission rate of 0.126 gram/second*(20)*. The characteristics of the Dow historical hazardous waste incinerator are found elsewhere*(20)*.

Data comparison. The outputs of ISCST3 and AEMOD are air concentrations (in μg/m^3) and deposition fluxes (dry, wet and total depositions, in g/m^2/yr) of TEQ dioxins. The results from the three scenarios are visualized using a commercial visualization product, TerraSeer STIS *(36)*. Air concentrations and deposition fluxes of the various scenarios are paired to allow for a side by side comparison using a quantile-

quantile plot, in which the quantiles of the first data set are graphed against the quantiles of the second data set *(37)*. A quantile is the fraction (or percent) of points below a selected value on the cumulative distribution function. Quantiles of each comparison variable are calculated and plotted by SigmaPlot software *(38)*.

5.3. Results and Discussion

Air Dispersion. Figure 5.3(a-c) shows the air concentration estimated by ISCST 3 for scenario 1 and 2 and by AERMOD for scenario 3. The map visually displays different spatial patterns of particulate TEQ in the air. The dispersion plume of scenario 1, in which surface air data are obtained from the Alpena station, and mixing heights are from the Flint station, spreads widely over the North and South-East side of the Dow plant (at the center of the map). The maximum air concentration in scenario 2 is the highest (10.76), followed by that of scenario 3 (10.58) and of scenario 1 (8.04) (Table 5.1).

Table 5.1. Data statistics of air concentrations predicted for scenario 1, 2 and 3.

Air Concentration	**Scenario 1**	**Scenario 2**	**Scenario 3**
Size	24258	24258	24258
Mean	3.59	3.43	1.94
Std Dev	1.70	2.04	1.35
Std. Error	0.011	0.013	0.009
C.I. of Mean	0.021	0.026	0.017
Range	8.04	10.69	10.29
Max	8.04	10.76	10.58
Min	0	0.06	0.29
Median	3.32	2.94	1.53
25th percentile	2.25	2.01	1.01
75th percentile	4.8	4.31	2.46

The plume in scenario 2, which used meteorological input data from Midland-Bay-Saginaw airport (MBS) and from Detroit (DTX) disperses mainly to the North-East side of the property. The plume also exhibits elevated concentrations relative to scenario 3. In the last scenario, the use of local meteorological conditions (Midland-Bay-Saginaw surface data) results not only in a change in plume direction, to the South- West side of the plant (scenario 1) but constrains the dispersion within the fine receptor grid out to 1 km from the plant. The air concentrations range from 0.3 to 10.3 ng/m^3air with a mean of 0.29 ng/m^3air (Table 5.1).

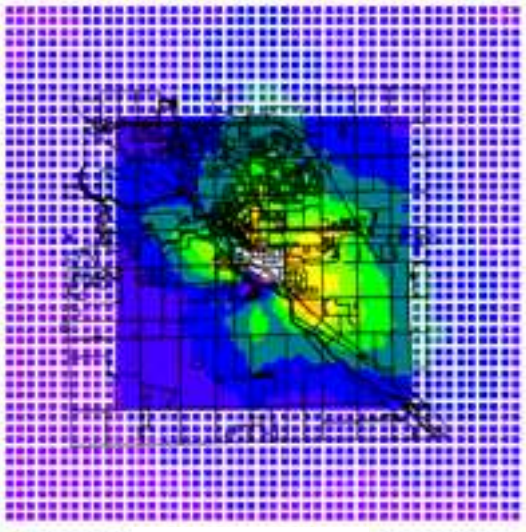

(a) Scenario 1

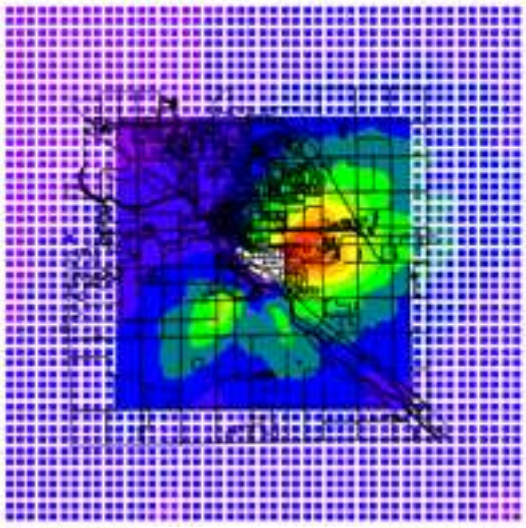

(b) Scenario 2

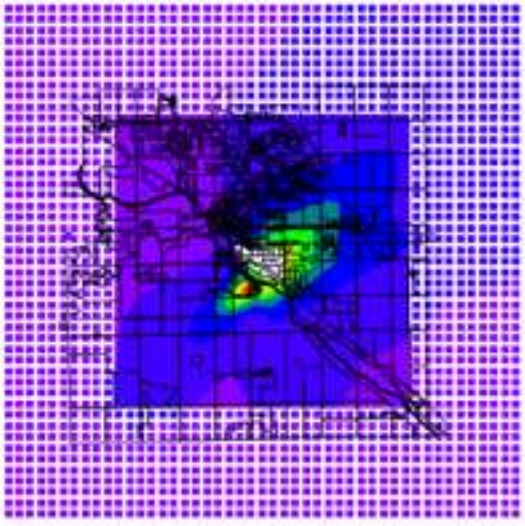

(c) Scenario 3

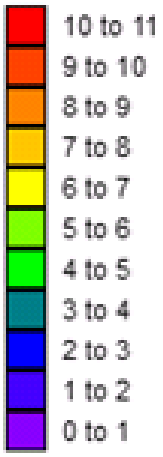

Figure 5.3. (a) Maps of TEQ air concentration (ng/m^3) predicted by the ISCST3 with meteorological data from surface station in Alpena (APN) and upper air station in Flint (FNT) during 1987-1991 and (b) with data from surface station in Midland-Saginaw-Bay airport (MBS) and upper air station in Detroit (DTX) during 2002-2006; (c) map of air concentration (ng/m^3) predicted by AERMOD with meteorological data from MBS surface station and DTX upper air station during 2001-2005. The receptor grid is nested with grid spacing=50m, 100 and 500 m for distances from property line= 1km, 1-5km, and 5-10 km. No receptors are assigned within the property lines. Background layer is the road network for Midland County.

In an attempt to explain the directional changes of the plume, wind directions and wind speeds are plotted in Figure 5.4. Wind direction and wind speed in scenario 2 and 3 were mostly identical as they are of the same station (MBS) except for 1 year difference in the 5 year data set. The winds were mainly in the North-East direction. Given that the location of the MBS airport is just few miles south of Midland, the wind direction is relevant to the city. On the contrary, the prevailing wind direction recorded at Alpena range from NE to SE (figure 5.4a), and are reflected in the dispersion plume.

There is a strong correlation between prevailing wind direction and the shape of the dispersion plumes observed in the three scenarios. In assessing the impact of meteorological inputs to performance of ISCST3 and AERMOD, Faulkner et al.*(10)* concluded that wind speed, temperature, solar radiation, and mixing heights below 160 m are sensitive parameters for the ISCST3 model, while albedo, surface roughness, wind speed, temperature, and cloud cover are sensitive for AERMOD case. The sensitivity analysis was conducted in a flat terrain near Amarillo, Texas using particulate matter (PM) as the modeled pollutant. Wind speed and direction are indeed an important attribute to air dispersion model in predicting air concentration of SO_2 as found in a study in tropical area, where different meteorological data scenarios were assessed*(12)*. Considering this strong relationship, scenarios 2 and 3 are assumed to more closely reflect the actual TEQ dispersion plume.

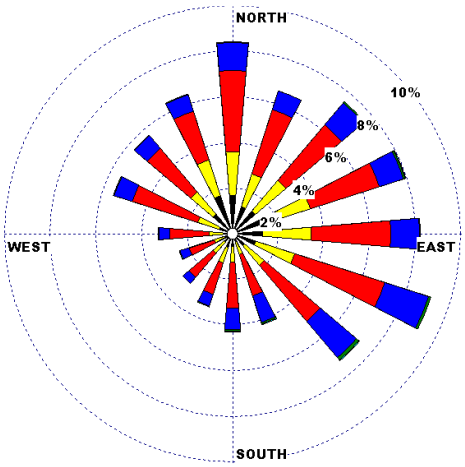

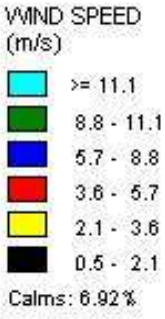

(a) Scenario 1

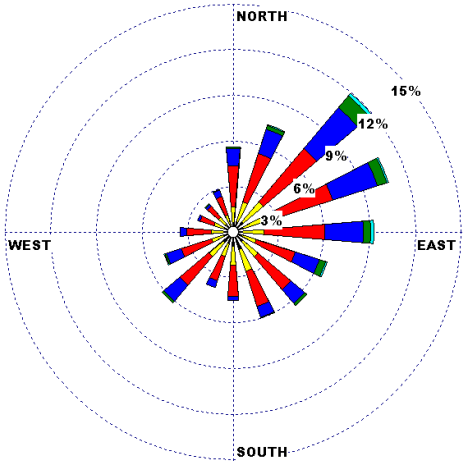

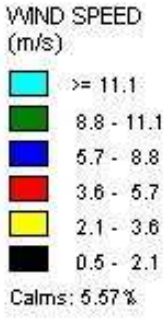

(b) Scenario 2

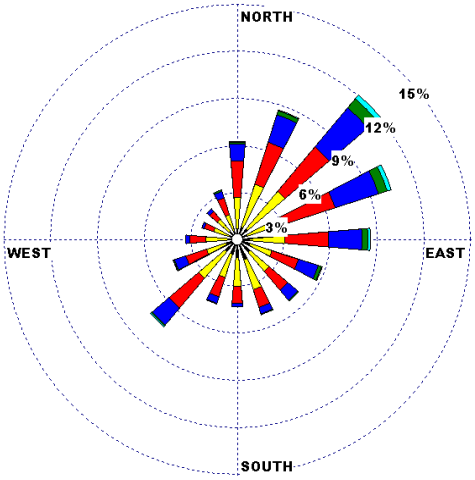

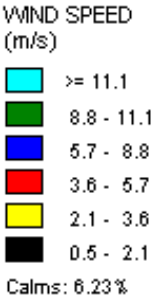

(c) Scenario 3

Figure 5.4(a-c). (a) Wind roses illustrate the wind flow vector (blowing to) and wind speed (m/s) recorded in the meteorological data for ISCST 3 model (scenario 1 of 1987-1991 at Alpena station and scenario 2 of 2002-2006 at MBS station) and for AERMOD model (scenario 3 of 2001-2005 at MBS station).

Dioxin Depositional Fluxes. Five-year dry and wet deposition fluxes predicted by the dispersion models are shown in Figure 5.5(a-c) and 5.6(a-c).

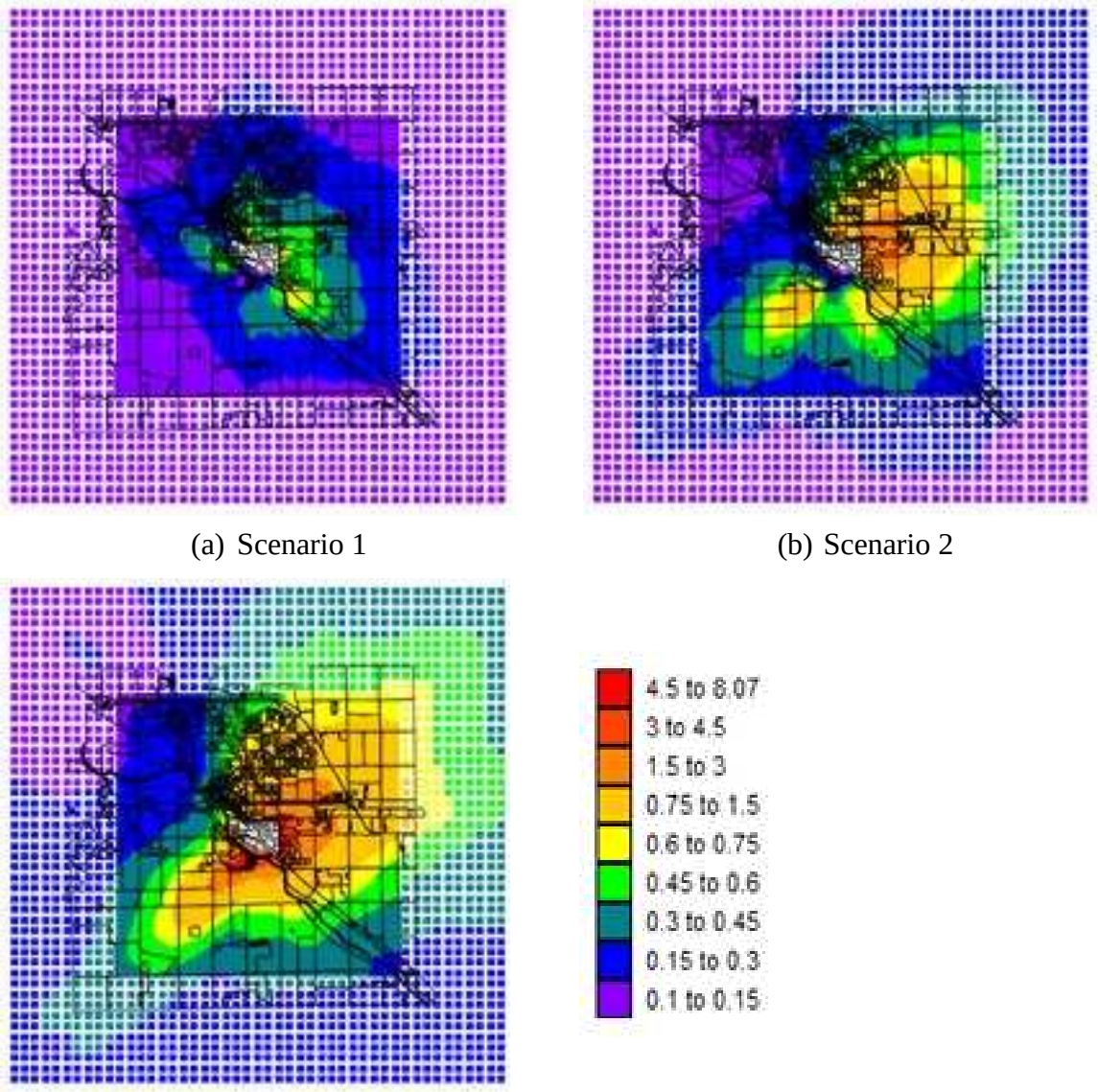

(a) Scenario 1

(b) Scenario 2

(c) Scenario 3

Figure 5.5(a-c). (a) Maps of 5 year dry deposition flux (mg/m^2) predicted by the ISCST3 with meteorological data from surface station in Alpena (APN) and upper air station in Flint (FNT) during 1987-1991 and (b) with data from surface station in Midland-Saginaw-Bay airport (MBS) and upper air station in Detroit (DTX) during 2002-2006; (c) map of 5 year dry deposition flux (mg/m^2) predicted by AERMOD with meteorological data from MBS surface station and DTX upper air station during 2001-2005.

It is apparent that the dry deposition fluxes in scenario 3 are the highest and those in scenario 1 are the lowest. The concentration ranges within a factor of more than 3 (Figure 5.5(a-c), Table 5.2).

Table 5.2. Statistics of dry deposition fluxes (mg/m^2-5years) of scenario 1, 2 and 3.

Dry deposition flux	**Scenario 1**	**Scenario 2**	**Scenario 3**
Size	24258	24258	24258
Mean	0.27	0.58	1.03
Std Dev	0.15	0.48	0.99
Std. Error	0.00	0.00	0.01
C.I. of Mean	0.00	0.01	0.01
Range	0.75	2.61	7.97
Max	0.75	2.62	8.07
Min	0.00	0.01	0.10
Median	0.23	0.43	0.68
25th percentile	0.14	0.26	0.39
75th percentile	0.37	0.75	1.28

The highest values are found in the immediate vicinity of the plant. Similar observations have been made for PCDDs/PCDFs in ISCST3 modeling *(19, 22)* from an incinerator. The direction of the dry deposition plumes is similar to the directions of the dispersion plumes shown earlier. Lohmann and Jones*(39)*, in their review of air concentrations and deposition patterns, point to a study conducted at three sampling sites in Germany (Wallenhorst, 1996) that showed a similarity between air concentrations and depositions.

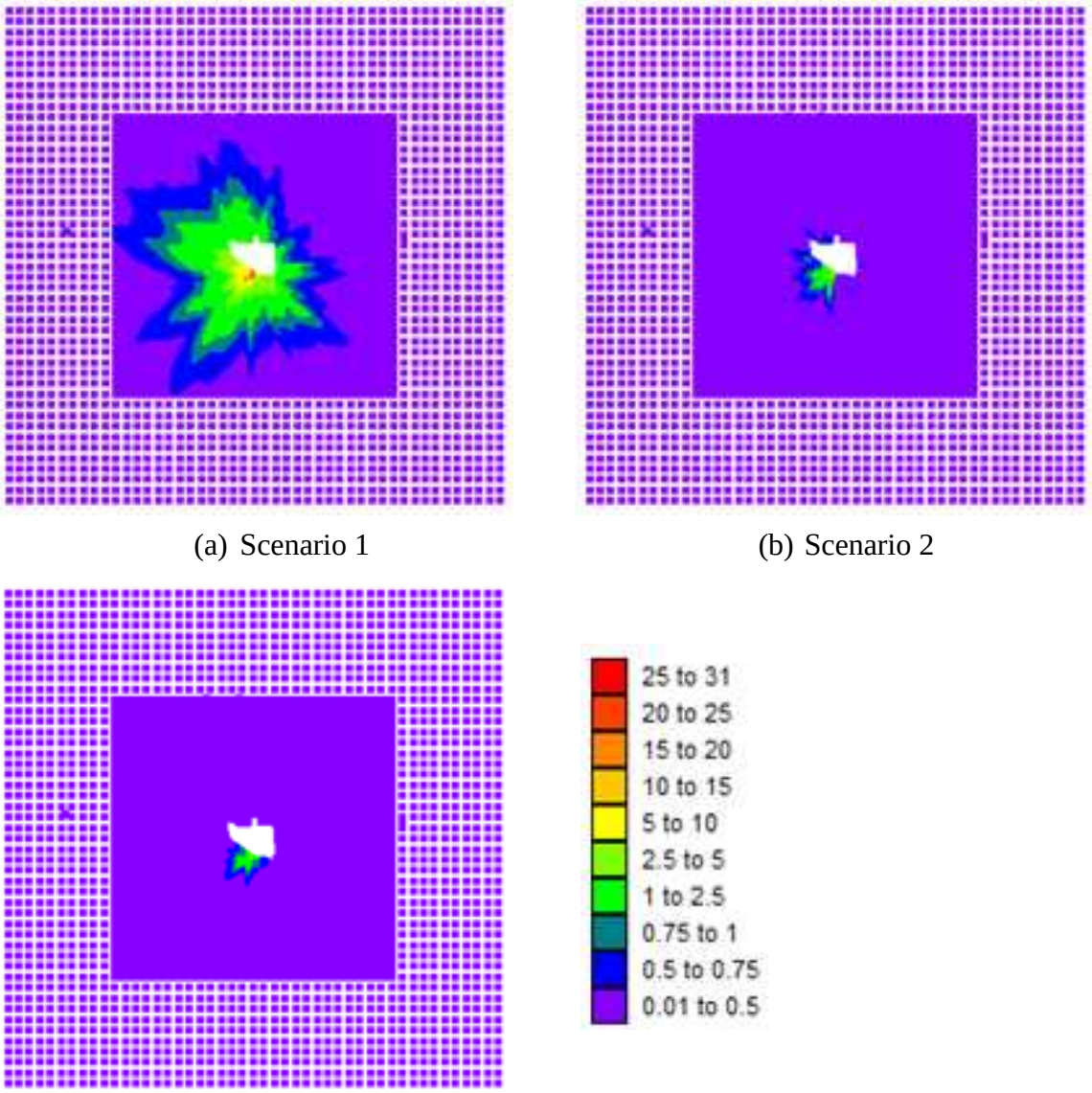

(a) Scenario 1

(b) Scenario 2

(c) Scenario 3

Figure 5.6(a-c). (a) Maps of 5 year wet deposition flux (mg/m^2) predicted by the ISCST3 with meteorological data from surface station in Alpena (APN) and upper air station in Flint (FNT) during 1987-1991 and (b) with data from surface station in Midland-Saginaw-Bay airport (MBS) and upper air station in Detroit (DTX) during 2002-2006; (c) map of 5 year dry deposition flux (mg/m^2) predicted by AERMOD with meteorological data from MBS surface station and DTX upper air station during 2001-2005. The road network of Midland County is omitted from the background for a better visualization.

As seen from Figure 5.6(a-c), wet deposition occurs in the close proximity and south-western side of the plant. The magnitude of the wet deposition flux is the highest among all scenarios and also surpasses the level of dry deposition for scenario 1. Although wet deposition has been observed to be the dominant pathway of removing dioxin from the air *(40)*, dry deposition appears to be the most important removal mechanism for dioxins in this situation and under the meteorological conditions in Midland *(12- 14)*. A summary table of precipitation intensity (Table 5.3) and wind roses from two stations located in Alpena and Midland-Bay-Saginaw (Figure 5.7) shows that the rain intensity observed in Alpena for scenario 1 during 1987-1991 was 0.04 mm/hour, while precipitation recorded in Midland for scenario 2 or 3 (although at only 42% data availability) during 2002-2006 was significantly lower, at an average of 0.01 mm/hour. Scenario 3 that used the same weather data at MBS, and thus would expect a low precipitation intensity as well. The wet deposition therefore was an important removal pathway of dioxins. However, due to the difference in specifics of the various meteorological stations (Alpena is in the far north of the plant versus Midland), the wet deposition in scenario 2 and 3 was lower than scenario 1. In fact, the dry deposition estimates in scenario 2 and 3 were about two orders of magnitude larger than the wet deposition fluxes.

Table 5.3 Summary of meteorological data used in scenario 1, 2 & 3.

	Scenario 1	**Scenario 2/3**
Year	1987-1991	2002-2006
Location	Alpena	Midland-Saginaw-Bay
Total number of hours	43824	43828
Average precipitation intensity	0.04 mm/hour	0.01 mm/hour
Dry hours	41760	18556
Dry hour frequency	97.51%	98.69%
Data availability	97.72%	42.90%
Number of hours used	42825	18802

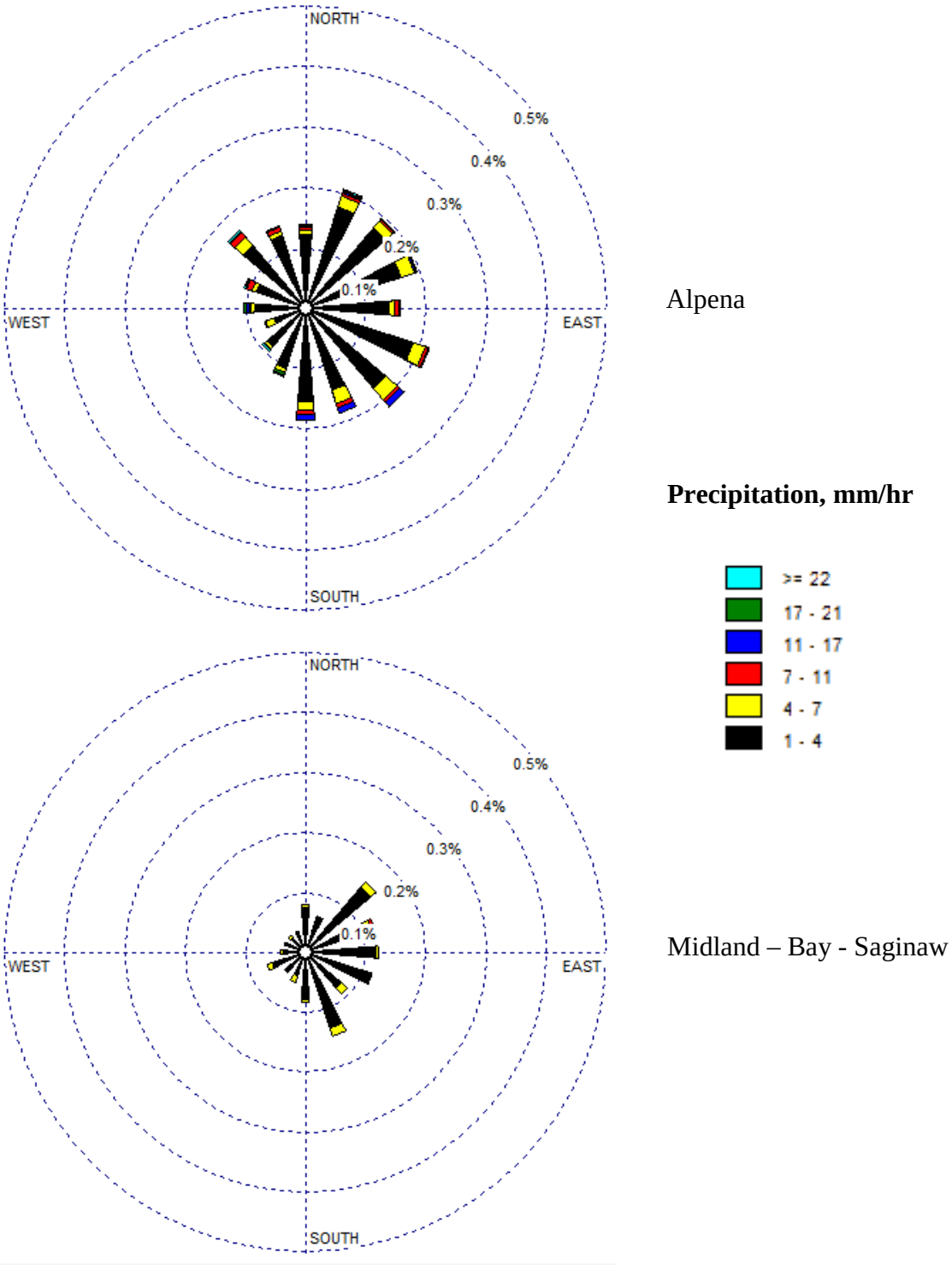

Figure 5.7. Rain rose recorded at meteorological station in Alpena (APN) (top) and at station in Midland-Bay-Saginaw (MBS) (bottom).

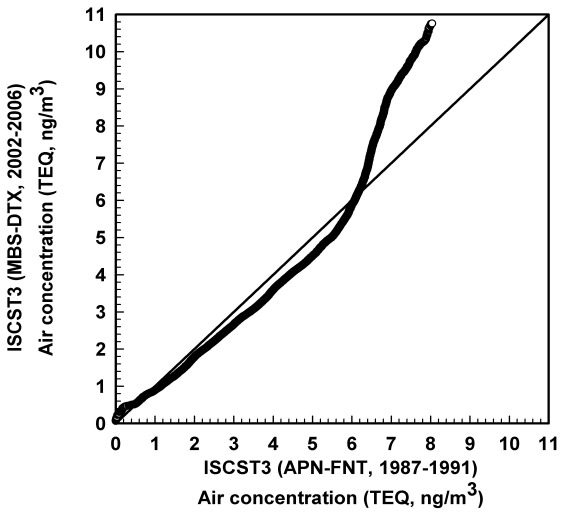

(a) Scenario 1 vs. scenario 2

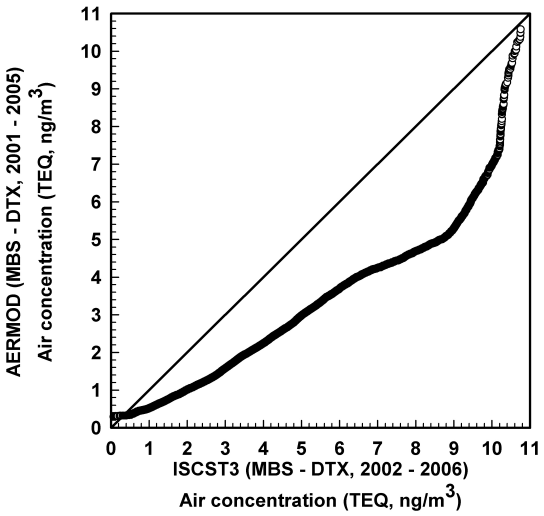

(b) Scenario 2 vs. scenario 3

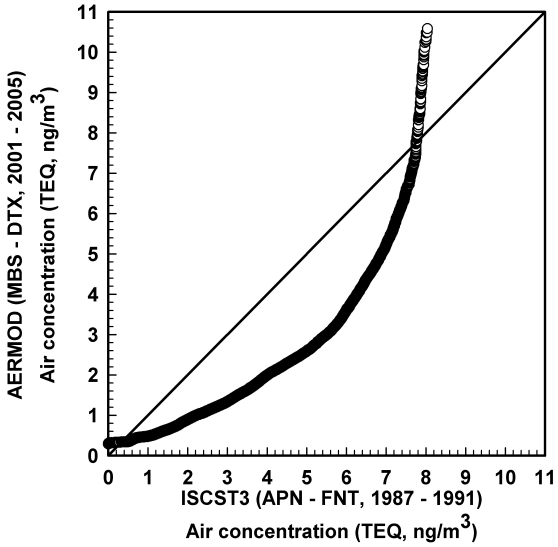

(c) Scenario 1 vs. scenario 3

Figure 5.8(a-c). (a) Q-Q plots of air concentration predicted in scenario 1 against that of scenario 2; (b) scenario 2 versus scenario 3 and (c) scenario 1 versus scenario 3.

It is of particular interest to compare model performances of ISCST3 and AERMOD to inform threshold values set by the regulatory agencies (*27*). A useful way to capture the high end tail of the distribution is by way of a Q-Q plot. A Q-Q plot is a graphical tool in which quantiles of one distribution (as read from X-axis) are plotted against the same quantiles of the other distribution (as read from the Y-axis). The units displayed on the two axes are actual values of the two distributions of scenario predictions from AERMOD and ISCST3, as in this study. Thus, for a given point on the Q-Q plot we know the value of each distribution at the same frequency. Data points that fall along the 45^{o} reference line indicate that the two distributions are similar.

The two distributions in Figure 5.8a are similar up to a value of 6 ng/m^3, indicating that the ISCST3 model with MBS/DTX data predicts much higher values at the right tail of the distribution. There is indeed a wide range of high values in air concentration estimated in scenario 2. When compared against scenario 3 (Figure 5.8b), the two distributions are completely different. Values of scenario 2 are consistently higher than those of scenario 3 for the same quantiles. However, the difference narrows down at the high end of the two distributions. ISCST3 was also found to overpredict the true observations as compared to AERMOD which slightly underpredicted the true observations of tracer SO_2 for the flat and rural terrain in Prairie Grass, Nebraska and Indianapolis*(6)*.

The Q-Q plot of air concentrations in scenario 1 versus scenario 3 demonstrates an obvious dissimilarity in the two distributions. The differences are mainly due to the differences in the model specifications of ISCST3 and AERMOD, and to a lesser extent because of the meteorological data used (APN/FNT vs. MBS/DTX). Indeed the changes

occur even in the range where the differences in meteorological data alone do not have an impact. The air concentrations predicted by ISCST3 are higher than predictions of AERMOD in the entire concentration distribution at the same location with the same source of meteorological data (Midland) (Figure 5.8c).

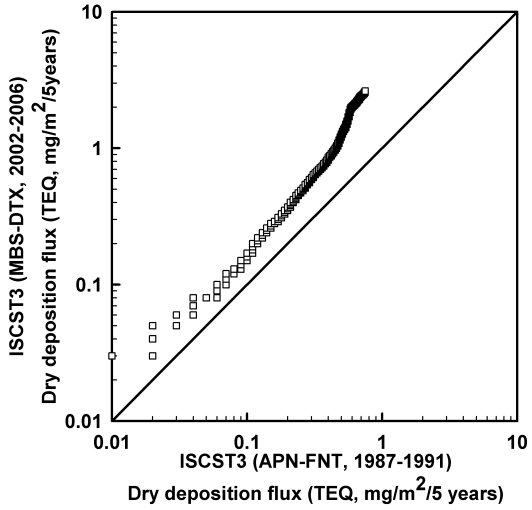

(a) Scenario 1 vs. scenario 2

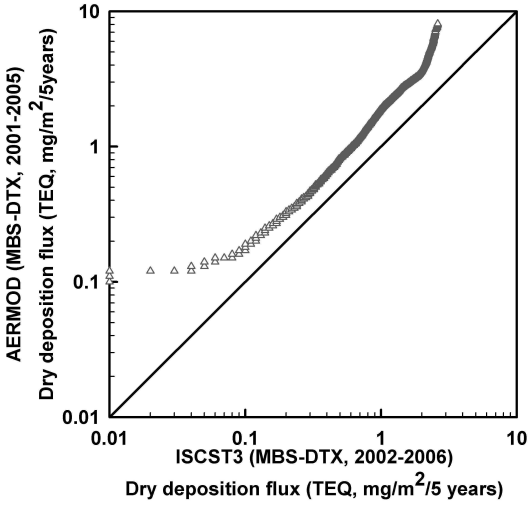

(b) Scenario 2 vs. scenario 3

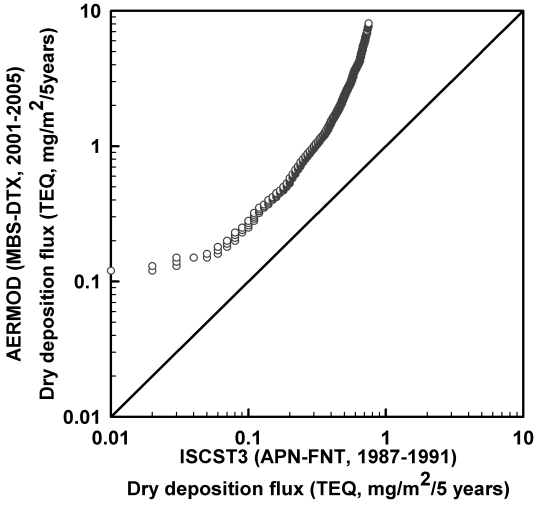

(c) Scenario 1 vs. scenario 3

Figure 5.9(a-c). (a) Q-Q plots of dry deposition flux predicted in scenario 1 against that of scenario 2; (b) scenario 2 versus scenario 3 and (c) scenario 1 versus scenario 3.

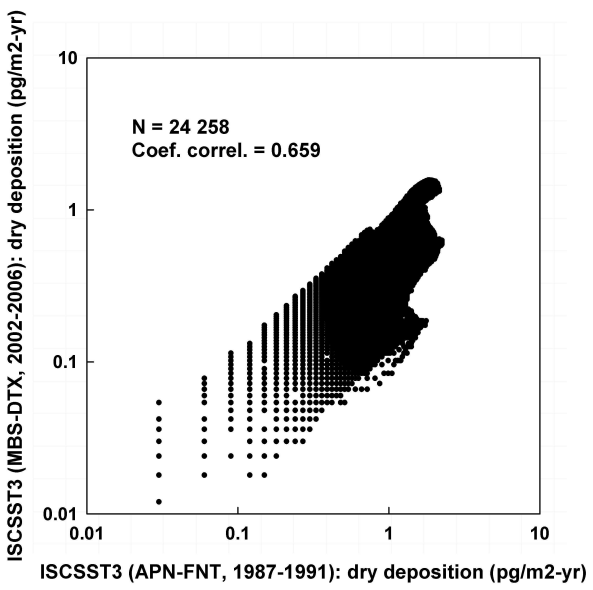

(a) Scenario 1 vs. scenario 2

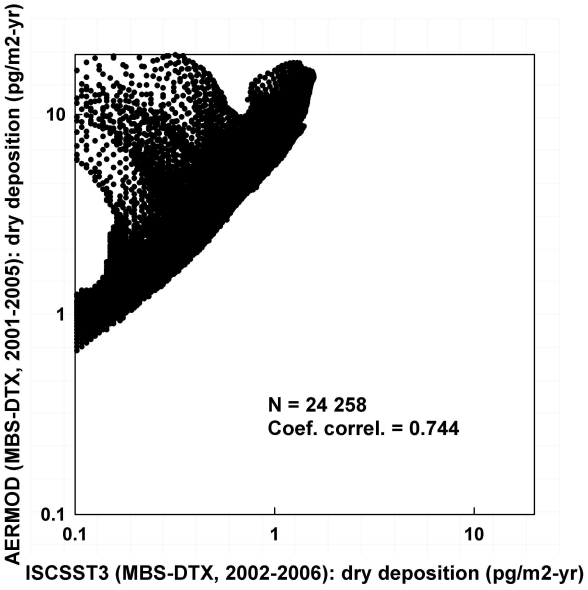

(b) Scenario 2 vs. scenario 3

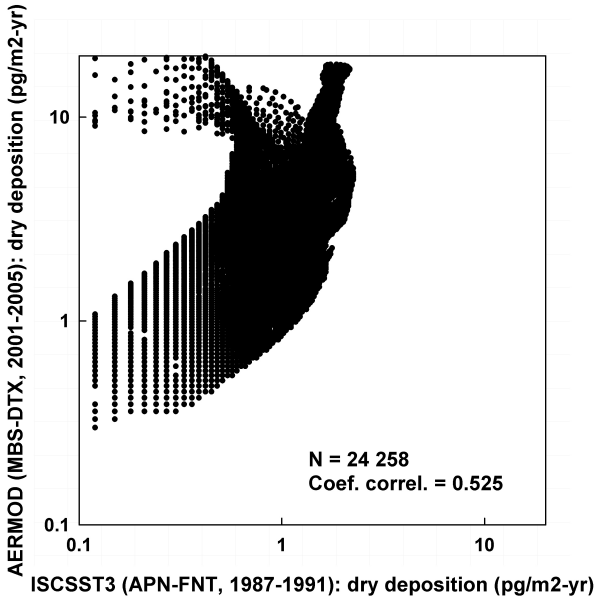

(c) Scenario 1 vs. scenario 3

Figure 5.10(a-c). (a) Scatter plots of dry deposition flux predicted in scenario 1 against that of scenario 2; (b) scenario 2 versus scenario 3 and (c) scenario 1 versus scenario 3.

When dry deposition fluxes are quantified (Figure 5.9a-c), we observed that AERMOD generally overpredicts dry deposition fluxes relative to ISCST3 (also seen in Figure 5.5(a-c)). This is curious, considering that, as described in an AERMOD supporting document*(41)*, the deposition algorithms in AERMOD are based on the deposition algorithms developed for ISCST3 by Wesely et al. *(42)*. Hence, the outcomes of deposition fluxes predicted by ISCST3 and AERMOD for the same model inputs would be expected to be the same in scenario 2 and 3. Figure 5.9b however shows that AERMOD consistently over predicted ISCST3 in dry deposition fluxes. A possible reason is in the postprocessing of available meteorological data by MDEQ for AERMOD from 2001-2005 (scenario 3) and by us for scenario 2 ISCST3. For example, as shown in Table 5.2, the ISCST3 compatible meteorological data formatting was based on 42% data availability, meaning the missing number of data hours was significant. Meanwhile, MDEQ provided us the AERMOD compatible meteorological data at 100% of data availability. The mixing height interpolation in our data processing might contribute to the difference in meteorological data outputs. A derived parameter such as surface roughness length, for example is very sensitive to the model *(10, 43, 44)*. The computed surface roughness values in scenario 2 in fact were different compared with the standard values in scenario 3, leading to the difference in dry deposition fluxes as seen in Figure 5.9b between these two scenarios. As for Figure 5.9a and Figure 5.9b the different meteorological data due to the selection of weather stations (Alpena, Flint versus MBS and Detroit) clearly affects the deposition fluxes.

As a result, precipitation density at those stations represents a big contribution on predictions of wet deposition fluxes in scenario 1 versus 2 and 3 (Figure 5.11a and Figure 5.11c). Meanwhile, wet deposition fluxes predicted by ISCST3 and AERMOD (Figure 5.11b) were found to be more similar as expected as the models adopted the same wet deposition formulations. The minor difference is due to differences in meteorological data processing.

Correlations between wet depositions among these scenarios also reflected similar observations seen in scatter plots (Figure 5.12): the highest correlation coefficient (R^2 = 0.909) resulted between scenario 2 and 3 for the same modeling site (Figure 5.12b); the second highest correlation coefficient (R^2=0.886) was between scenario 1 and 3 (Figure 5.12c). Correlations among wet depositions in these scenarios were higher than those relations among dry depositions (Figure 5.10 (a-c)).

.

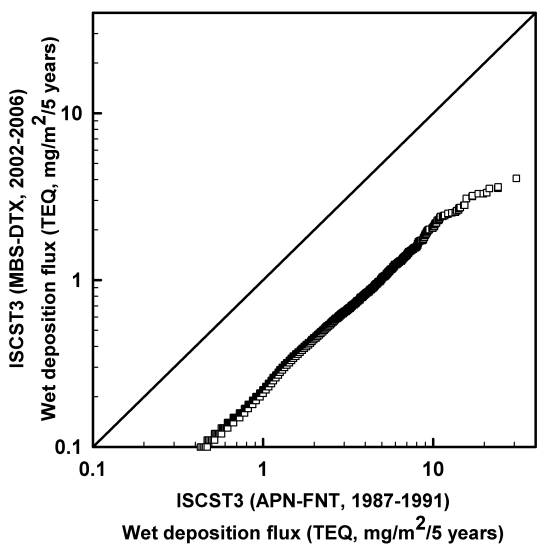

(a) Scenario 1 vs. scenario 2

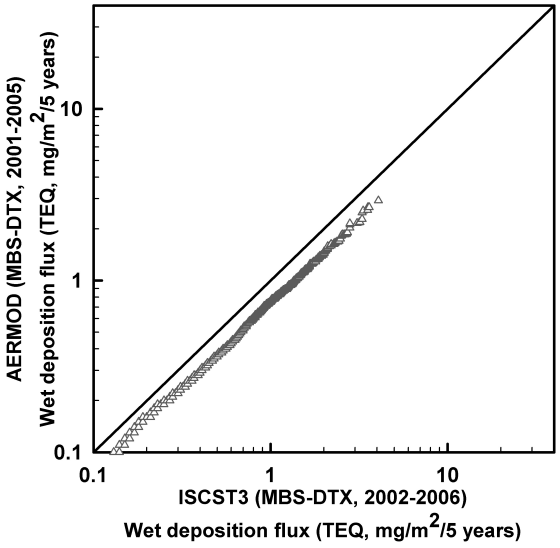

(b) Scenario 2 vs. scenario 3

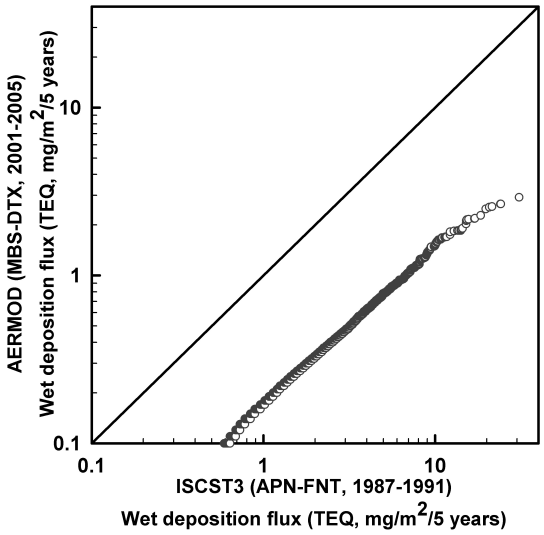

(c) Scenario 1 vs. scenario 3

Figure 5.11(a-c). (a) Q-Q plots of wet deposition flux predicted in scenario 1 against that of scenario 2; (b) scenario 2 vs. scenario 3 and (c) scenario 1 vs. scenario 3.

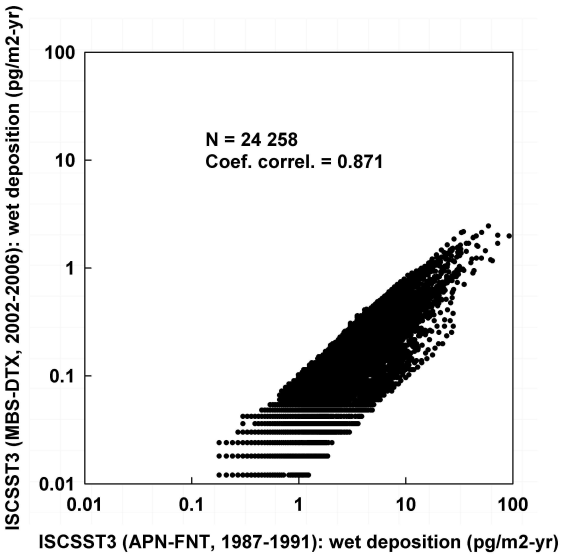

(a) Scenario 1 vs. scenario 2

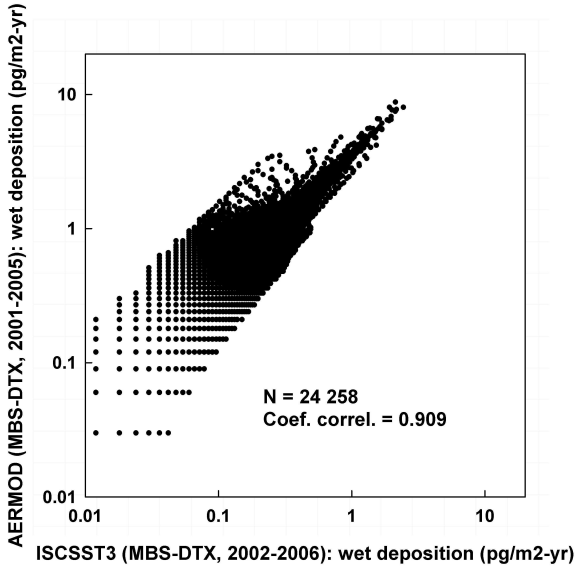

(b) Scenario 2 vs. scenario 3

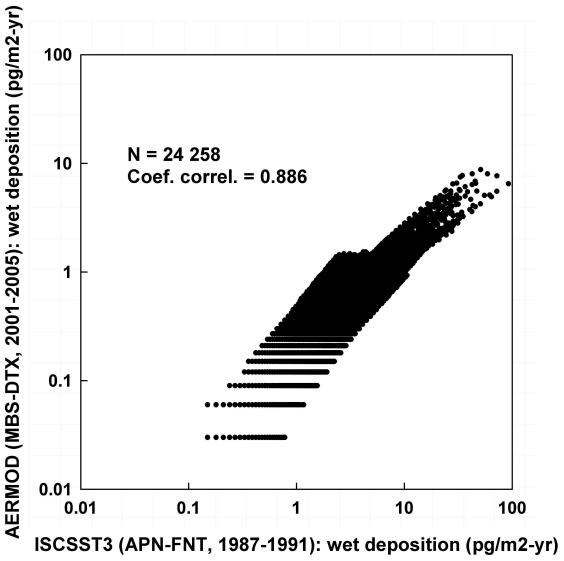

(c) Scenario 1 vs. scenario 3

Figure 5.12(a-c). (a) Q-Q plots of wet deposition flux predicted in scenario 1 against that of scenario 2; (b) scenario 2 versus scenario 3 and (c) scenario 1 versus scenario 3.

It is of interest to assess whether the correlation between predicted and measured soil concentrations is improved when using scenario 2 and 3. TEQ values predicted from the coupled ISCST3-geostat model used 53 soil samples from the Michigan Department of Environmental Quality dioxin soil sampling events (MDEQ; ref to Goovaerts paper?). The TEQ predictions were compared to the 51 measered soil samples collected during the University of Michigan Dioxin Exposure Study (UMDES) field campaign (*20, 21*). Figures 5.13 (a,b) represent histograms of these two data sets, (MDEQ 53) and (UMDES 51). The two distributions are both skew right with maximum values of 450 ppt TEQ (of MDEQ set) and of 920 ppt TEQ (of UMDES set).

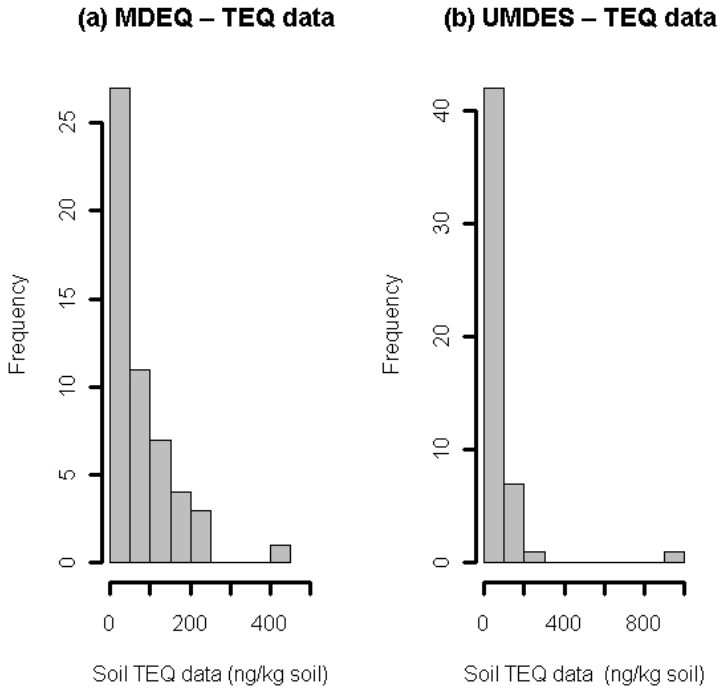

Figure 5.13 (a-b). Histograms of available soil TEQ data from (a) the Michigan Department of Environmental Quality (MDEQ-TEQ, 53 samples) and (b) the University of Michigan Dioxin Exposure Study (UMDES-TEQ, 51 samples) in Midland.

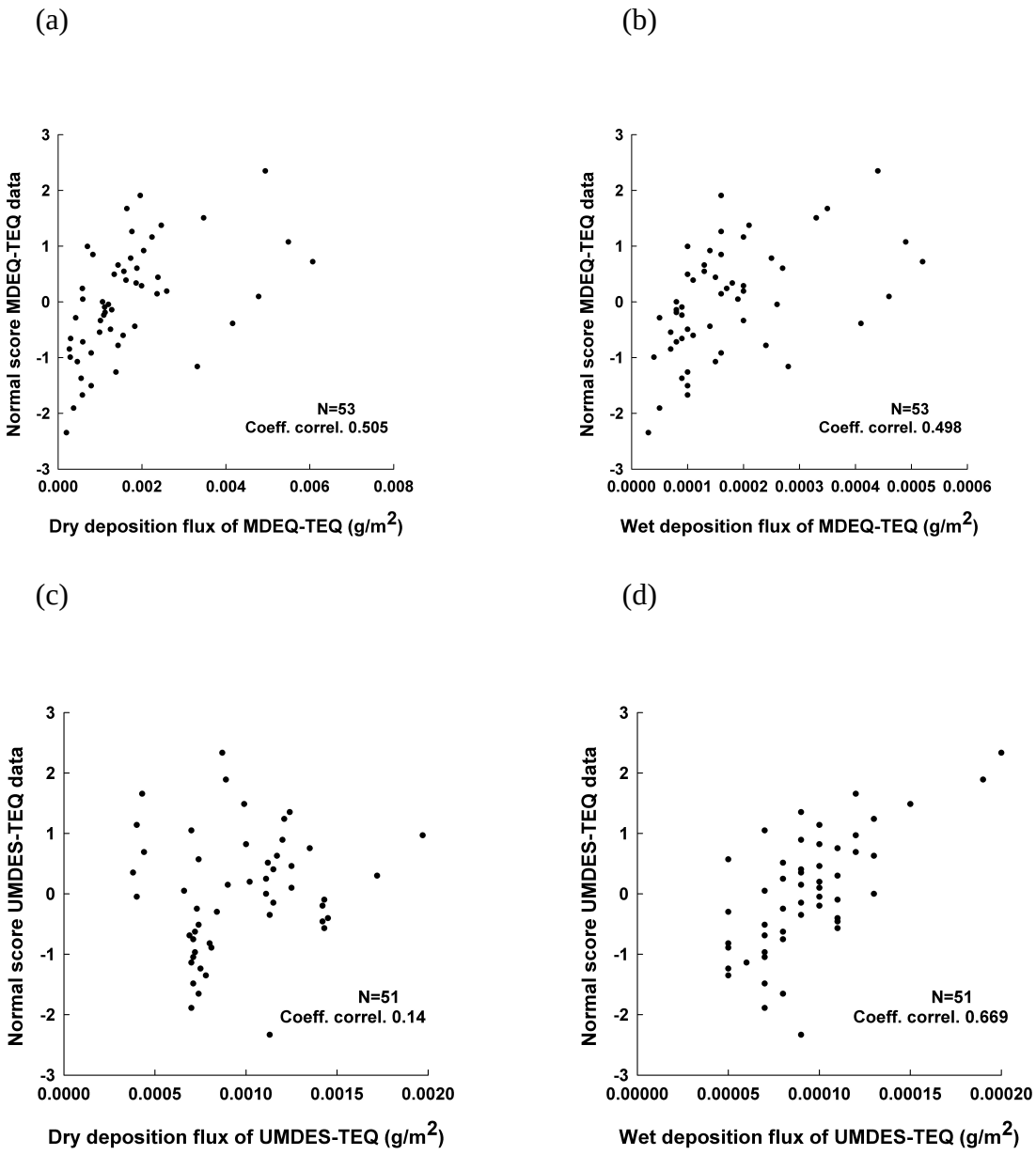

Figure 5.14 (a,b,c,d). Scatter plots of dry (a,c) and wet (b,d) deposition flux predicted by ISCST3 versus normal score transformations of MDEQ-TEQs data and UMDES-TEQs.

When the wet deposition flux predicted by AERMOD was plotted against the normal score transformations of UMDES-TEQ data, the correlation coeffiecient was the highest ($R^2 = 0.669$). Dry deposition flux has no correlation with soil data (Figure 5.14

(c,d)). In the case of ISTST3 prediction, dry deposition fluxes were correlated with the MDEQ-TEQ measurements (Figure 5.14 (a,b)). When the total fluxes estimated by ISTST3 and AERMOD were regressed against UMDES and MDEQ data, the correlation coefficients were similar (0.44 vs. 0.41). Deposition fluxes predicted by AERMOD did not improve the correlation with soil measurements which may be due to the differences in TEQ data sets (MDEQ and UMDES). In addition, since the UMDES soil samples were taken preferentially in the north of the Dow plant, where the majority of the population resides, the data set is regionally-biased.

The results from ISCST3 and AERMOD predictions coupled with geostatistical models were validated at 51 receptor nodes closest to the locations of 51 UMDES soil sampling data (less than grid node spacing of 50 feet) using 100 realizations of TEQ predictions at each of these receptors. Figure 5.15 shows the boxplots of these 100 realizations at each validating location,. When the 51 boxplots simulated by ISCST3-geostat (scenario 1) were overlain onto 51 boxplots simulated by AERMOD-geostat (scenario 3), a comparison could be made between both models. The UMDES soil data at these locations are shown as triangles on the same figure. The figure shows that the simulated TEQ distribution at each location was capable of capturing the true soil TEQ for most locations in both scenarios.

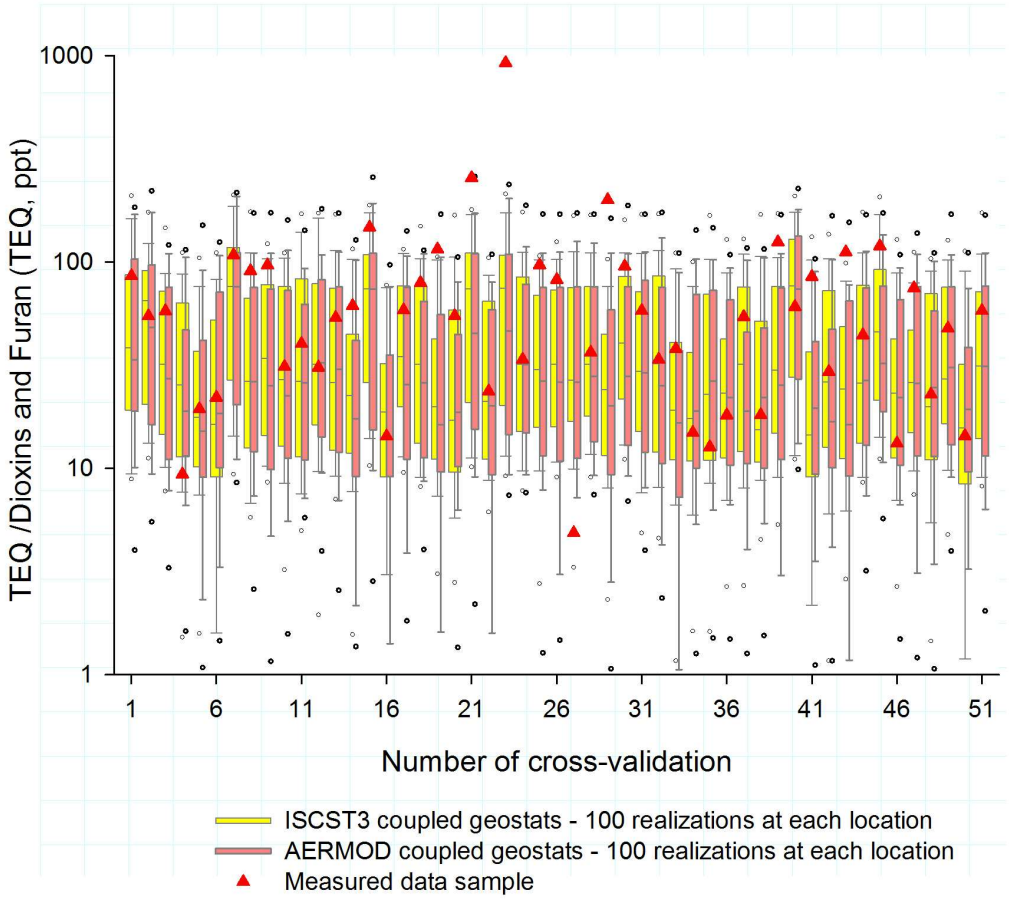

Figure 5.15. Boxplots of 100 TEQ simulated values resulted from ISCST3-geostat model (scenario 1) and AERMOD-geostat model (scenario 3).

The capability of the distribution to capture the true values measured using different probability intervals (PI) of the 100 realization distribution: the 0.1-PI ranges between the 45th and 55th percentile; 0.2-PI, a range between 40th and 60th percentiles; and p-PI, a range bounded between (1-p)/2 and (1+p)/2 percentiles. To quantitatively evaluate whether the true measurements fall within the PIs, the empirical PIs based on the real data were plotted against the theoretical PIs, to yield a probability plot (Figure 5.16). A model is said to be accurate if the fraction of the true values that falls into a *p*-PI is

equal or greater than *p (45)*. For example, at 0.5-PI a model is accurate if the fraction of the true values between the 25th and 75th percentile across all total available validated samples is greater than 50%. At all p-PIs, the numbers of true values that fall into these probability intervals exceeded what we would expect.

For the prediction to be accurate, the scatter points at each p-PI on figure 5.16 need to be above the 45 degree line. However, for the prediction to be precise, the points need to be as close to the line as possible. Based on the goodness of fit for theAERMOD-geostat model, there was only minor improvement compared to ISCST3-geostat model predictions.

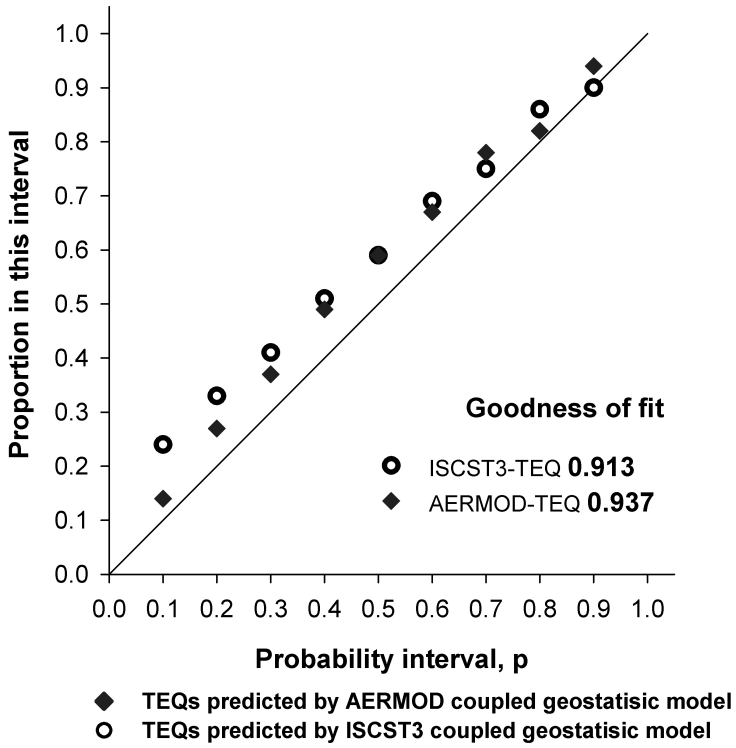

Figure 5.16. Probability plot of TEQ predictions by ISCST3-geostat and AERMOD-geostat model.

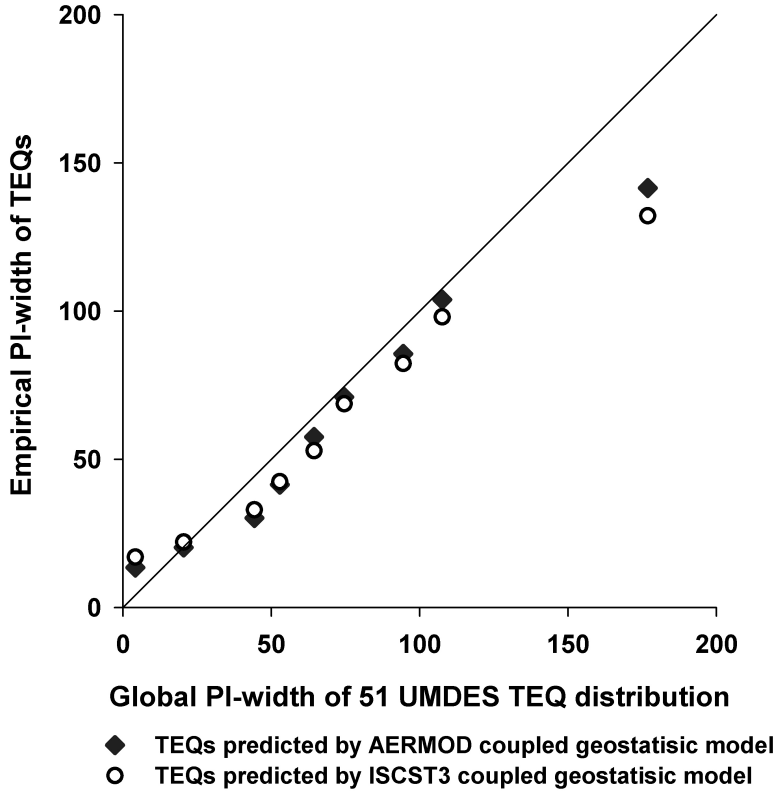

Figure 5.17. Accuracy plot of TEQ predictions by ISCST3-geostat and AERMOD-geostat model.

It was also noticed that the predicted TEQs are less uncertain than the 51 soil measured data because the empirical PI-widths of TEQs predictions are narrower than the PI-width of the distribution of the original 51 UMDES data (Figure 5.17).

5.4. Conclusions

Is was observed that the air concentrations and deposition fluxes predicted by AERMOD using on-site meteorological data (MBS, DTX) were different than the results obtained by Goovaerts et al (2008)*(20)* using ISCST3. In the AERMOD application, dry

deposition is the main removal pathway for dioxins and dioxin dispersion in air is less extensive than the predicted depositional 'plume' on the ground. The differences observed in the performance of AERMOD over ISCST3 are not due to terrain considerations or downwash building effects, which are incorporated in AERMOD but are optional in ISCST3, as our modeling site is considered flat and rural. Apart from that, model differences stem from the process improvements in AERMOD formulations (such as Gaussian distribution in lateral and bi-Gaussian distribution in vertical direction in convective boundary layer; the dividing stream concept in planetary boundary layer among others). It appears that the change in selecting weather stations has a major impact on input variables (wind direction, precipitation amount among others), and resultant estimates. The meteorological data processed for ISCST3 by PCRAMMET processor using various data sources might also contribute to the differences in model predictions of wet and dry particle depositions in a comparison to the results obtained from the meteorological data processed by AERMET for AERMOD model. Despite the variability of meteorological data and the change in air dispersion model, the correlation between predicted wet and dry deposition fluxes and actual soil measurements did not significantly improve. Ultimately, the geographical bias of sampled locations is likely the major cause for the low correlations.

References

(1) EPA, U., User's Guide for the Industrial Source Complex (ISC 3) Dispersion Models **1995,** Vol. 1

(2) EPA, U., EPA SCRAM website. In 2009.

(3) EPA, U., The American Meteorological Society/Environmental Protection Agency Regulatory Model Improvement Committee (AERMIC) *AERMOD* **2006**.

(4) EPA, U., User's Guide for the AMS/EPA Regulatory Model - AERMOD. **2006**

(5) Cimorelli, A. J.; Perry, S. G.; Venkatram, A.; Weil, J. C.; Paine, R. J.; Wilson, R. B.; Lee, R. F.; Peters, W. D.; Brode, R. W., AERMOD: A dispersion model for industrial source applications. Part I: General model formulation and boundary layer characterization. *Journal of Applied Meteorology* **2005,** 44, (5), 682-693.

(6) Perry, S. G.; Cimorelli, A. J.; Paine, R. J.; Brode, R. W.; Weil, J. C.; Venkatram, A.; Wilson, R. B.; Lee, R. F.; Peters, W. D., AERMOD: A dispersion model for industrial source applications. Part II: Model performance against 17 field study databases. *Journal of Applied Meteorology* **2005,** 44, (5), 694-708.

(7) Hanna, S. R.; Egan, B. A.; Purdum, J., Evaluation of the ADMS, AERMOD, and ISC3 dispersion models with the OPTEX, Duke Forest, Kincaid, Indianapolis and Lovett field datasets. *International Journal of Environment and Pollution* **2001,** 16, (1-6), 301-314.

(8) Spanton, A. M.; Hall, D. J.; Dunkerley, F.; Griffiths, R. F.; Bennett, M., A dispersion model intercomparison archive. *International Journal of Environment and Pollution* **2005,** 24, (1-4), 4-10.

(9) Isakov, V.; Venkatram, A.; Touma, J. S.; Koracin, D.; Otte, T. L., Evaluating the use of outputs from comprehensive meteorological models in air quality modeling applications. *Atmospheric Environment* **2007,** 41, (8), 1689-1705.

(10) Faulkner, W. B.; Shaw, B. W.; Grosch, T., Sensitivity of Two Dispersion Models (AERMOD and ISCST3) to Input Parameters for a Rural Ground-Level Area Source. *Journal of the Air & Waste Management Association* **2008,** 58, (10), 1288-1296.

(11) Faulkner, W. B.; Powell, J. J.; Lange, J. M.; Shaw, B. W.; Lacey, R. E.; Parnell, C. B., Comparison of dispersion models for ammonia emissions from a ground-level area source. *Transactions of the Asabe* **2007,** 50, (6), 2189-2197.

(12) Lopez, J., Influence of the micro meteorological parameters in the estimation of the atmospheric dispersion using the AERMOD. *Air Pollution X* **2002,** 11, 83-92.

(13) Scott, P. K.; Proctor, D., Soil suspension/dispersion modeling methods for estimating health-based soil cleanup levels of hexavalent chromium at chromite ore processing residue sites. *Journal of the Air & Waste Management Association* **2008,** 58, (3), 384-403.

(14) Hill, R.; Taylor, J.; Lowles, I.; Emmerson, K.; Parker, T., A new model validation database for evaluating AERMOD, NRPB R91 and ADMS using krypton-85 data from BNFL Sellafield. *International Journal of Environment and Pollution* **2005,** 24, (1-4), 75-87.

(15) Brizio, E.; Genon, G.; Poggio, M., Results of atmospheric dispersion model for the localization of a MSW incinerator. *Development and Application of Computer Techniques to Environmental Studies X* **2004,** 11, 147-156.
(16) Silverman, K. C.; Tell, J. G.; Sargent, E. V., Comparison of the industrial source complex and AERMOD dispersion models: Case study for human health risk assessment. *Journal of the Air & Waste Management Association* **2007,** 57, (12), 1439-1446.
(17) Basham, J. P.; Whitwell, I., Dispersion modelling of dioxin releases from the waste incinerator at Avonmouth, Bristol, UK. *Atmospheric Environment* **1999,** 33, (20), 3405-3416.
(18) Yoshida, K.; Ikeda, S.; Nakanishi, J.; Tsuzuki, N., Validation of modeling approach to evaluate congener-specific concentrations of polychlorinated dibenzo-p-dioxins and dibenzofurans in air and soil near a solid waste incinerator. *Chemosphere* **2001,** 45, (8), 1209-1217.
(19) Floret, N.; Viel, J. F.; Lucot, E.; Dudermel, P. M.; Cahn, J. Y.; Badot, P. M.; Mauny, F., Dispersion modeling as a dioxin exposure indicator in the vicinity of a municipal solid waste incinerator: A validation study. *Environmental Science & Technology* **2006,** 40, (7), 2149-2155.
(20) Goovaerts, P.; Trinh, H. T.; Demond, A.; Franzblau, A.; Garabrant, D.; Gillespie, B.; Lepkowski, J.; Adriaens, P., Geostatistical modeling of the spatial distribution of soil dioxins in the vicinity of an incinerator. 1. Theory and application to Midland, Michigan. *Environmental Science & Technology* **2008,** 42, (10), 3648-3654.
(21) Goovaerts, P.; Trinh, H. T.; Demond, A. H.; Towey, T.; Chang, S. C.; Gwinn, D.; Hong, B.; Franzblau, A.; Garabrant, D.; Gillespie, B. W.; Lepkowski, J.; Adriaens, P., Geostatistical modeling of the spatial distribution of soil dioxin in the vicinity of an incinerator. 2. Verification and calibration study. *Environmental Science & Technology* **2008,** 42, (10), 3655-3661.
(22) Lorber, M.; Eschenroeder, A.; Robinson, R., Testing the USA EPA's ISCST-Version 3 model on dioxins: a comparison of predicted and observed air and soil concentrations. *Atmospheric Environment* **2000,** 34, (23), 3995-4010.
(23) Koester, C. J.; Hites, R. A., Wet and Dry Deposition of Chlorinated Dioxins and Furans. *Environmental Science & Technology* **1992,** 26, (7), 1375-1382.
(24) Eitzer, B. D.; Hites, R. A., Polychlorinated dibenzo-p-dioxins and dibenzofurans in the ambient atmosphere of Bloomington, Indiana. *Environ. Sci. Technol.* **1989,** 23, (11), 1389-1395.
(25) Eitzer, B. D.; Hites, R. A., Atmospheric transport and deposition of polychlorinated dibenzo-p-dioxins and dibenzofurans. *Environ. Sci. Technol.* **1989,** 23, (11), 1396-1401.
(26) MDEQ, Meteorological Data Support Document. In Michigan Department of Environmental Quality: 2009.
(27) EPA, U. *Michigan Dioxin Studies Dow Chemical Building 703 Incinerator Exhaust And Ambient Air Study*; 1987.
(28) Schecter, A.; Birnbaum, L.; Ryan, J. J.; Constable, J. D., Dioxins: An overview. *Environmental Research* **2006,** 101, (3), 419-428.

(29) Paustenbach, D. J., The practice of exposure assessment: A state-of-the-art review (Reprinted from Principles and Methods of Toxicology, 4th edition, 2001). *Journal of Toxicology and Environmental Health-Part B-Critical Reviews* **2000,** 3, (3), 179-291.
(30) MDEQ, Dow Hazardous Waste Facility Operating License Information In Michigan Department of Environmental Quality (MDEQ) 2009.
(31) Webmet, Lakes Environmental Software In.
(32) NCDC, Integrated Surface Database. In.
(33) Lee, R., Russell Lee Consulting. In 2009.
(34) NCDC, Radiosonde Database In.
(35) EPA, U. *Comparison of regulatory design concentrations AERMOD vs ISCST3, CTDMPLUS, ISC-PRIME*; 2003.
(36) TerraSeer *Space-Time Intelligence System (STIS)*, 2008.
(37) NIST/SEMATECH, NIST/SEMATECH e-Handbook of Statistical Method. In 2009.
(38) Systat *SigmaPlot*, 9.0.
(39) Lohmann, R.; Jones, K. C., Dioxins and furans in air and deposition: A review of levels, behaviour and processes. *The Science of The Total Environment* **1998,** 219, (1), 53-81.
(40) Nopmongcol, U.; Khamwichit, W.; Fraser, M. P.; Allen, D. T., Estimates of heterogeneous formation of secondary organic aerosol during a wood smoke episode in Houston, Texas. *Atmospheric Environment* **2007,** 41, (14), 3057-3070.
(41) EPA *AERMOD Deposition Algorithms – Science Document (Revised Draft)*; 2004.
(42) Wesely, M. L. D. P. V. S. J. D. *Deposition Parameterizations for the Industrial Source Cmplex (ISC3) Model*; Argonne National Laboratory: 2002.
(43) Grosch, T. G.; Lee, R. F., Sensitivity of the AERMOD air quality model to the selection of land use parameters. *Air Pollution Vii* **1999,** 6, 803-812.
(44) Hanna, S. R.; Paine, R.; Heinold, D.; Kintigh, E.; Baker, D., Uncertainties in air toxics calculated by the dispersion models AERMOD and ISCST3 in the Houston ship channel area. *Journal of Applied Meteorology and Climatology* **2007,** 46, 1372-1382.
(45) Deutsch, C. V., *Direct assessment of local accuracy and precision.* Kluwer Academic Publishing: Dordrecht, 1997; p 115–125.

Chapter 6

Prediction of congener specific dioxin deposition from an incinerator: the AERMOD air dispersion model

6.1. Introduction

Incineration of chlorinated containing organic waste at high temperature has been demonstrated to result in the emission of dioxins and furan pollutants to the atmosphere *(1-4)*. Often, the air dispersion of these pollutants and their deposition are assessed by a regulatory air dispersion model to quantify the extent and impact of incinerators on urban populations *(5-10)*. In the previous chapter, we introduced the newly promulgated AERMOD model developed by the US EPA to predict the dispersion and deposition of total dioxins, expressed as toxic equivalents (TEQs).

This chapter will describe the application of AERMOD to estimate congener specific dioxin dispersion and deposition from a historical incinerator in Midland, Michigan. Prior work on dioxin-specific congener emissions from incinerators indicated

that 1,2,3,4,6,7,8-HpCDD, OCDD; 1,2,3,4,6,7,8-HpCDF and OCDF are predominant dioxin congeners across emission profiles from hazardous waste incinerators and municipal waste incinerators *(11-18)*. It was also noted that PeCDF, 2,3,7,8-TeCDF and 1,2,3,4,7,8-HxCDF *(16, 17)* were among the main contributors to total TEQs, and the incinerator emission profile was observed to have a direct influence on ambient air concentrations*(13-18)*. Since individual dioxin and furan congeners exhibit variable emission profiles and physicochemical properties, it can be expected that the dispersion and deposition fluxes will be affected.

The above mentioned attributes were incorporated in the model allowing AERMOD to perform predictions of congener air concentrations, as well as dry and wet deposition fluxes in gaseous and particulate deposition modes. The addition of a gaseous deposition mode, which is typically not included in dispersion modeling, would capture the fractions of dioxins and furans known to be associated both in gaseous and particulate phase. Although gaseous and particulate deposition algorithms are built as options for the Industrial Source Complex (ISC) model and were revised for the AERMOD model*(19)*, these modes are not often seen in the literature because the pollutants which were modeled (NO_x, SO_2, ammonia, etc.) are not associated with both gaseous and particulate phases as dioxin like compounds. Gaseous phase deposition of dioxins is more applicable to the lesser chlorinated dioxins (TCDD, TeCDF) and furans (PeCDD, PeCDF) while particulate phase deposition tends to be more associated with the heavier congeners (HpCDD/D or OCDD/F) based on the partitioning properties of these specific congeners *(20, 21)*.

Since the model outputs of wet and dry dioxin deposition fluxes are used as inputs for the geostatistical analysis of soil contamination with individual congeners*(8),* these fluxes need to be calculated on a congener-specific basis. Ten dioxin and furan congeners, each representing its homologue group, were selected: 2,3,7,8-Tetrachlorodibenzo-p-dioxin (TCDD); 1,2,3,4,7-Pentachlorodibenzo-p-dioxin (PCDD); 1,2,3,4,7,8-Hexachlorodibenzo-p-dioxin (1,2,3,4,7,8-HxCDD);1,2,3,4,6,7,8-Heptachlorodibenzo-p-dioxin (1,2,3,4,67,8-HpCDD); Octachlorodibenzo-p-dioxin (OCDD); 2,3,7,8-Tetrachlorodibenzofuran (TeCDF); 2,3,4,7,8-Pentachlorodibenzofuran (PeCDF); 1,2,3,4,7,8-Hexachlorodibenzofuran (1,2,3,4,7,8-HxCDF); 1,2,3,4,6,7,8-Heptachlorodibenzofuran (1,2,3,4,6,7,8-HpCDF) and Octachlorodibenzofuran (OCDF).

The objectives of this chapter therefore are to (1) estimate air concentrations, wet and dry deposition of dioxins using the best available data and to (2) investigate the relative importance of dioxin removal pathways by dry and wet deposition in the gas phase and in the particulate phase.

VI.2. Materials and Methods

The AERMOD air dispersion model generates both air concentrations and deposition fluxes using the same model run, however, gaseous phase deposition and particulate phase deposition need to be calculated separately *(22, 23).* Ten dioxin congeners will be used in AERMOD gaseous and particulate deposition algorithms to predict the dioxin deposition and air concentration plume emitted from the incinerator.

Modeling Site:

The study area is the vicinity of the Dow Chemical Company facility in Midland, Michigan as described in detail elsewhere (Chapter 3). Dioxin contamination in Midland soils is believed to have been impacted by the operation of hazardous waste incinerators since the 40s *(24)*. Halogenated materials were among the processed wastes, amounting to about 200 tons daily as reported in 1984 *(25)* and the burning of those materials produced dioxins as byproducts *(4)*. Although a new incinerator complex with high dioxin removal efficiency (99.9999%) is in place, our modeling is based on the incinerator complex 830, which was demolished in 2002 prior to the operation of the current incinerator*(26)*.

The area surrounding the Dow Plant incinerator was divided into a nested receptor grid comprising 3 sub-grids of different resolutions: a fine grid with spacing of 50 m from the plant boundary out to 1000 m; a medium grid with spacing of 100 m to 5000 m and a coarse grid with spacing of 500 m from 5000 m to 10000m. AERMOD generates its output, air concentration, dry, wet and total deposition flux for each receptor point over the course of meteorological data period from 2001 to 2005 provided by Michigan Department of Environmental Quality *(27)*. The plant incinerator is located in the middle of the modeling grid (Figure 6.1).

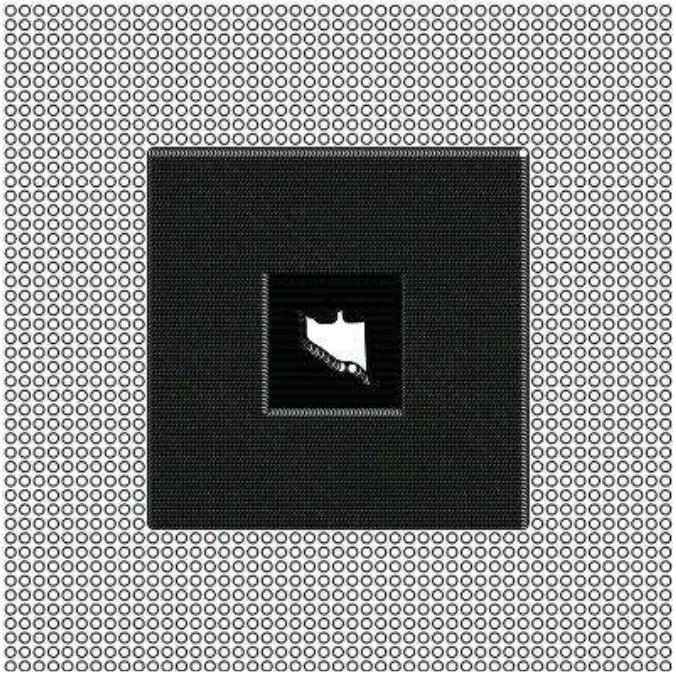

Figure 6.1. Three nested grids of receptors, including fine grid with spacing of 50 m out to 1 km; medium grid with spacing of 100 m out to 5 km and coarse grid with spacing of 500 m out to 10 km away from the plant incinerator. Plant boundary is in white at the centre of the receptor grid.

Land Use Type and Seasonal Categories:

Land cover data are retrieved from the 1992 National Land Cover Data *(28)* for the Tri Counties of Michigan: Bay, Midland and Saginaw. The data are visualized in a map of the ArcGIS program (Figure 6.2). The land use categories are grouped according to wind directions in 36 directions in which each direction covers 10 degrees. The first segment corresponds to the land use category for wind directions at 10 degrees. The further directions follow in clockwise order with the last segment corresponding to wind directions north at 360 degrees. Nine land use categories in AERMOD gaseous

deposition are classified. Wind rose data measured for 5 years during 2001-2005 at Midland-Bay-Saginaw International Airport are embedded in the land use map of the three counties. The land uses coded according to each increment clockwise of wind directional segments from 0 to 360 degree include urban land, no vegetation, agriculture land, suburban areas, and forested areas *(19)*.

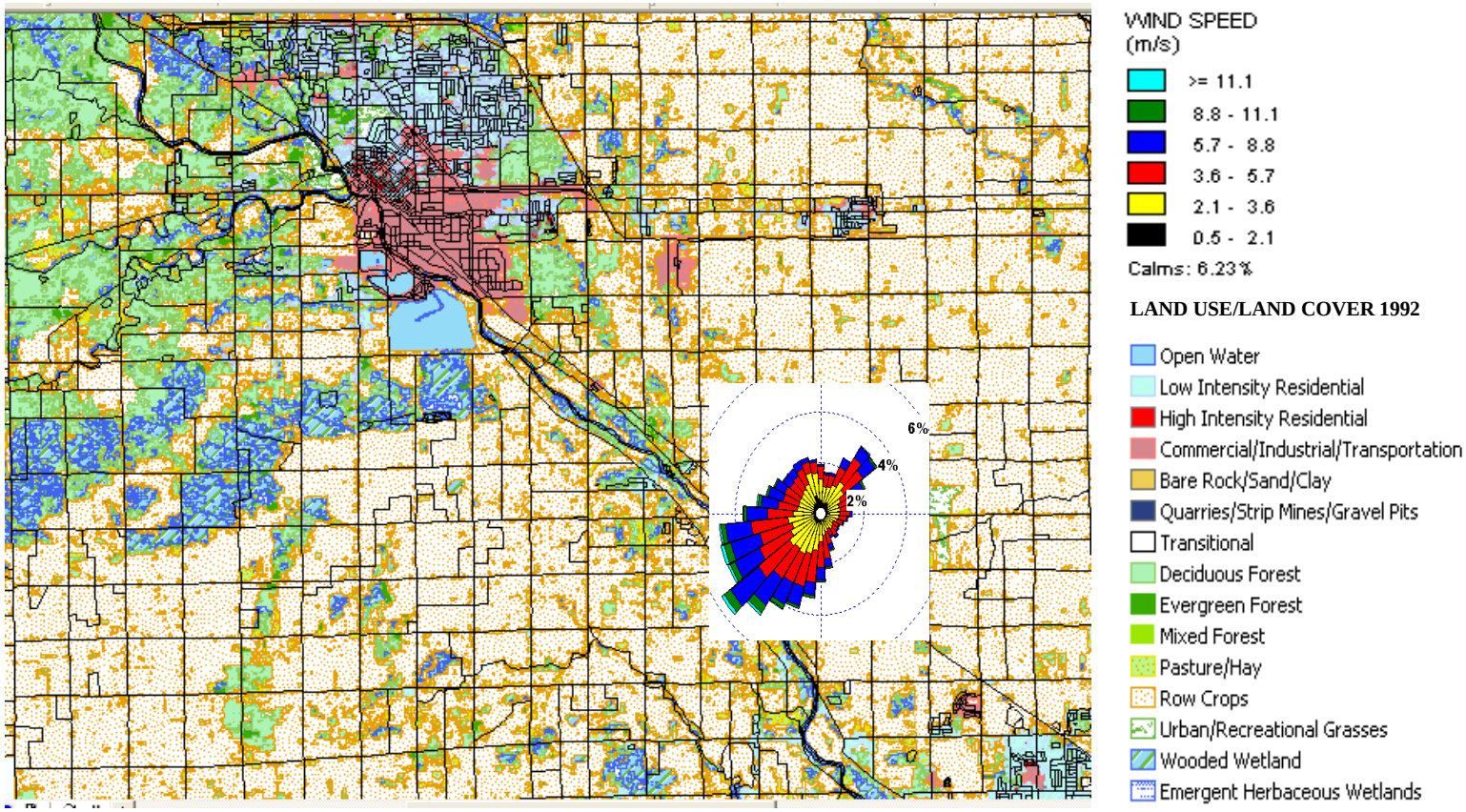

Figure 6.2. Land use type/cover in Midland County, Michigan in 1992. The wind rose at the Tri Cities (Midland-Bay-Saginaw) airport is considered relevant to the modeling site is shown.

The gas deposition in AERMOD requires that seasonal information is incorporated with respect to land use (Table 6.1). There are five categories defined as follows*(19)*:

- Seasonal Category 1: Midsummer with lush vegetation
- Seasonal Category 2: Autumn with unharvested cropland
- Seasonal Category 3: Late autumn after frost and harvest, or winter with no snow
- Seasonal Category 4: Winter with snow on ground
- Seasonal Category 5: Transitional spring with partial green coverage or short annuals.

Table 6.1. Definitions of Land Use Categories

Land Use Category	Definition
1	Urban land, no vegetation
2	Agriculture Land
3	Rangeland
4	Forest
5	Suburban areas, grassy
6	Suburban areas, forested
7	Bodies of water
8	Barren land, mostly desert
9	Non-forested wetlands

The weather conditions associated with crops in Michigan can be described as long months of cold weather. Twelve calendar months are grouped according to the five categories as follows:

- December to March: Seasonal category 4
- April to May: Seasonal category 5
- June to August: Seasonal category 1
- September to October: Seasonal category 2
- November: Seasonal category 3

Physical-Chemical Properties of Dioxin Congeners

The properties of dioxins needed for AERMOD modeling are: water solubility, vapor pressure, Henry constant, diffusivity in water, etc. The full records of these properties are found in Appendix 6.1 and 6.2 *(19)*. The partitioning ratios between vapor/ gaseous phase and particulate phase of dioxin congeners are based on data presented in Eitzer and Hites *(29-32)*. These data (Table 6.2) were based on ambient air analysis in Bloomington, Indiana, in which the lesser chlorinated dioxin congeners were found to be highly variable and increasingly present in the gaseous phase as the atmospheric temperature increased. The temperatures at which gaseous and particulate phase accumulation of dioxins/ furans in ambient air samples was conducted covered a wide range of atmospheric temperatures from 3^{o}C to 28^{o}C. The data confirmed that temperature indeed has an important effect on the distribution of dioxins and furans between gaseous and particulate phase as has been observed elsewhere *(33)*. Since we modeled deposition of dioxins using a 5 year meteorological data average, we used the average distribution of dioxins in the particulate phase (Table 6.2) to convert total emission rates of dioxin

congeners into gaseous emission rates, particulate emission rates as well as dioxin deposition fluxes under wet and dry deposition conditions.

Table 6.2. Distribution of dioxins and furans which are in the particulate phase (4-D = TCDD; 4-F=TeCDF…) based on air monitoring data *(29)*

Reference	4-D	5-D	6-D	7-D	8-D	4-F	5-F	6-F	7-F	8-F
Temp = 20ºC	23.00	37.00	66.00	87.00	96.00	14.00	31.00	64.00	87.00	91.00
Temp = 3ºC	40.00	87.00	100.00	100.00	100.00	100.00	60.00	88.00	100.00	98.00
Temp = 18ºC	8.00	28.00	45.00	88.00	100.00	ND	28.00	30.00	93.00	100.00
Temp = 28ºC	5.00	13.00	45.00	60.00	100.00	ND	0.00	38.00	78.00	98.00
Average	19.00	41.25	64.00	83.75	99.00	57.00	29.75	55.00	89.50	96.75

Dioxin Emission Profile:

Reports on dioxin emissions from the incinerator stack at the Dow Chemical Facility in Midland were limited before 1992 *(24, 25)*, and, hence, retrieval of historical emissions of dioxins is very difficult. The reported values often are in terms of total TEQ *(25)*; for example, prior to1983 the emission was reported to be greater than 12 g TEQ/year and emission measured in 1984 was already reduced by more than 95% to 0.3 g/year TCDD equivalents. A two orders of magnitude reduction in TEQ emission was observed in 1992, at which time the full emission profile was measured, resulting in 0.0333 g TEQ-$WHO_{TEF\text{-}2005}$ *(34)*. The reduction in total discharge of dioxins and furans was due to the implementation of corrective actions required for its incinerator operating licenses *(25, 26, 35)*.

We used emission rates for 10 dioxin and furan congeners based on the stack test reported by US. EPA in 1992 *(25, 34)*. The emission rate of each congener was adjusted following the gaseous and particulate fraction as discussed earlier. The emission rate of each congener was averaged after 4 stack test runs and was considered the total emission rate, including gaseous and particulate components. Given the fact that dioxins are associated with both particulate and gaseous phases, the total emission rate of each congener was converted into a vapor emission rate and a particle emission rate by multiplying the total emission rate with the average distribution of dioxins in the particulate phase (Table 6.2). A scaling factor of 360 (representing the ratio between total TEQ emission in 1983 and in 1992) was then applied to adjust the particulate and vapor phase emission rates.

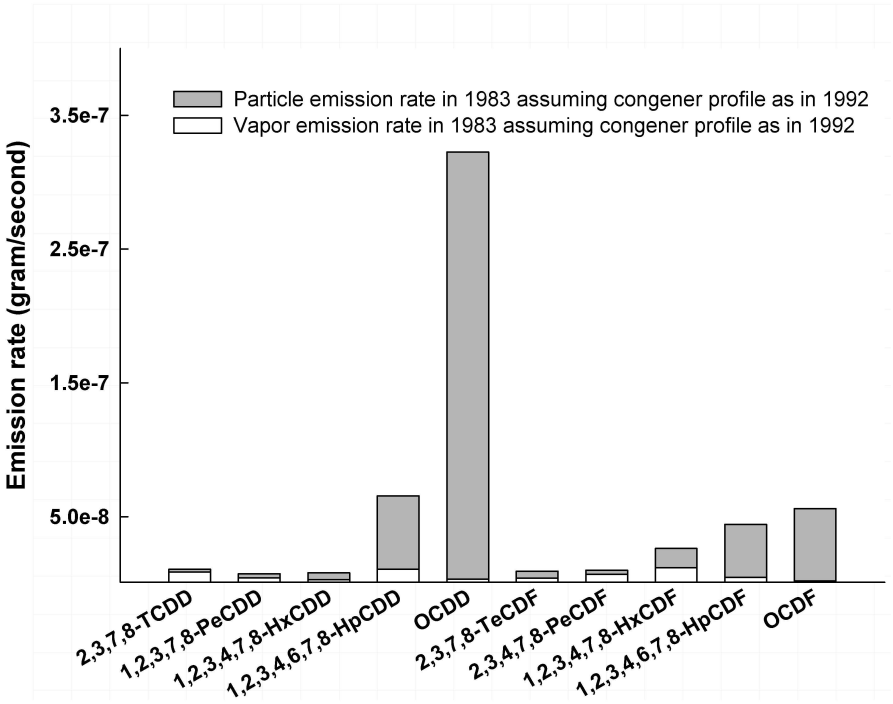

Figure 6.3. Emission rates of gaseous and particulate phases of dioxin congeners following the emission profile in 1992 adjusted to emission level in 1983 of the Dow Chemical Company.

Figure 6.3 shows both gaseous and particulate emission rates of 10 selected dioxins and furans following the emission profile of 1992, after multiplication by 360 to adjust to the level of 1983 emission. The emission profile of Dow was a typical profile from a hazardous waste incinerator that emitted HpCDD, OCDD, HpCDF and OCDF as major byproducts. The fractions of vapor emission rates are significant for the lesser chlorinated dioxin congeners but not for the higher chlorinated dioxin and furan compounds.

Fluxes of dioxins in gas and particle form by dry and wet deposition

The air dispersion modeling employs wet and dry deposition algorithms to obtain deposition fluxes of PCDDs/PCDFs in gaseous and particulate phases. Four possible combinations of deposition/dioxin phase are thus investigated:

a. particle-bound dry deposition (particle-dry);

b. gaseous phase dry deposition (gas-dry);

c. particle-bound wet deposition (particle-wet);

d. gaseous phase wet deposition (gas-wet)

Combinations of the particle-dry and gas-dry depositions, particle-wet and gas-wet depositions result in the total dry deposition and total wet deposition fluxes of dioxins and furans.

AERMOD Air Dispersion Model

A detailed description of AERMOD and its modeling formulations are found elsewhere *(19, 23, 36-38)* and described in chapter 3. AERMOD was used both in particulate and gaseous phase deposition. Dioxin deposition fluxes were obtained by these two mechanisms and by wet and dry deposition pathways. To support the application of AERMOD, meteorological data prepared by the meteorological pre-processor AERMET are crucial. The meteorological data used in this work were prepared by Michigan Department of Environmental Quality (MDEQ) from 2001-2005, the period that UMDES study was conducted. The surface and upper air meteorological data obtained from Midland-Bay-Saginaw airport and from White Lake in Detroit *(27)* for each year are surface data and profiling data. Five year meteorological data files were then compiled as a 5 year surface file and a 5 year profiling file. The former file contained hourly surface parameters such as sensible heat flux, heights of convective layer and of mechanical mixing layer, Monin-Obukhov length, and precipitation amount among others. The latter profiling data file included vertical gradients of temperature, wind speed and turbulence computed from the radiosonde data. The details of AERMET data files are described in detail elsewhere *(39)*

The modeling conditions for AERMOD were based on a unitary emission rate of 1gram/second for 10 dioxin congeners using both gaseous and particulate algorithms. The outputs included air concentrations and dioxin deposition fluxes (calculated separately for gaseous and particulate forms, were multiplied by conversion factor derived from the 1992 emission profile and 1983 emission level as shown in Figure 6.3).

Data visualization was conducted using ArcMap of ESRI *(40)* and STIS, a commercial product of Terra-Seer *(41)*. The windrose of the MBS weather station was plotted using software of Lakes Environmental Softwares *(42)*. Other figures were plotted using SigmaPlot, version 11.0 of Systat Inc.*(43)*.

VI.3. Results and discussion

The absolute values of the estimated dry and wet deposition fluxes are shown in Table 6.4 and Figure 6.4 (a,b). Figure 6.4 (a,b) presents the absolute values of deposition fluxes for the 4 possible pathways, leaving out the lower tail values of the ten congeners. Each box-plot represents the distribution range of the fifth (5th) to the ninety-fifth (95^{th}) percentiles of each congener's deposition flux. The upper tail values of the distributions are of particular interest, as low deposition fluxes are found at further distance from the sources. The maximum values of deposition fluxes are provided in the figure as well. Mean values of wet deposition fluxes of particulate phase PCDD/F range from 2 pg/m^2 of PeCDD to 152 pg/m^2 of OCDD. Mean values of wet deposition of dioxin in gaseous phase are one order of magnitude smaller than those of particulate phase PCDD/F.

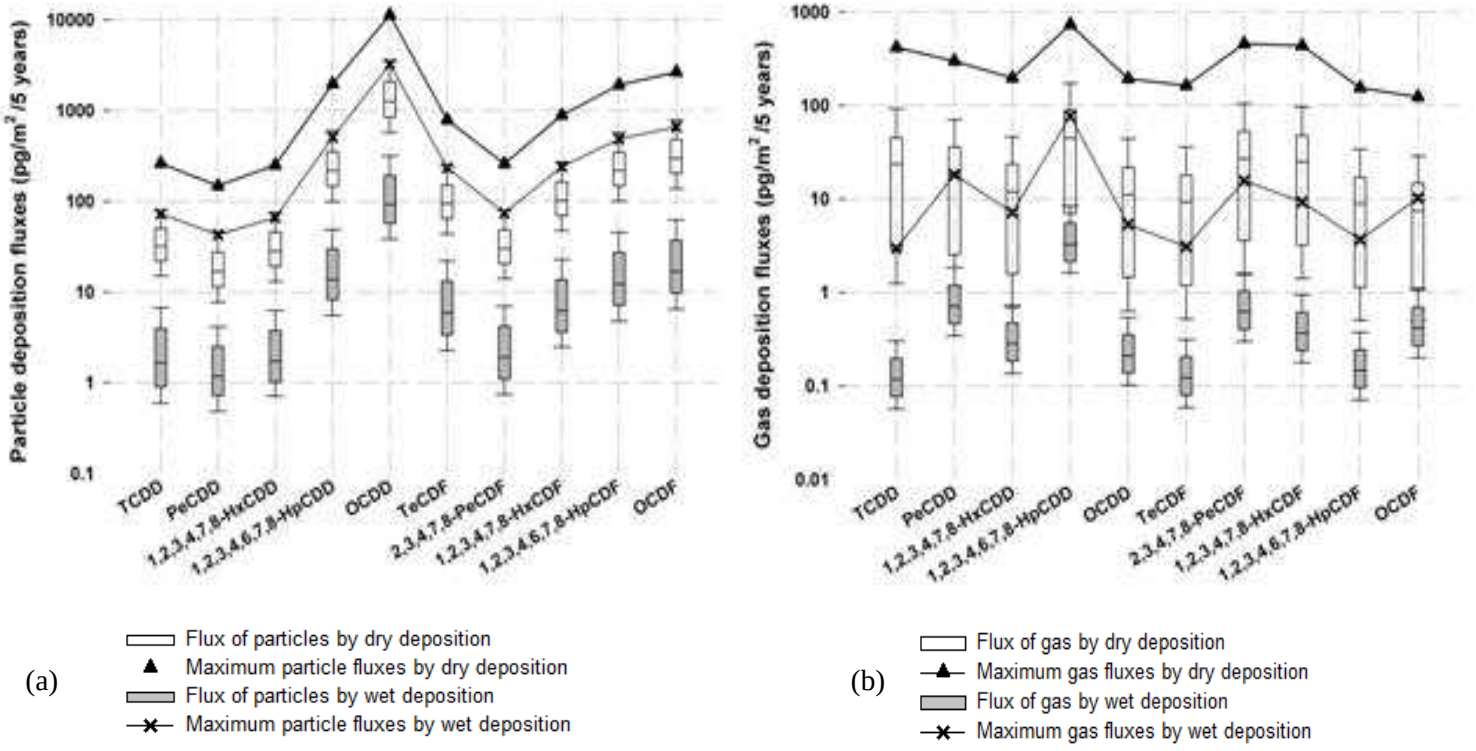

Figure 6.4. (a,b) Boxplot of particle (a) and gas fluxes (b) of dioxins and furans by dry and wet deposition

The wet deposition fluxes are smaller in both gas and particle deposition mode, as quantified by the gray box plots in Figure 6.4(a) and Figure 6.4(b). The maximum values for the wet deposition mode are on average one to two orders of magnitude below the maximum values for the dry deposition mode. Dry deposition fluxes of gaseous and particle phase PCDD/F dioxins are quantified by white box plots. The connecting lines of maximum values for dry and wet depositions in each figure create a range of deposition values for the ten congeners. As seen in Figure 6.4(a), the band width is mostly constant across PCDD/F congeners within an order of magnitude. As described in the previous section, the particle deposition algorithm is a function of deposition velocity which is computed from various resistances (aerodynamic and quasi-laminar sub-layer resistance) within the atmospheric sub-layers. The deposition velocity is also a function of particles size. In the particle-dry deposition algorithm, we applied a detailed particle size distribution for each congener based on data described in a municipal waste incinerator study *(44)*, where the particle size distribution was well known and the fraction of size category above 10 micron in diameter is more than 10% (Method 1).

Since the obtained particle size distribution does not include a coarse fraction that is greater than 10 μm, method 2 applies a dry particle deposition algorithm in which the particle size is distributed in two size categories (fine particles with diameter smaller than 2.5 μm and coarse particles with greater than 10 μm; *(45)*. Methods 1 and 2 for the particle-dry deposition case are different with respect to computing the dry deposition velocity *(45)*. Based on the results, it appears that the differences in size distributions of particulate-phase dioxin congeners are not very significant in explaining deposition fluxes.

Details of particle size distribution are shown in Table 6.3 below. The data are computed from the original work of Chao *(44)*, who measured particle-associated dioxins at two experimental sites. The mass fraction associated with particle size categories in Table 6.3 were averaged based on measured values at these two sites following the logarithmic mean method. The mass fraction of dioxins was averaged following geometric means of the available measured values.

Table 6.3. Dioxin particle size distribution computed based on original data of Chao (2004) *(44)*.

Compounds	**Mass Fraction**				
	Representative diameter (μm)				
	0.13	**0.76**	**4.24**	**31.62**	**Total**
2,3,7,8-TeCDD		0.90		0.10	1.00
1,2,3,7,8-PeCDD	0.28	0.51	0.19	0.03	1.00
1,2,3,4,7,8-HxCDD	0.39	0.45	0.13	0.03	1.00
1,2,3,6,7,8-HxCDD	0.42	0.43	0.12	0.03	1.00
1,2,3,7,8,9-HxCDD	0.42	0.44	0.12	0.03	1.00
1,2,3,4,6,7,8-HpCDD	0.36	0.51	0.11	0.02	1.00
OCDD	0.23	0.58	0.16	0.02	1.00
2,3,7,8-TeCDF	0.29	0.31	0.29	0.11	1.00
1,2,3,7,8-PeCDF	0.32	0.37	0.23	0.08	1.00
2,3,4,7,8-PeCDF	0.36	0.39	0.19	0.06	1.00
1,2,3,4,7,8-HxCDF	0.40	0.43	0.13	0.04	1.00
1,2,3,6,7,8-HXCDF	0.41	0.42	0.13	0.04	1.00
2,3,4,6,7,8-HxCDF	0.46	0.41	0.10	0.03	1.00
1,2,3,7,8,9-HxCDF	0.38	0.37	0.20	0.05	1.00
1,2,3,4,6,7,8-HpCDF	0.44	0.44	0.08	0.03	1.00
1,2,3,4,7,8,9-HpCDF	0.45	0.44	0.08	0.03	1.00
OCDF	0.49	0.40	0.08	0.03	1.00
ΣPCDD/Fs					
TEQs (fg I-TEQ m-cu)	0.38	0.42	0.15	0.05	1.00

In this table, four particle size categories are specified. The data showed that most of dioxin congeners are associated with fine particles (greater than 75% of dioxin mass are

with particles with less than 0.75 μm in diameter) except for TeCDF (60%) and PeCDF (68%).

Table 6.4. Descriptive statistics of particle and gas deposition fluxes by dry and wet deposition.

Particle-bound dry deposition (particle-dry, pg/m2)	**MIN**	**MAX**	**MEDIAN**	**MEAN**
TCDD	2.9	262.4	32.0	41.2
PeCDD	1.6	148.1	16.8	22.8
1,2,3,4,7,8-HxCDD	2.7	249.9	28.2	37.7
1,2,3,4,6,7,8-HpCDD	21.4	1964.7	216.5	293.7
OCDD	124.6	11305.4	1258.3	1725.1
TeCDF	8.6	791.1	94.4	124.1
2,3,4,7,8-PeCDF	2.8	258.3	30.2	40.0
1,2,3,4,7,8-HxCDF	9.7	887.8	101.9	135.6
1,2,3,4,6,7,8-HpCDF	21.0	1913.9	216.4	287.6
OCDF	28.7	2647.2	297.7	396.2
Gaseous phase dry deposition (gas-dry, pg/m2)				
TCDD	0.6	416.9	23.6	35.7
PeCDD	0.5	298.0	18.1	27.6
1,2,3,4,7,8-HxCDD	0.3	196.5	11.9	18.1
1,2,3,4,6,7,8-HpCDD	1.4	733.3	44.7	68.2
OCDD	0.3	193.4	11.2	17.0
TeCDF	0.3	163.8	9.3	14.0
2,3,4,7,8-PeCDF	0.7	456.9	26.8	40.9
1,2,3,4,7,8-HxCDF	0.7	436.3	25.0	37.5
1,2,3,4,6,7,8-HpCDF	0.3	154.5	8.9	13.3
OCDF	0.2	123.3	7.5	11.4
Particle-bound wet deposition (particle-wet, pg/m2)				
TCDD	0.1	72.8	1.7	3.0
PeCDD	0.1	42.9	1.2	2.0
1,2,3,4,7,8-HxCDD	0.2	66.0	1.7	3.0
1,2,3,4,6,7,8-HpCDD	1.1	506.1	13.7	23.2
OCDD	9.6	3231.9	92.6	151.8
TeCDF	0.4	233.6	5.9	10.2
	MIN	**MAX**	**MEDIAN**	**MEAN**

Particle-bound dry deposition (particle-dry, pg/m2)				
2,3,4,7,8-PeCDF	0.1	73.7	1.9	3.3
1,2,3,4,7,8-HxCDF	0.4	241.1	6.2	10.7
1,2,3,4,6,7,8-HpCDF	0.8	483.9	12.3	21.3
OCDF	1.1	661.5	16.8	29.1
Gaseous phase wet deposition (gas-wet, pg/m2)				
TCDD	0.0	3.0	0.1	0.2
PeCDD	0.1	18.2	0.7	1.0
1,2,3,4,7,8-HxCDD	0.0	7.2	0.3	0.4
1,2,3,4,6,7,8-HpCDD	0.5	77.0	3.3	4.5
OCDD	0.0	5.3	0.2	0.3
TeCDF	0.0	3.1	0.1	0.2
2,3,4,7,8-PeCDF	0.1	15.7	0.6	0.8
1,2,3,4,7,8-HxCDF	0.1	9.3	0.4	0.5
1,2,3,4,6,7,8-HpCDF	0.0	3.7	0.1	0.2
OCDF	0.1	10.2	0.4	0.6

The fluxes of gas phase PCDD/F appeared to vary substantially, as indicated by a fluctuation of band width of the maximum values between the dry and wet deposition mode by two orders of magnitude (Figure 6.4b). This variation can be explained by the wide range of input values for gaseous deposition calculations, including site characteristics and physical-chemical properties of the congeners. For example, the deposition velocity used for gaseous dry deposition is a function of both land use types and seasonal categories *(46).* The variables for this calculation include depositional resistance parameters, such as gas-surface phase resistance, and stomatal resistance *(45).* Descriptive statistics of the 4 combinations of gaseous, particulate phase and of dry and wet deposition pathways are presented in Table 6.4. The physical-chemical properties of

dioxin congeners range over multiple orders of magnitude as well (Appendix 6.1 and 6.2).

The relative particle and gas fluxes contributed by dry and wet deposition are summarized in Table 6.5. Based on the flux estimates, dry deposition of particles appeared to be the dominant removal pathway of dioxins from the atmosphere, with fluxes ranging from 43% for PeCDD to 91% for OCDF/ OCDD. HxCDD/F and HpCDD/F also exhibited high portions (greater than 60%) via the particle-dry removal pathway. The higher chlorinated compounds are generally associated with larger particles and the fact that high portions of these congeners were observed in the particulate-dry deposition pathway is similar to results reported by Kaupp and McLachlan *(47)*.

That study estimated that particles with a diameter greater than 1.35 μm contributed to 60-70% of the particle-dry deposition fluxes, and that the fine particles with diameter less than 1 μm are removed by rain by more than 50%. Another study *(48)* came to similar conclusions. We observed that the higher chlorinated dioxins and furans contributed largely in particle-dry deposition fluxes and the lesser chlorinated compounds were mainly associated with particle-wet deposition fluxes. In contrast, the HpCDD/F and OCDD/F contribution was slightly higher in particle wet deposition fluxes than that of other congeners. The difference may be due to the meteorological data since precipitation and temperature of each site are different, leading to the diverging conclusions on the role of particle-wet deposition. Particle deposition fluxes increased with decreasing temperature *(29, 32, 47, 49-52)*. Gaseous phase deposition has rarely been investigated in the literature however, one study in Japan *(21)* suggested that contributions of gas-dry deposition fluxes of lesser chlorinated dioxin compounds might

be significant. Our study confirmed that gas-dry deposition fluxes of TCDD, PeCDD and PeCDF is indeed significant.

Table 6.5. Relative particle and gas deposition fluxes by dry and wet deposition

Chemical	Relative deposition flux contributed by			
	Dry deposition of particles	Dry deposition of gas	Wet deposition of particles	Wet deposition of gas
TCDD	51.39%	44.61%	3.80%	0.20%
PeCDD	42.71%	51.76%	3.71%	1.82%
1,2,3,4,7,8-HxCDD	63.77%	30.58%	5.00%	0.65%
1,2,3,4,6,7,8-HpCDD	75.40%	17.51%	5.95%	1.14%
OCDD	91.07%	0.90%	8.01%	0.02%
TeCDF	83.54%	9.45%	6.90%	0.11%
2,3,4,7,8-PeCDF	47.05%	48.12%	3.84%	0.99%
1,2,3,4,7,8-HxCDF	73.57%	20.36%	5.80%	0.27%
1,2,3,4,6,7,8-HpCDF	89.20%	4.13%	6.61%	0.06%
OCDF	90.61%	2.60%	6.66%	0.13%

As TeCDF is predominantly present in a larger particle size category (4.25 micron in diameter at 29% of mass fraction), the deposition flux of TeCDF would be expected to be higher and comparable to the dry deposition fluxes of the higher chlorinated dioxins and furans (84% and 91%, respectively). In summary, we observed a trend in particle-phase dioxin and furan fluxes (both under dry and wet conditions), whereby particulate-driven fluxes increase as the chlorine level of PCDD/F increases. Deposition fluxes of gas-phase dioxins vary among the congeners. The variability of the particle fluxes between dry and wet deposition (Figure 6.4b) also is likely controlled by the variability in particle emission rates. Figure 6.3 shows that PeCDD and PeCDF exhibit lower emission rates than HxCDD and HxCDF, which, in turn, are lower than that of OCDD.

We modeled the dioxin deposition plume on nested grids comprising a fine grid with spacing of 50 m from the plant boundary out to 1,000 m, a medium grid with spacing of 100 m out to 5,000 m, and a coarse grid with spacing of 500 m out to 10,000 m *(7, 8)*. Table 6.6 shows the relative deposition fluxes at these three grids, indicating that the predicted dioxin and furan deposition occurs close to the source of emission. The total mass of PCDD/F deposited on the outer coarse grid is less than 2.5% of total deposition for all congeners. Our prediction maps of deposition fluxes therefore can leave out the coarse grid area without loosing information about the shape and magnitude of congener-specific spatial PCDD/F distributions.

Table 6.6. Relative dioxin fluxes by wet and dry deposition on three nested receptor grids

Deposition	Fine grid (%)	Medium grid (%)	Coarse grid (%)
TCDD particle-dry	51.89%	45.53%	2.58%
TCDD gas-dry	58.50%	39.48%	2.02%
TCDD particle-wet	71.11%	28.21%	0.68%
TCDD gas-wet	58.44%	39.60%	1.96%
PeCDD particle-dry	54.40%	43.24%	2.37%
PeCDD gas-dry	58.67%	39.36%	1.98%
PeCDD particle-wet	67.47%	31.47%	1.05%
PeCDD gas-wet	58.77%	39.32%	1.91%
1,2,3,4,7,8-HxCDD particle-dry	54.12%	43.48%	2.40%
1,2,3,4,7,8-HxCDD gas-dry	58.67%	39.35%	1.97%
1,2,3,4,7,8-HxCDD particle-wet	68.47%	30.58%	0.95%
1,2,3,4,7,8-HxCDD gas-wet	58.63%	39.44%	1.93%
1,2,3,4,6,7,8-HpCDD particle-dry	54.77%	42.88%	2.34%
1,2,3,4,6,7,8-HpCDD gas-dry	58.63%	39.40%	1.98%
1,2,3,4,6,7,8-HpCDD particle-wet	67.76%	31.22%	1.03%
1,2,3,4,6,7,8-HpCDD gas-wet	58.96%	39.16%	1.88%
OCDD particle-dry	54.96%	42.71%	2.32%
OCDD gas-dry	58.71%	39.31%	1.98%
OCDD particle-wet	66.87%	32.02%	1.11%
OCDD gas-wet	58.55%	39.50%	1.94%
TeCDF particle-dry	52.83%	44.67%	2.50%
TeCDF gas-dry	58.33%	39.62%	2.05%
TeCDF particle-wet	69.28%	29.85%	0.87%
TeCDF gas-wet	58.47%	39.57%	1.96%
2,3,4,7,8-PeCDF particle-dry	53.29%	44.25%	2.46%
2,3,4,7,8-PeCDF gas-dry	58.78%	39.25%	1.97%
2,3,4,7,8-PeCDF particle-wet	68.95%	30.14%	0.90%
2,3,4,7,8-PeCDF gas-wet	58.61%	39.46%	1.94%
1,2,3,4,7,8-HxCDF particle-dry	53.64%	43.92%	2.44%
1,2,3,4,7,8-HxCDF gas-dry	58.18%	39.75%	2.06%
1,2,3,4,7,8-HxCDF particle-wet	68.88%	30.21%	0.91%
1,2,3,4,7,8-HxCDF gas-wet	58.46%	39.58%	1.96%
1,2,3,4,6,7,8-HpCDF particle-dry	53.85%	43.72%	2.42%
1,2,3,4,6,7,8-HpCDF gas-dry	58.07%	39.85%	2.08%
1,2,3,4,6,7,8-HpCDF particle-wet	69.17%	29.95%	0.88%
1,2,3,4,6,7,8-HpCDF gas-wet	58.46%	39.58%	1.96%
OCDF particle-dry	53.94%	43.64%	2.42%
OCDF gas-dry	58.63%	39.39%	1.98%
OCDF particle-wet	69.16%	29.96%	0.88%
OCDF gas-wet	58.86%	39.24%	1.90%

The congener-specific deposition fluxes of congeners resulting from dry and wet deposition processes are shown using the same color scale of deposition fluxes, to allow for easy comparison between congeners (Figure 6.5; 6.6). The following observations can be made. First, the North-East direction of the deposition plume for both dry and wet deposition reflects the prevailing wind direction and wind speed recorded at the Midland-Bay-Saginaw airport, only a few miles away of Midland (Figure 6.2). Second, the dry deposition fluxes increase with chlorine level and are elevated for HpCDD, OCDD, HxCDF and OCDF. Third, the dry deposition flux and extent of the OCDD plume are one to two orders of magnitude higher than the wet deposition fluxes. These observations concur with results reported in the literature *(32, 47-49)*. Fourth, except for OCDD, the plume of wet deposition fluxes (both in term of gas and particle fluxes) is concentrated close to the source with higher fluxes at the South West direction of the plant. Although differences are observed for HpCDD, OCDD, HpCDF and OCDF, the magnitude of wet deposition of these congeners are low, contributing less than 10% to the total deposition flux (Table 6.6).

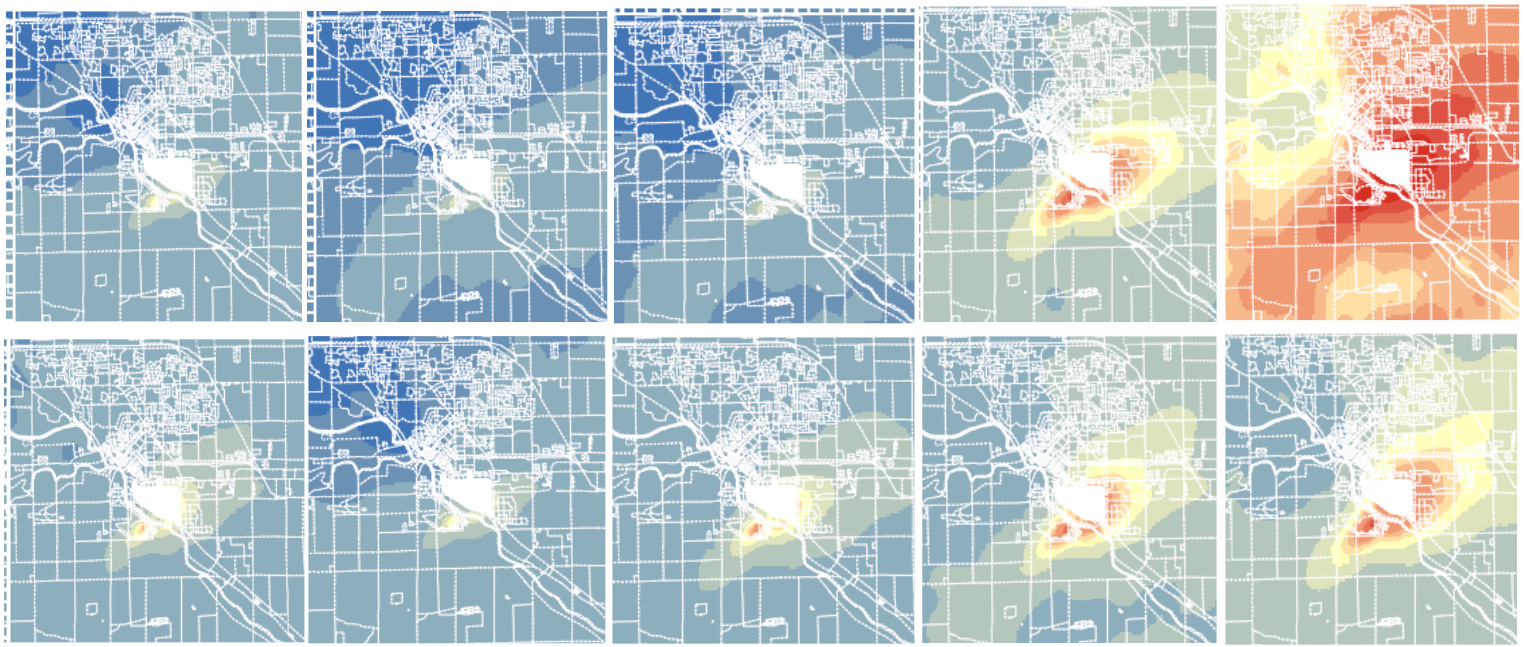

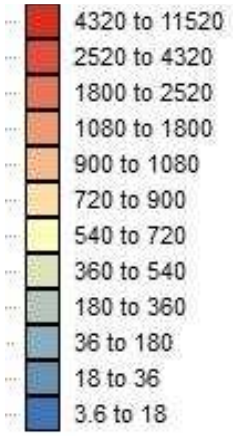

Upper row from left to right: total dry deposition flux (pg/m^2/5years) of TCDD; PeCDD; 1,2,3,4,7,8-HxCDD; 1,2,3,4,6,7,8-HpCDD; OCDD.

Middle row from left to right: total dry deposition flux (pg/m^2/5years) of TeCDF; 2,3,4,7,8-PeCDF; 1,2,3,4,7,8-HxCDF; 1,2,3,4,6,7,8- HpCDF; OCDF.

Figure 6.5. Total dry deposition fluxes of dioxins (upper row) and furans (middle row). The scales of fluxes are depicted in the last three boxes on the right of the lower row. Scale unit of the fluxes is pg/m^2/5years.Grid of census blocks is embedded in each map of Midland. The pollutant source, plant incinerator is located at the middle of the map, in white.

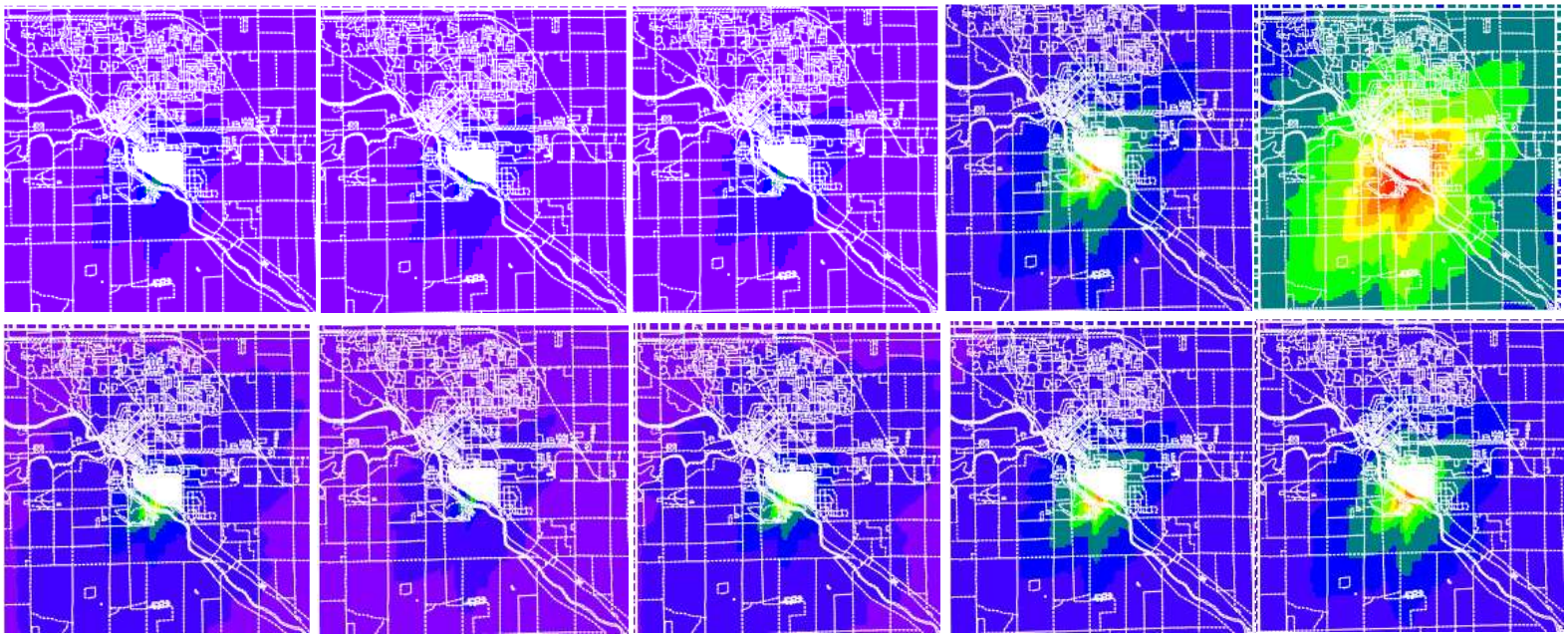

Upper row from left to right: total wet deposition flux (pg/m2/5years) of TCDD; PeCDD; 1,2,3,4,7,8-HxCDD; 1,2,3,4,6,7,8-HpCDD; and OCDD.

Lower row from left to right: total wet deposition flux (pg/m2/5years) of TeCDF; 2,3,4,7,8-PeCDF; 1,2,3,4,7,8-HxCDF; 1,2,3,4,6,7,8-HpCDF; and OCDF.

Figure 6.6. Total wet deposition fluxes of dioxins (upper row) and furans (middle row). The scales of fluxes are depicted in the last three boxes on the right of the lower row. Scale unit of the fluxes is $pg/m^2/5years$.Grid of census blocks is embedded in each map of Midland. The pollutant source, plant incinerator is located at the middle of the map, in white.

Air concentration predicted by AERMOD for 10 dioxin and furan congeners

The spatial distributions of air concentrations predicted by AERMOD for the ten dioxin and furan congeners yielded similar plume shapes as they are calculated following the Gaussian dispersion equation and similar directions impacted by wind speed and other meteorological data. Each congener yields different air concentrations (Figure 6.7) because they are scaled to their emission rates (Figure 6.3.). A typical quantile map of air concentration distributions of TCDD is shown in Figure 6.8. Color bands represent the 10 quantile ranges of the air concentration distribution. The concentration plume is shaped along the North East direction similar to the prevailing wind direction.

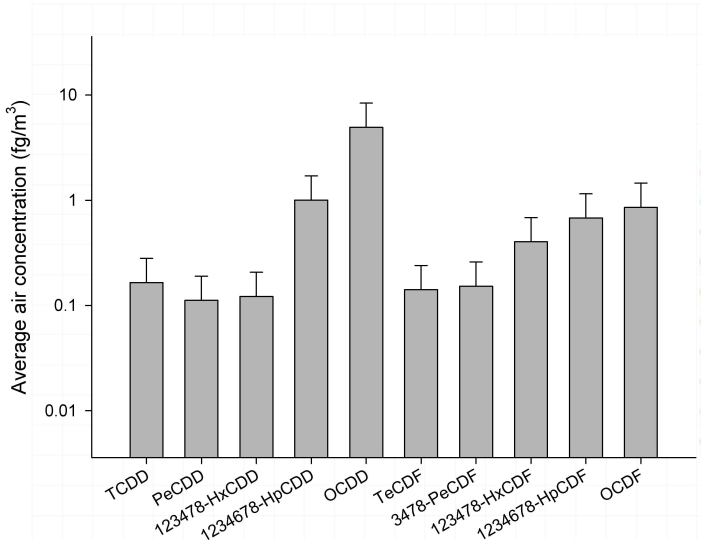

Figure 6.7. Air concentration pattern by mean values. Error bar represents the standard deviation.

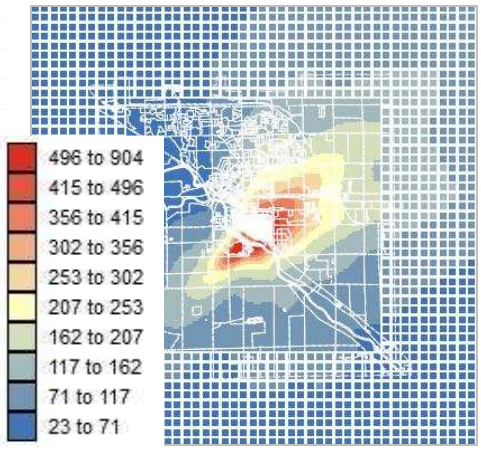

Figure 6.8. Map of air concentration of TCDD predicted by AERMOD with 1992 emission profile adjusted to 1983 emission level (attogram/m^3). Census block layout of Midland is embedded in the map. The plant is located at middle of the map, in white.

The AERMOD estimates for congener-specific air concentrations and deposition fluxes based on the 1992 Dow Chemical Plant incinerator stack emissions adjusted to emission level of 1983 indicated very low concentrations of these contaminants both in air and by deposition on land. Figure 6.8 is a map of TCDD air concentration prediction, which indicates that the TCDD in air ranged from 0.02 fg/m^3 to 0.9 fg/m^3, while OCDD ranged from 0.9 to 27 fg/m^3. These estimates may be an underestimate of the actual measured levels of dioxin in ambient air, based on the following rationale. From the literature, the ambient air levels of total tetra to octa-PCDD/PCDF (and the ΣTEQ) are as follows: remote < 0.5 pg/m^3 (ΣTEQ < 10 fg/m^3); rural ~0.5–4 pg/m^3 (ΣTEQ ~20–50 fg/m^3); and urban/industrial ~10–100 pg/m^3 (ΣTEQ ~100–400 fg/m^3) *(53)*. The fact that AERMOD predictions of air concentrations using 1992 stack emission profile adjusted to 1983 emission level were 2-3 orders of magnitude lower than these reported values (fg/m^3 versus pg/m^3) indicated that even in the 1983-1984 time frame, the emission from Dow incinerators was not the dominant contributor to ambient dioxin levels. In fact, a report from Dow also mentioned that air dispersion modeling work using 1985 emissions could not explain the dioxin level in ambient air *(54)*. Dyke and Amendola *(55)* recently collected dioxin inventories at 6 chlorine facilities in the US, including the Dow Chemical Company's Midland facility during 2000- 2002. They estimated that the total I-TEQ released from these facilities to air ranged from 0.0038 to 3.08 gram/year. These below background emissions of PCDDs/PCDFs further indicate that waste processing operations of the incinerator after 1983 are minor contributors to ambient air concentrations. A second explanation could be that the model specifications and inputs are insufficient to capture actual TEQ and congener specific emissions. Based on the

validation work performed prior to release of this model (Chapter 5), it appears that the model is capable of a predictive accuracy within an order of magnitude.

Our modeling results further indicated that deposition fluxes of dioxins are dominated by the higher chlorinated compounds (HpCDD, OCDD, HpCDF and OCDF). We observed that dry deposition of gas-phase dioxins is a potentially important pathway for the lesser chlorinated PCDD/F congeners (tetra-, penta PCDD/F), contributing from 30 to 50% to total deposition. Wet deposition is less important for these congeners, but this process contributes 10% of the deposition of higher chlorinated congeners (OCDD, OCDF). These observations are similar to those reported earlier *(21)*. However, other literature reports indicated that wet deposition is a major removal pathway or is an equally important removal pathway as dry deposition for dioxins from the atmosphere *(32, 48)*. The difference is likely attributable to the meteorological conditions under which deposition occurs. For example, the sites at which wet and dry deposition fluxes were measured were Bloomington, Indiana *(32)* and Houston, Texas *(48)* where longer periods of warm weather and intense storm activity occur relative to Midland, Michigan. A decrease in temperature was found to be associated with an increase in dry particle deposition *(32, 49, 51, 52)* which may explain the dominant particle-dry removal pathway observed in our study.

VI.4. Conclusions

Aiming at the objects of exploring the air concentration and deposition fluxes in the gas and in the particle phase by wet and dry deposition, the application of AERMOD in predicting dispersion and deposition of dioxin congeners described in this chapter improved model predictions of TEQ dispersion plumes and deposition fluxes in comparison to ISCST3 (Chapters 4 and 5). First, the congener-specific dioxin analysis showed that both dry and wet processes impact HpCDF/D and OCDD/F, whereas dry deposition of particles is important for TeCDF. Second, the site characteristics and detailed meteorological data also showed effects on gas dry deposition, the direction of the dioxin plume and dominant removal pathway of particle-dry deposition. Third, the incorporation of gas phase dry deposition indicated the importance of gas-dry removal pathways for tetra and penta dioxins and furans. Fourth, the partitioning of the total emissions rate into gaseous and particulate emission rates was supported. Lastly, the congener-specific emission profile (1992) demonstrated a predominance of hepta and octa dioxins and furans near the source. Although the emission rate was adjusted to 1983, the obtained model outputs were still well below observed ambient data. The lack of a historical emission profile impacted our ability to predict the distribution of dioxin concentration in the air and deposition on the ground, but even under conservative assumptions the incinerator output cannot explain ambient levels, indicating other contributing sources. In our previous work (Chapters 4 and 5), dioxin TEQs were estimated using available soil TEQs to guide soil sampling. However, TEQ is not a real pollutant and therefore does not have physicochemical meaning, which limits the value of the model output. As individual congeners can be modeled, the weighted sum of these

congeners would result in a more accurate prediction of TEQ values to identify the extent and magnitude of a dioxin plume emitted from an incinerator stack.

Appendix 6.1. Physical properties of dioxins *(19)*

							Le Bas	Diffusivity	Diffusivity
		Chemical	Molecular Weight (g mol-1)	Melting Point (°C)	Boiling Point (°C)	Molecular Volume	Molar Volume (cm3 mol-1)	in Air Da	in Water Dw x 105
Chemical	CAS No.							(cm2 s-1)	(cm2 s-1)
2,3,7,8-TCDD	1746-01-6	C12H4O2Cl4	321.98	305	446.5	241.4	267.8	0.05196	0.4392
1,2,3,7,8-PeCDD	39227-61-7	C12H3O2Cl5	356.43	195	464.7	260.1	288.7	0.04998	0.3993
1,2,3,4,7,8-HxCDD	39227-26-8	C12H2O2Cl6	390.87	273	487.7	278.7	309.6	0.04822	0.3626
1,2,3,4,6,7,8-HpCDD	35822-46-9	C12HO2Cl7	425.32	265	507.2	297.4	330.5	0.04663	0.3287
OCDD	3268-87-9	C12O2Cl8	459.76	322	510	316.1	351.4	0.04519	0.2973
2,3,7,8-TCDF	51207-31-9	C12H4OCl4	305.98	227	438.3	235.3	260.3	0.05269	0.4544
2,3,4,7,8-PeCDF	51207-31-4	C12H3OCl5	340.42	196	464.7	253.9	281.2	0.05063	0.4132
1,2,3,4,7,8-HxCDF	70658-26-9	C12H2OCl6	374.87	225.5	487.7	272.6	302.1	0.0488	0.3754
1,2,3,6,7,8-HxCDF	57117-44-9	C12H2OCl6	374.87	232	487.7	272.6	302.1	0.0488	0.3754
1,2,3,4,6,7,8-HpCDF	67462-39-4	C12HOCl7	409.31	236	507.2	291.3	323	0.04715	0.3406
OCDF	39001-02-0	C12OCl8	443.76	258	537	310	343.9	0.04566	0.3083

Appendix 6.2. Properties of dioxin congeners *(19)*

Chemical		Vapor Pressure	Aqueous Solubility	Henry's Law constant, H			Washout Ratio, Wg		
	CAS No.	(Pa)	(mmol m-3)	(Pa m3 mol-1)	log Kow	log Kcw	(unitless)	rcl (s cm-1)	log Kp
2,3,7,8-TCDD	1746-01-6	2.00 x 10-7	6 x 10-5	3.34	6.8	6.66	7.42 x 102	7.84	-2.94
1,2,3,7,8-PeCDD	39227-61-7	8.80 x 10-8	3.31 x 10-4	0.266	7.4	7.25	9.32 x 103	5.47 x 10-1	-1.21
1,2,3,6,7,8-HxCDD	39227-26-8	5.10 x 10-9	1.13 x 10-5	0.451	7.8	7.63	5.50 x 103	1.2	-1.11
1,2,3,4,6,7,8-HpCDD	35822-46-9	7.50 x 10-10	5.64 x 10-6	0.133	8	7.83	1.86 x 104	5.97 x 10-1	-0.31
OCDD	3268-87-9	1.10 x 10-10	1.61 x 10-7	0.684	8.2	8.02	3.62 x 103	4.94	-0.81
2,3,7,8-TCDF	51207-31-9	2.00 x 10-6	1.37 x 10-3	1.46	6.1	5.98	1.70 x 103	9.67	-3.28
1,2,3,7,8-PeCDF	51207-31-4	3.50 x 10-7	6.93 x 10-4	0.505	6.5	6.37	4.91 x 103	3.99	-2.41
1,2,3,4,7,8-HxCDF	70658-26-9	3.20 x 10-8	2.20 x 10-5	1.45	7	6.86	1.71 x 103	1.11 x 101	-2.41
1,2,3,6,7,8-HxCDF	57117-44-9	3.50 x 10-8	4.72 x 10-5	0.741	NA	NA	3.35 x 103	NA	NA
1,2,3,4,6,7,8-HpCDF	67462-39-4	4.70 x 10-9	3.30 x 10-6	1.43	7.4	7.25	1.73 x 103	1.27 x 101	-2.01
OCDF	39001-02-0	5.0 x 10-10	2.61 x 10-6	0.191	8	7.83	1.30 x 104	1.42	-0.51

References

(1) Bumb, R. R.; Crummett, W. B.; Cutie, S. S.; Gledhill, J. R.; Hummel, R. H.; Kagel, R. O.; Lamparski, L. L.; Luoma, E. V.; Miller, D. L.; Nestrick, T. J.; Shadoff, L. A.; Stehl, R. H.; Woods, J. S., Trace Chemistries of Fire: A Source of Chlorinated Dioxins. *Science* **1980,** 210, (4468), 385-390.

(2) Lustenhouwer, J. W. A.; Olie, K.; Hutzinger, O., Chlorinated dibenzo-p-dioxins and related compounds in incinerator effluents: A review of measurements and mechanisms of formation. *Chemosphere* **1980,** 9, (7-8), 501-522.

(3) Hutzinger, O.; Choudhry, G. G.; Chittim, B. G.; Johnston, L. E., Formation of Polychlorinated Dibenzofurans and Dioxins during Combustion, Electrical Equipment Fires and PCB Incineration. *Environmental Health Perspectives* **1985,** 60, 3-9.

(4) EPA Available: Exposure and Human Health Reassessment of 2,3,7,8-Tetrachlorodibenzo-p-Dioxin (TCDD) and Related Compounds National Academy Sciences (NAS) Review Draft. http://www.epa.gov/ncea/pdfs/dioxin/nas-review/pdfs/part1_vol1/dioxin_pt1_vol1_ch02_dec2003.pdf Accessed June 16, 2009,

(5) Nadine Fréry, A. Z., Hélène Sarter, Grégoire Falq, Mathilde Pascal, Bénédicte Bérat, Perrine De Crouy-Chanel, Jean-Luc Volatier, Anne Thébault *Étude d'imprégnation par les dioxines des populations vivant à proximité d'usines d'incinération d'ordures ménagères*; Institut de veille sanitaire (InVS), Département santé environnement (DSE), l'Agence française de sécurité sanitaire des aliments (Afssa): 2009; p 146.

(6) Fowles, J.; Noonan, M.; Stevenson, C.; Baker, V.; Gallagher, L.; Read, D.; Phillips, D., 2,3,7,8-Tetrachlorodibenzo-p-dioxin (TCDD) plasma concentrations in residents of Paritutu, New Zealand: Evidence of historical exposure. *Chemosphere* **2009,** 75, (9), 1259-1265.

(7) Goovaerts, P.; Trinh, H. T.; Demond, A. H.; Towey, T.; Chang, S. C.; Gwinn, D.; Hong, B.; Franzblau, A.; Garabrant, D.; Gillespie, B. W.; Lepkowski, J.; Adriaens, P., Geostatistical modeling of the spatial distribution of soil dioxin in the vicinity of an incinerator. 2. Verification and calibration study. *Environmental Science & Technology* **2008,** 42, (10), 3655-3661.

(8) Goovaerts, P.; Trinh, H. T.; Demond, A.; Franzblau, A.; Garabrant, D.; Gillespie, B.; Lepkowski, J.; Adriaens, P., Geostatistical modeling of the spatial distribution of soil dioxins in the vicinity of an incinerator. 1. Theory and application to Midland, Michigan. *Environmental Science & Technology* **2008,** 42, (10), 3648-3654.

(9) Floret, N.; Viel, J. F.; Lucot, E.; Dudermel, P. M.; Cahn, J. Y.; Badot, P. M.; Mauny, F., Dispersion modeling as a dioxin exposure indicator in the vicinity of a municipal solid waste incinerator: A validation study. *Environmental Science & Technology* **2006,** 40, (7), 2149-2155.

(10) Lorber, M.; Eschenroeder, A.; Robinson, R., Testing the USA EPA's ISCST-Version 3 model on dioxins: a comparison of predicted and observed air and soil concentrations. *Atmospheric Environment* **2000,** 34, (23), 3995-4010.
(11) Alcock, R. E.; Gemmill, R.; Jones, K. C., Improvements to the UK PCDD/F and PCB atmospheric emission inventory following an emissions measurement programme. *Chemosphere* **1999,** 38, (4), 759-770.
(12) Chang, M. B.; Lin, J.-J.; Chang, S.-H., Characterization of dioxin emissions from two municipal solid waste incinerators in Taiwan. *Atmospheric Environment* **2002,** 36, (2), 279-286.
(13) Cheng, P. S.; Hsu, M. S.; Ma, E.; Chou, U.; Ling, Y. C., Levels of PCDD/FS in ambient air and soil in the vicinity of a municipal solid waste incinerator in Hsinchu. *Chemosphere* **2003,** 52, (9), 1389-1396.
(14) Bakoglu, M.; Karademir, A.; Durmusoglu, E., Evaluation of PCDD/F levels in ambient air and soils and estimation of deposition rates in Kocaeli, Turkey. *Chemosphere* **2005,** 59, (10), 1373-1385.
(15) Kim, B. H.; Lee, S. J.; Mun, S. J.; Chang, Y. S., A case study of dioxin monitoring in and around an industrial waste incinerator in Korea. *Chemosphere* **2005,** 58, (11), 1589-1599.
(16) Lee, C. C.; Chen, H. L.; Su, H. J.; Guo, Y. L.; Liao, P. C., Evaluation of PCDD/Fs patterns emitted from incinerator via direct ambient sampling and indirect serum levels assessment of Taiwanese. *Chemosphere* **2005,** 59, (10), 1465-1474.
(17) Oh, J.-E.; Choi, S.-D.; Lee, S.-J.; Chang, Y.-S., Influence of a municipal solid waste incinerator on ambient air and soil PCDD/Fs levels. *Chemosphere* **2006,** 64, (4), 579-587.
(18) Kim, D. G.; Min, Y. K.; Jeong, J. Y.; Kim, G. H.; Kim, J. Y.; Son, C. S.; Lee, D. H., Ambient air monitoring of PCDD/Fs and co-PCBs in Gyeonggi-do, Korea. *Chemosphere* **2007,** 67, (9), 1722-1727.
(19) Wesely, M. L. D. P. V. S. J. D. *Deposition Parameterizations for the Industrial Source Cmplex (ISC3) Model*; Argonne National Laboratory: 2002.
(20) Basham, J. P.; Whitwell, I., Dispersion modelling of dioxin releases from the waste incinerator at Avonmouth, Bristol, UK. *Atmospheric Environment* **1999,** 33, (20), 3405-3416.
(21) Yoshida, K.; Ikeda, S.; Nakanishi, J.; Tsuzuki, N., Validation of modeling approach to evaluate congener-specific concentrations of polychlorinated dibenzo-p-dioxins and dibenzofurans in air and soil near a solid waste incinerator. *Chemosphere* **2001,** 45, (8), 1209-1217.
(22) EPA, U., User's Guide for the Industrial Source Complex (ISC 3) Dispersion Models **1995,** Vol. 1
(23) EPA, U., User's Guide for the AMS/EPA Regulatory Model - AERMOD. **2006**
(24) EPA, U. *Michigan Dioxin Studies Dow Chemical Building 703 Incinerator Exhaust And Ambient Air Study*; 1987.
(25) EPA *Michigan Dioxin Studies Atmospheric Sampling Fact Sheet*; 1983.
(26) CH2MHILL *Closure plan for the 703 and 830 incinerators* CH2MHILL: 2003; p 32.
(27) MDEQ, Meteorological Data Support Document. In Michigan Department of Environmental Quality: 2009.

(28) MDEQ, Michigan Geographic Data Library. In Michigan Department of Information Technology: 2009.
(29) Eitzer, B. D.; Hites, R. A., Dioxins and furans in the ambient atmosphere: A baseline study. *Chemosphere* **1989,** 18, (1-6), 593-598.
(30) Eitzer, B. D.; Hites, R. A., Polychlorinated dibenzo-p-dioxins and dibenzofurans in the ambient atmosphere of Bloomington, Indiana. *Environ. Sci. Technol.* **1989,** 23, (11), 1389-1395.
(31) Eitzer, B. D.; Hites, R. A., Atmospheric transport and deposition of polychlorinated dibenzo-p-dioxins and dibenzofurans. *Environ. Sci. Technol.* **1989,** 23, (11), 1396-1401.
(32) Koester, C. J.; Hites, R. A., Wet and Dry Deposition of Chlorinated Dioxins and Furans. *Environmental Science & Technology* **1992,** 26, (7), 1375-1382.
(33) Bidleman, T. F., Atmospheric transport and air-surface exchange of pesticides. *Water Air and Soil Pollution* **1999,** 115, (1-4), 115-166.
(34) EPA/OSW, 1996 National Dioxin Database. **1996**.
(35) MDEQ, Dow Hazardous Waste Facility Operating License Information In Michigan Department of Environmental Quality (MDEQ) 2009.
(36) EPA *Addendum to User's Guide for the AMS/EPA Regulatory model AERMOD* 2004; p 40.
(37) Cimorelli, A. J.; Perry, S. G.; Venkatram, A.; Weil, J. C.; Paine, R. J.; Wilson, R. B.; Lee, R. F.; Peters, W. D.; Brode, R. W., AERMOD: A dispersion model for industrial source applications. Part I: General model formulation and boundary layer characterization. *Journal of Applied Meteorology* **2005,** 44, (5), 682-693.
(38) EPA, U., The American Meteorological Society/Environmental Protection Agency Regulatory Model Improvement Committee (AERMIC) *AERMOD* **2006**.
(39) EPA *Addendum to User's Guide for the AERMOD Meteorological Data Preprocessor, AERMET* 2004
p19.
(40) ESRI *ArcMap*, 9.1; 1999-2005.
(41) TerraSeer *Space-Time Intelligence System (STIS)*, 2008.
(42) LakeEnvironmentalSoftwares *WRPLOT - Windrose Plot for Meteorological Data* 5.9; Lake Environmental Softwares: 1988-2008.
(43) Systat *SigmaPlot* 11.0; Systat Inc.: 2008.
(44) Chao, M. R.; Hu, C. W.; Chen, Y. L.; Chang-Chien, G. P.; Lee, W. J.; Chang, L. W.; Lee, W. S.; Wu, K. Y., Approaching gas-particle partitioning equilibrium of atmospheric PCDD/Fs with increasing distance from an incinerator: measurements and observations on modeling. *Atmospheric Environment* **2004,** 38, (10), 1501-1510.
(45) Cimorelli, A. P. G. V. A. e. a. *AERMOD: Description of Model formulation* 2004; p 91.
(46) EPA *AERMOD Deposition Algorithms – Science Document (Revised Draft)*; 2004; p 22.
(47) Kaupp, H.; McLachlan, M. S., Atmospheric particle size distributions of polychlorinated dibenzo-p-dioxins and dibenzofurans (PCDD/Fs) and polycyclic aromatic hydrocarbons (PAHs) and their implications for wet and dry deposition. *Atmospheric Environment* **1999,** 33, (1), 85-95.

(48) Correa, O.; Raun, L.; Rifai, H.; Suarez, M.; Holsen, T.; Koenig, L., Depositional flux of polychlorinated dibenzo-p-dioxins and polychlorinated dibenzofurans in an urban setting. *Chemosphere* **2006,** 64, (9), 1550-1561.
(49) Oka, H.; Kakimoto, H.; Miyata, Y.; Yonezawa, Y.; Niikawa, A.; Kyudoh, H.; Kizu, R.; Hayakawa, K., Atmospheric deposition of polychlorinated dibenzo-p-dioxins (PCDDs) and polychlorinated dibenzofurans (PCDFs) in Kanazawa, Japan. *Journal of Health Science* **2006,** 52, (3), 300-307.
(50) Moon, H. B.; Kannan, K.; Lee, S. J.; Ok, G., Atmospheric deposition of polycyclic aromatic hydrocarbons in an urban and a suburban area of Korea from 2002 to 2004. *Archives of Environmental Contamination and Toxicology* **2006,** 51, (4), 494-502.
(51) Shih, M. L.; Lee, W. S.; Chang-Chien, G. P.; Wang, L. C.; Hung, C. Y.; Lin, K. C., Dry deposition of polychlorinated dibenzo-p-dioxins and dibenzofurans (PCDD/Fs) in ambient air. *Chemosphere* **2006,** 62, (3), 411-416.
(52) Moon, H. B.; Lee, S. J.; Choi, H. G.; Ok, G., Atmospheric deposition of polychlorinated dibenzo-p-dioxins (PCDDs) and dibenzofurans (PCDFs) in urban and suburban areas of Korea. *Chemosphere* **2005,** 58, (11), 1525-1534.
(53) Lohmann, R.; Jones, K. C., Dioxins and furans in air and deposition: A review of levels, behaviour and processes. *Science of the Total Environment* **1998,** 219, (1), 53-81.
(54) EPA, Soil Screening Survey At Four Midwestern Sites **1985**, 163.
(55) Dyke, P. H.; Amendola, G., Dioxin releases from US chemical industry sites manufacturing or using chlorine. *Chemosphere* **2007,** 67, (9), S125-S134.

Chapter 7

Validation of the Local Uncertainty Model to Predict Soil Concentrations of Dioxin Congeners in the Vicinity of an Incinerator

7.1. Introduction

The regulatory AERMOD air dispersion model *(1)* currently is in the process of replacing the ISCST3 *(2)* model to predict air concentration and deposition fluxes from incinerators. In our modeling work (Chapters 5 and 6), we applied both ISCST3 and AERMOD to assess the dispersion plume and deposition fluxes of total dioxin toxic equivalents (TEQ) and specific dioxin congeners.

Our results indicated that the deposition fluxes of dioxins are dominated by the higher chlorinated compounds (HpCDD, OCDD, HpCDF and OCDF). We observed that dry deposition of gas-phase dioxins is important for the lesser chlorinated PCDD/F congeners (tetra-, penta PCDD/F), with contributions ranging from 30 to 50% to the total deposition. Wet deposition is less important for these congeners, but this process contributes 10% of the deposition of higher chlorinated congeners (OCDD, OCDF). The air dispersion modeling results, however underpredicted the ambient level of dioxins measured around municipal incinerators. This is presumably due to inaccurate

measurements in earlier decades when the emissions were highest or because the incinerator emissions were low relative to other sources. For example, if the emission rates from the 1992 incinerator stack test (when Dow was operating a 99.9999% efficient process) at the Dow Chemical Company *(3)* are applied as the model input, the discrepancy in the modeling results and ambient level of dioxins ranges from 3 to 4 orders of magnitude. The total TEQ equivalent of dioxin emission at Dow in 1992 was reported to be as low as 0.033 grams. Dyke and Amendola *(4)* concluded that the air releases of dioxins at 6 chlorine production facilities, including Dow Chemical at Midland, were not significant, with inventory levels ranging from 0.0038 g I-TEQ to 3.08 g I-TEQ for the year 2000. Before 1992, there are very few emission data reported for the Dow Chemical Hazardous Waste Incinerator (HWI), of which the highest level of dioxin release in TCDD equivalents was greater than 12 grams in 1983 *(5), (6)*. Predictions of air concentrations and deposition fluxes based on simulations from the air dispersion model thus can not fully explain the level of ambient air dioxins in the vicinity of the incinerator of Dow Chemical as (at least the 1992) emission level was already low due to regulatory compliance. To test the hypothesis whether dioxin contamination in Midland soils can be explained by historical emissions from the incinerator complex, we previously used information from dry and wet deposition fluxes based on the air dispersion model (ISCST3) to analyze spatial trend of dioxins in Midland soil *(7, 8)*. This exercise *(7)*indicated that dry and wet deposition fluxes were correlated with soil data ($r = 0.641$ and $r = 0.344$ for dry and wet deposition, respectively). These two variables and their interaction term were regressed against the normal score transformation of soil data, explaining 43.7% of the total variance in soil TEQ concentrations. The geostatistical

model which used the air dispersion model-generated maps of spatial distributions surrounding the Dow Chemical Plant in Midland, Michigan was used to determine the probability of a soil concentration being above the threshold value of 90 ppt, the criteria specified by the Michigan Department of Environmental Quality (MDEQ) for dioxin remediation *(9)*. The geostatistics-based aggregated concentrations at the census block support level informed the soil sampling design at the University of Michigan Dioxin Exposure Study for the Midland area *(10)*.

Cross validation of concentrations based on the air dispersion models such as ISCST3 and AERMOD is limited *(8)*. Model validation for AERMOD is often based on comparing the model predictions (air concentrations) against the available air samples *(11-15)*. Although AERMOD or ISCST3 can predict contaminant deposition fluxes, the direct comparison of model outputs and ground level concentrations of contaminants are more difficult. Literature reports have coupled the dispersion model with soil models – what is a soil model*(16, 17)* or statistical models *(7, 8, 18)* to obtain soil concentration predictions. For example, Goovaerts et al. (2008) used a probabilistic approach *(7, 8)* to assess local uncertainties of the predictions, and demonstrated that predicted TEQ quantiles were within the uncertainty range of soil values more than 50% of the time. This chapter further explores the air dispersion model and geostatiscal modeling approach to predict spatial distribution of specific dioxin congeners emitted from the incinerator in Midland.

7.2. Materials and Methods

Previous work (Goovaerts et al., 2008ab) introduced the theory and application of geostatistical modeling as well as a validation exercise for predicting TEQ distribution in soil (see also Chapter 3) *(10)*. Using the same approaches, this Chapter assesses the spatial distributions of 10 specific congeners using the new air dispersion model (AERMOD instead of ISCST3); the emission profile of the 1992 Dow stack test (because it provided complete dioxin-specific information instead of just TEQ); the higher bulk dioxin emission of 1983; and by incorporating partitioning properties of dioxin congeners.

As opposed to our 2008 papers (where we did not discriminate between particulate and vapor phases), this Chapter describes the dry and wet deposition fluxes of each dioxin congener as the sum of both deposition fluxes via particulate and vapor phase deposition pathways. Ten dioxin and furan congeners were selected: 2,3,7,8-Tetrachlorodibenzo-p-dioxin (TCDD); 1,2,3,4,7-Pentachlorodibenzo-p-dioxin (PCDD); 1,2,3,4,7,8-Hexachlorodibenzo-p-dioxin (1,2,3,4,7,8-HxCDD);1,2,3,4,6,7,8-Heptachlorodibenzo-p-dioxin (1,2,3,4,67,8-HpCDD); Octachlorodibenzo-p-dioxin (OCDD); 2,3,7,8-Tetrachlorodibenzofuran (TeCDF); 2,3,4,7,8-Pentachlorodibenzofuran (PeCDF); 1,2,3,4,7,8-Hexachlorodibenzofuran (1,2,3,4,7,8-HxCDF); 1,2,3,4,6,7,8-Heptachlorodibenzofuran (1,2,3,4,6,7,8-HpCDF) and Octachlorodibenzofuran (OCDF).

Dioxin congeners are modeled with their specific physiochemical properties, which are not applicable to TEQ in our previous work *(7, 8)*. Data inputs (meteorological data, dioxin emission profile and site characteristics) for AERMOD were collected for the

Midland area *(19-22).* The observed trend in wet and dry deposition fluxes for dioxin homologues indicates a domination by the higher chlorinated compounds, and shows that dry deposition is more important than wet deposition for the lesser chlorinated dioxin congeners. The predictive trends using AERMOD differ from those based on ISCST3, in part because the latter was based on TEQ which allows less resolution. 51 UMDES soil samples of dioxin congeners will be used in the model validation step, which should allow for an improved correlation between the predicted and measured trends. Lastly, AERMOD produced dry and wet deposition fluxes that will be incorporated into a geostatistical model using sequential Gaussian simulation (sGS) to compute soil concentrations for every receptor of a 261 by 261 grid with spacing of 50 m between grid nodes as same as described in Chapter 4 with ISCST3 model.

Geostatistical Model. The procedure of geostatistical modeling was detailed in *(7, 8)* and was described in Chapter 3. The set of 51 soil congener data that were used in the model were treated as follows:

1. The congener concentrations were normal score transformed to correct for the strongly positively skewed sample. Because the UMDES samples were preferentially located in census blocks with expected high concentrations of dioxins (based on the prior ISCT3 model predictions), sample statistics likely overestimate the magnitude of the contamination over the entire modeled area.
2. The 51 transformed data were regressed against the deposition (wet and dry) values predicted by AERMOD using the emission profile of 1992 and the bulk emission of 1983. Meteorological data and site information were collected from

the Midland area, as described in Chapters 5 and 6). This resulting regression model was used to predict the congener concentration and standard error at the nodes of the 261×261 simulation grid centered on the incinerator. The grid, which has a 50 m spacing, does not include any node within the boundary of the plant.

3. The spatial variability of regression residuals was modeled using a variogram based on the 51 measured data.
4. Sequential Gaussian simulation was used to simulate the spatial distribution of congener values conditionally to the 51 UMDES congener observations, the trend model inferred from the calibration of the deposition data (step 2) and the pattern of correlation modeled in step 3. One hundred realizations were generated over the 261×261 simulation grid.
5. Point simulated values were averaged within each census block to yield a simulated block value (upscaling). This averaging was repeated for each realization, yielding a set of 100 simulated values for each census block. E-type mean over100 realizations were derived.

The procedure SAS GLM *(23)* was used for the regression, while normal score transform was conducted using the program *nscore* in the public domain software library, GSLIB*(24)*. Sequential Gaussian simulation with local means was implemented by modifying the FORTRAN source code Sgsim in GSLIB. Semivariogram models, aggregation within census blocks and mapping were accomplished using TerraSeer STIS (Space-Time Intelligence System)*(25)*, a commercially available product.

Validation of the Geostatistical Model of Uncertainty. Details of validation procedure was described in chapter 3. Boxplot, probability plot and accuracy plot were used to validate the predictions at 51 closest grid nodes to the locations of the UMDES soil samples.

7.3. Results and Discussion

UMDES dioxin congener concentrations. Figure 7.1 (a-k) shows the histograms of the 51 soil data of 10 congeners used in the geostatistical modeling. UMDES soil concentrations are skewed right, where particularly OCDD, TeCDF and PeCDF, OCDF have big outliers. For example, the maximum observation of OCDD was 15,300 ng/g soil, while the mean value was 4,600 ng/g soil; the maximum observation of TeCDF was 1720 ppt while its mean value was 46.5 ppt; and the maximum observation value of PeCDF was 822 ppt while its mean value was 25 ppt. We observed that soil concentrations of the 5 furan congeners are distributed with more extreme values than those of the 5 dioxin congeners among the 51 soil available data. Extreme outliers in the distribution of the true observations will likely affect the point simulation values. As required by sequential Gaussian simulation, soil data are first normal transformed to avoid the skewedness in the data distribution*(26)*.

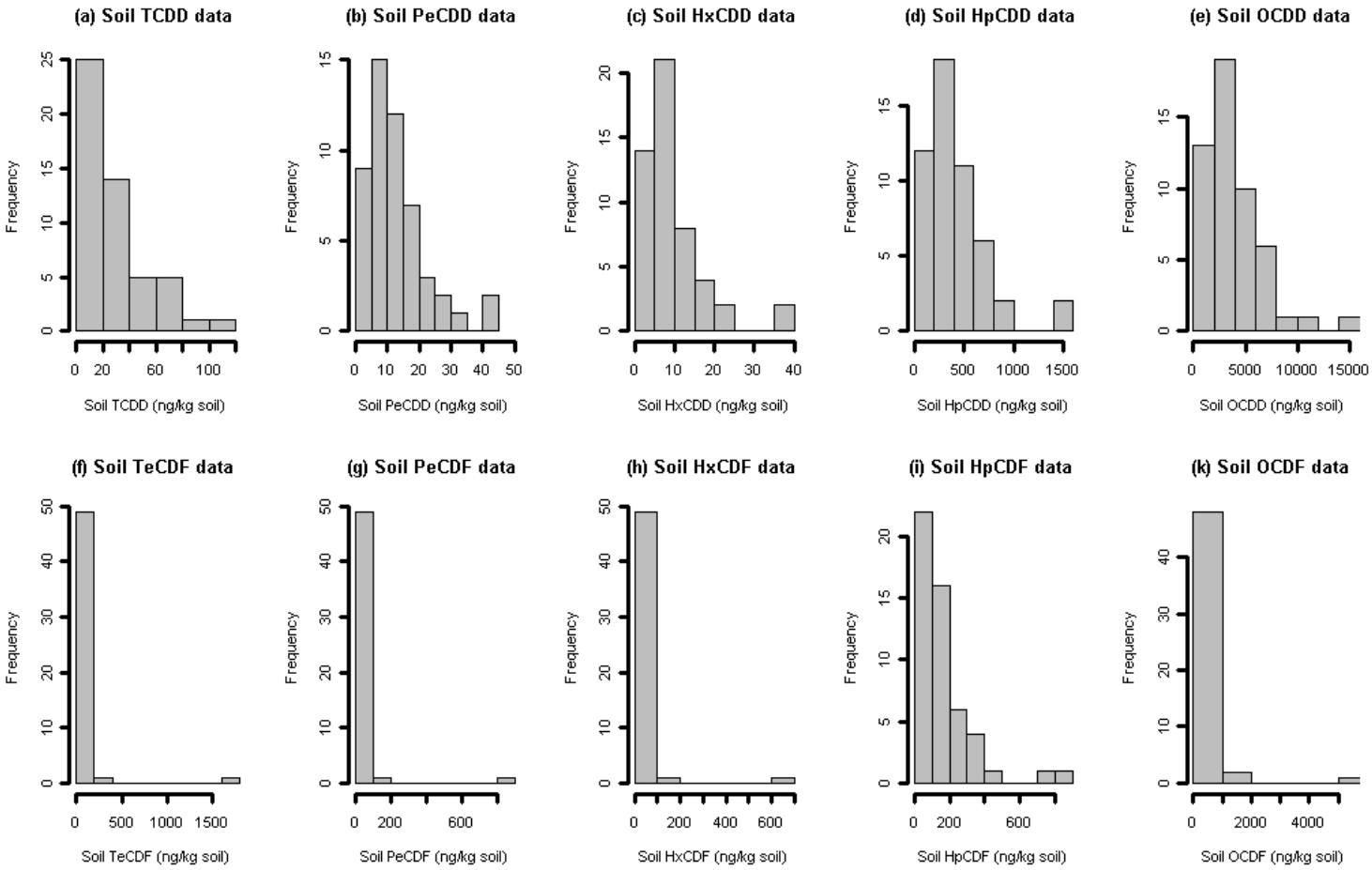

Figure 7.1 (a-k). Histograms of 51 soil dioxin congener data measured within 261x261 grid nodes.

Table 7.1: Descriptive statistics of congener concentration in soil (N = 51).

Column	Mean	Std Dev	Std. Error	C.I. of Mean	Max	Min	Median	25%	75%
TCDD	27.1	24.0	3.4	6.7	117.0	0.9	20.3	9.7	34.1
PeCDD	12.6	9.0	1.3	2.5	42.3	0.7	10.5	6.2	16.0
HxCDD	9.7	7.7	1.1	2.2	36.9	0.8	7.6	3.9	12.6
HpCDD	419.4	303.8	42.5	85.4	1600.0	42.4	343.0	209.5	548.0
OCDD	3922.9	2805.7	392.9	789.1	15300.0	422.0	3220.0	1805.0	4950.0
TeCDF	52.3	243.0	34.0	68.4	1720.0	1.1	6.6	2.8	16.8
PeCDF	29.5	114.8	16.1	32.3	822.0	1.3	6.6	3.4	15.4
HxCDF	31.3	97.6	13.7	27.4	684.0	1.4	11.6	4.9	19.8
HpCDF	171.0	169.8	23.8	47.8	885.0	20.1	121.5	65.7	200.3
OCDF	436.5	772.8	108.2	217.4	5500.0	31.6	280.0	148.5	453.3

Geostatistical model. Dry and wet deposition fluxes of each congener were regressed against normal score transformed 51 available soil data to derive a residual trend of normal score predictions. This spatial trend and the semivariogram parameters of the normal score residuals are then incorporated in sequential Gaussian simulations. Auto correlations from the congeners' variograms are at distances of 284 m for most of the compounds TCDD, PeCDD, HxCDD, HpCDD, OCDD and OCDF; at range of 400 m for PeCDF and HxCDF; and at 6-700 m for TeCDF and HpCDD. (Figure 7.2(a,b)).

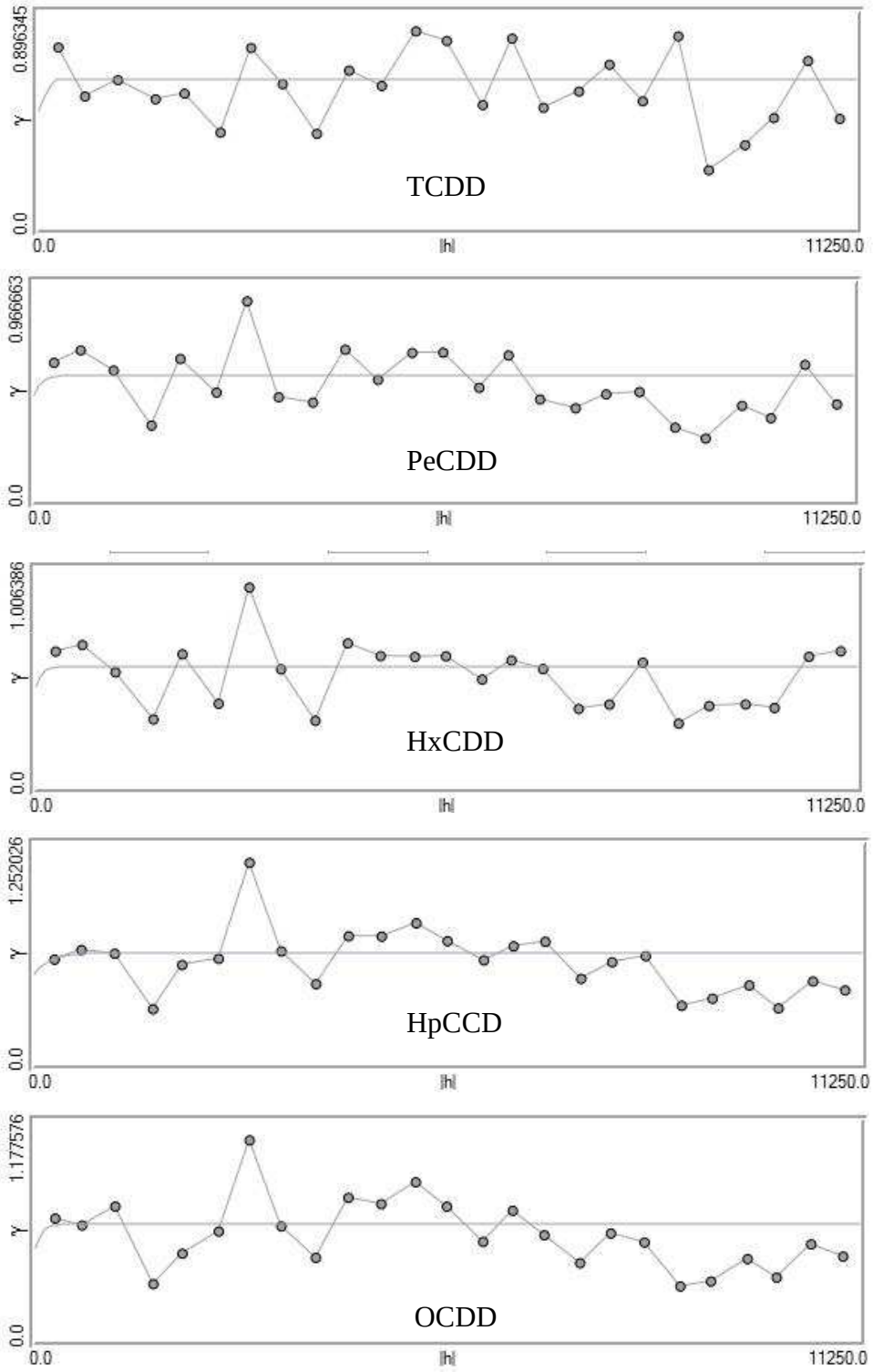

Figure 7.2 a. Variograms of 5 dioxin congeners.

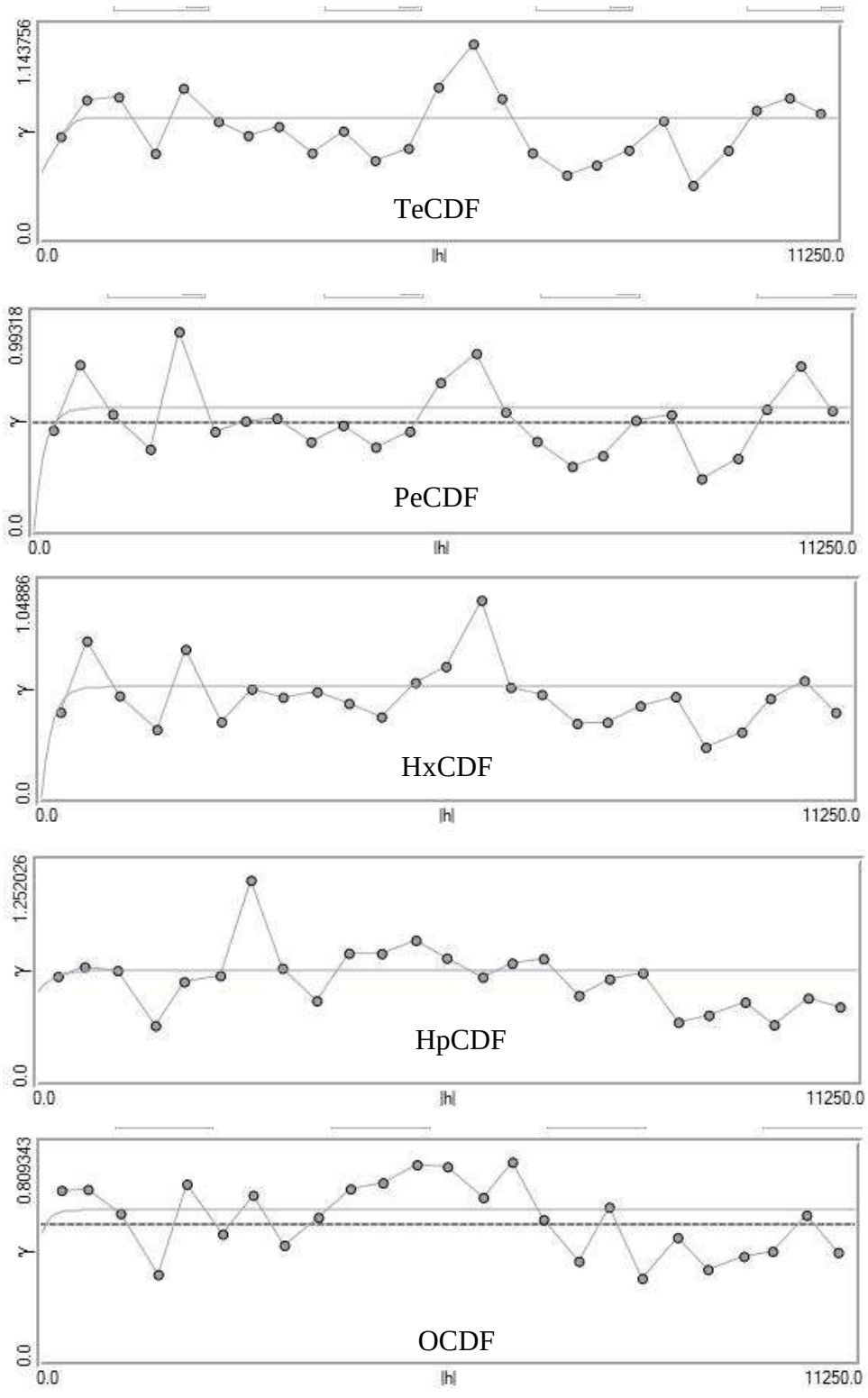

Figure 7.2b. Variograms of 5furan congeners.

Table 7.2 and Figure 7.3 (a,b,c,d) show the correlation coefficients of dry deposition flux and wet deposition fluxes with normal score transformed soil data for each congener. Congeners are in short abbreviation (4-D for TCDD, 5-D for PeCDD, etc.)

Table 7.2. Regressions of dry and wet deposition fluxes against available soil data.

Normal score transformation of congeners	4-D	5-D	6-D	7-D	8-D	4-F	5-F	6-F	7-F	8-F
Dry deposition flux (correlation coefficient)	0.05	0.17	0.06	0.14	0.17	-0.08	0.08	0.02	0.1	0.09
Wet deposition flux (correlation coefficient)	0.65	0.71	0.70	0.67	0.67	0.64	0.71	0.71	0.74	0.69
Total variance in soil data explained by regression model (R-square)	0.64	0.67	0.66	0.56	0.55	0.13	0.17	0.24	0.39	0.40

We observed that wet depositions were highly correlated (70%) with soil congener data while dry depositions were much less correlated (30% or less). As in our previous reported results using the meteorological data from Alpena (for surface data) and Flint station (for upper air data) during 1987-1991, the TEQ-based soil concentrations were better correlated with dry deposition fluxes (predicted by ISCST3; r = 0.64) and less correlated with wet deposition fluxes (r=0.34)*(7)*. As the meteorological data used in the AERMOD model were from Midland, we observed an opposite trend. Wet deposition was clearly correlated with dioxin congeners while dry deposition was not. The results were similar to observations from Koester and Hites at a sampling site in Bloomington, Indiana. *(27)*.

SAS program regressed normal score data of each congener with its wet and dry deposition variables as well as with the interaction term between these two variables. The total variance in soil data explained by the regression R-square value indicated that

dioxin congeners are better predicted than furan congeners (more than 50% of total variance is explained, table 7.2). In case of TEQ, the ISCST3 coupled geostatistical model explained 43.7% of total variance in soil TEQ concentrations *(7)*.

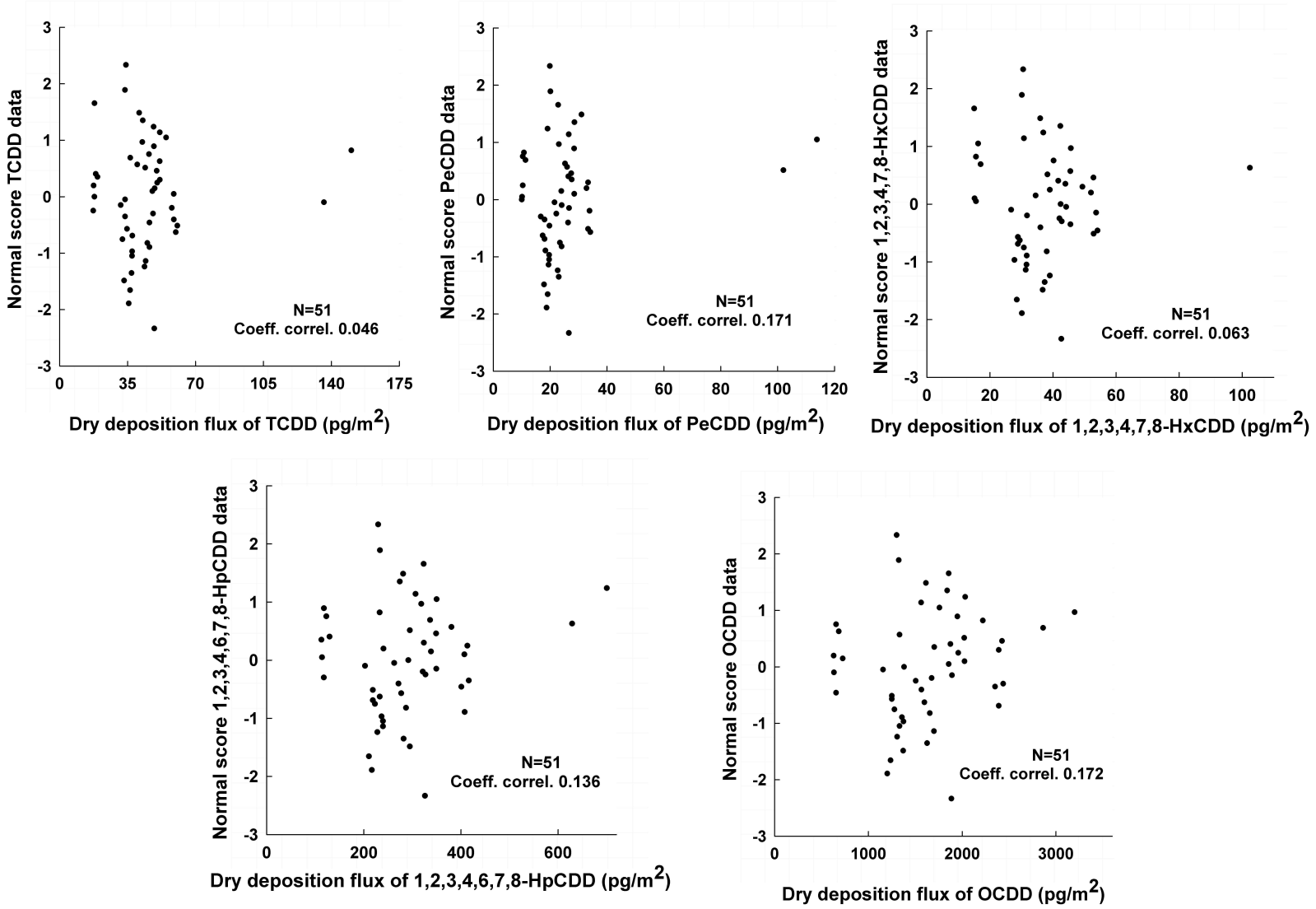

Figure 7.3a. Scatter plots of dry deposition fluxes and normal score transformations of dioxins at 51 sampled locations.

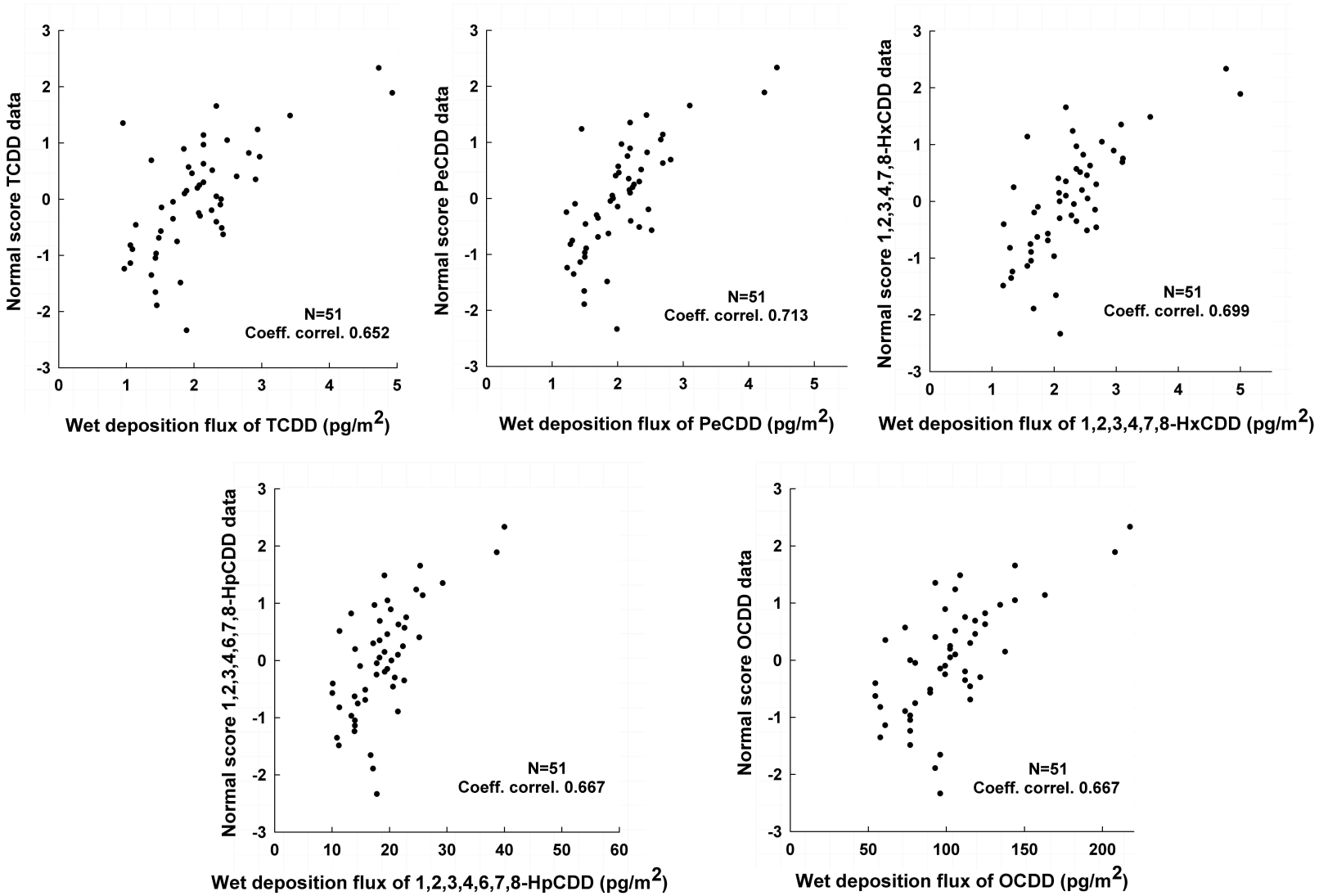

Figure 7.3b. Scatter plots of wet deposition fluxes and normal score transformation of dioxins at 51 sampled locations.

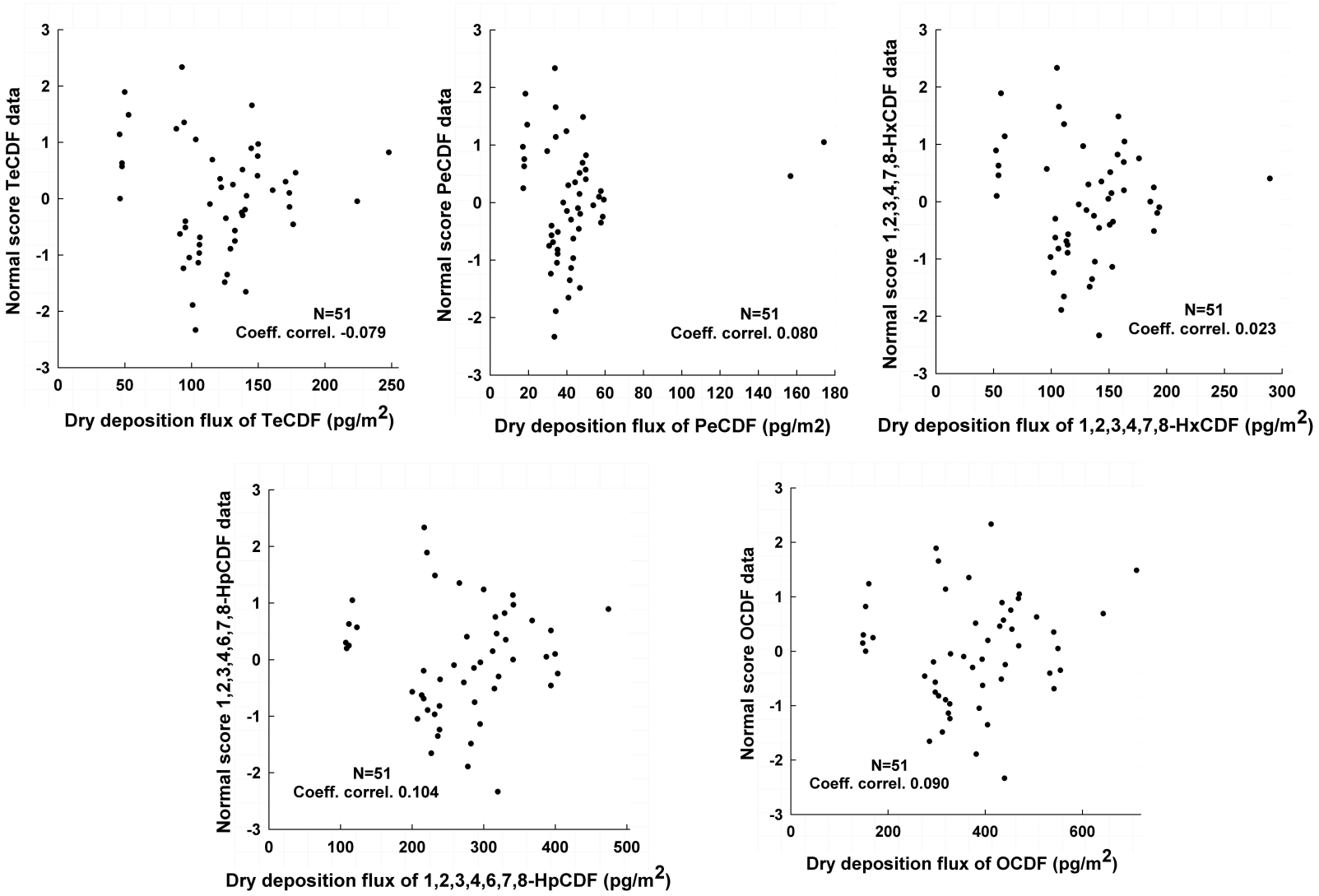

Figure 7.3c. Scatter plots of dry deposition fluxes and normal score transformations of furans at 51 sampled locations.

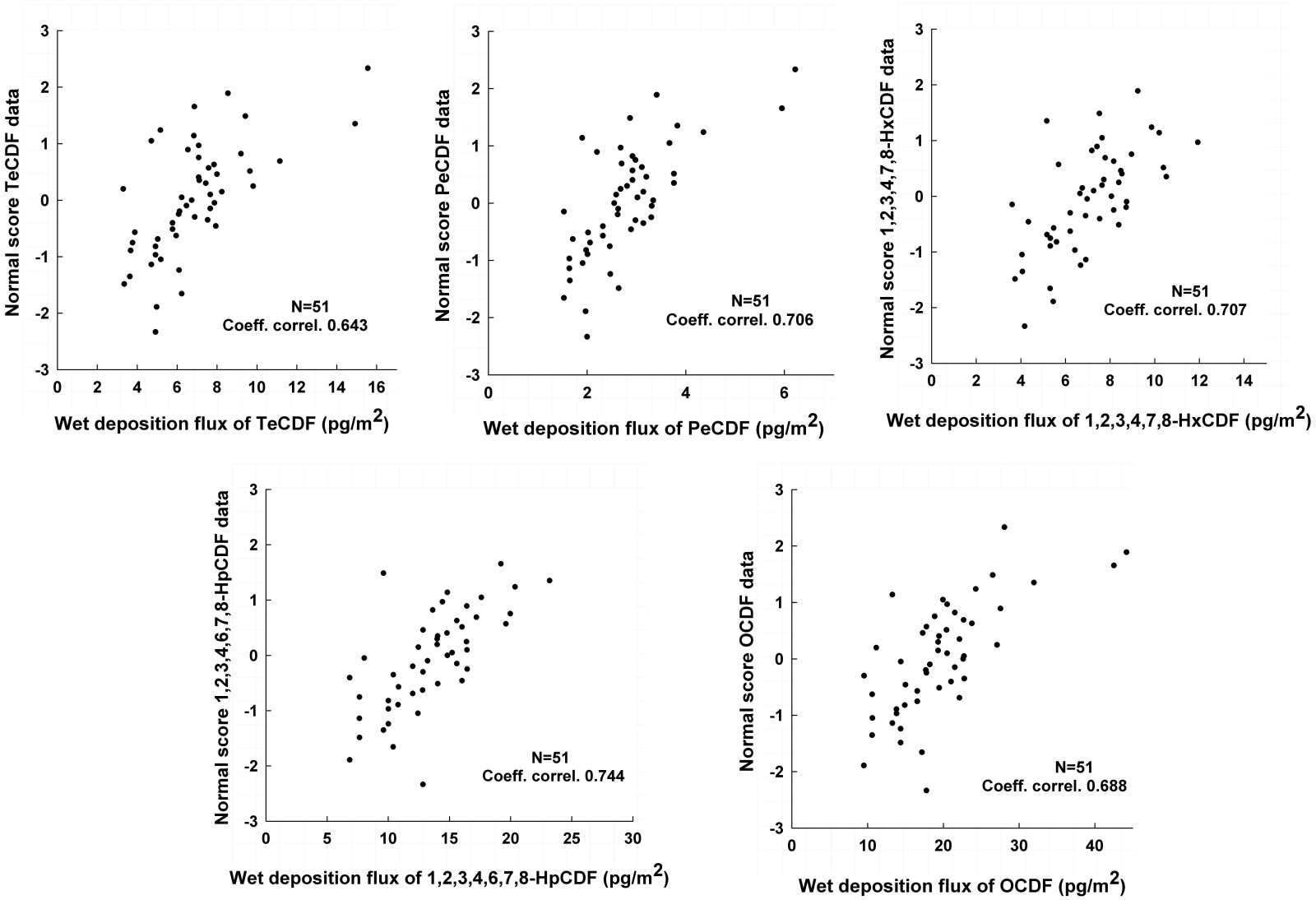

Figure 7.3d. Scatter plots of wet deposition fluxes and normal score transformations of 5 furans at 51 sampled locations.

For each congener, the point-simulated values at 261x261 grid nodes exhibit a similar pattern (Figure 7.4), which showed higher values in close proximity to the incinerator (middle of the figure, in white area). The high values are dominating in the south and south-west of the plant, where high correlations between soil data and wet deposition are observed. The spatial distribution of soil data also has impacts on the plume shape as high soil concentration values are more likely found close to the plant. We observed a similar trend in our previous work in that the highest soil TEQs are predicted closest to the incinerator stack, reflecting the locations where the highest dioxin values were measured*(7, 8)*. Figure 7.4 illustrates examples of mean point simulated values obtained for TCDD (top-left), TeCDF (top-right); PeCDD (bottom-left) and PeCDF (bottom-right). PeCDF is dominant across the entire area, probably due to the high maximum soil measurements. The concentration plumes of TCDD, TeCDF and PeCDD have a similar shape along the south-west direction and reflect high values close to the plant. All the maps have the same color scale for the concentrations of the 4 congeners. As seen from these maps, the red color was used to describe the dominance of predicted PeCDF concentrations. In a full observation for all 10 congeners, it is difficult to use a color spectrum to represent the variability in concentrations from the minimum to maximum concentrations across all congeners, especially for hepta and octa dioxins. The dominance of the heavier congeners such as hepta and octa reflects the congener-specific emission profile (1992), which demonstrated a predominance of hepta and octa dioxins and furans near the source. To simplify the congener plume representations, we averaged the point simulated values into census-block averaged values for each congener and weighted for their toxic equivalency factor attributions *(28)*. The dioxin and furan congeners' TEQ-weighted concentrations are presented in Figure 7.5(a,b).

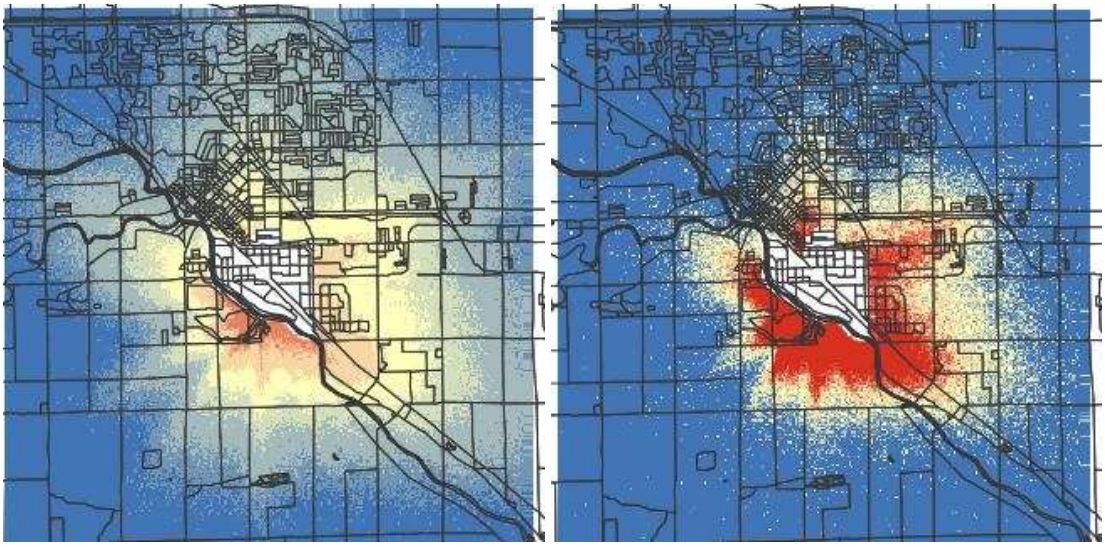

TCDD **TeCDF**

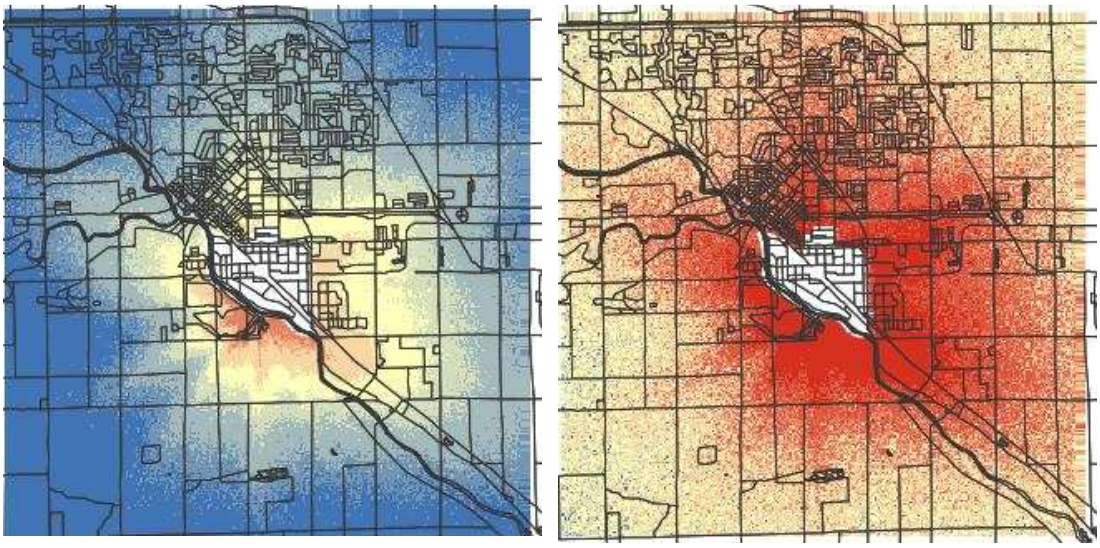

PeCDD **PeCDF**

Figure 7.4. Mean point simulated values over 100 realizations at 261x261 grid nodes. The selected sub-figures are for the 4 high TEQ weighted-congeners, including TCDD (top-left), PeCDD (bottom-left), TeCDF (top-right) and PeCDF (bottom-right). Scales of concentrations are in ng/g of soil.

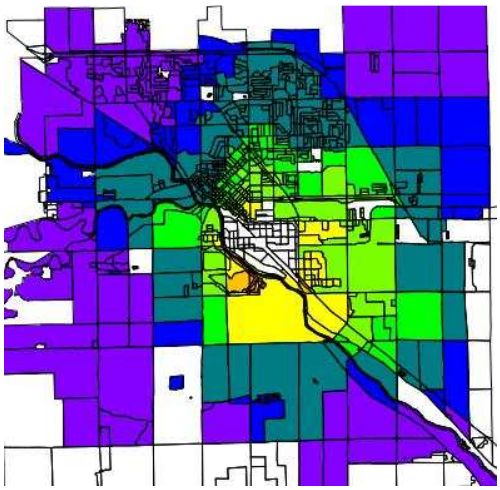

TCDD

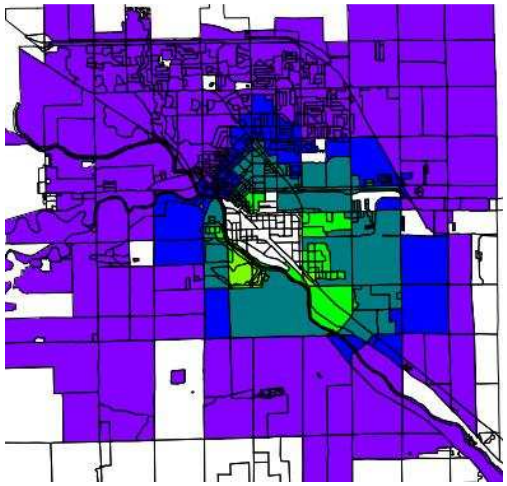

PeCDD

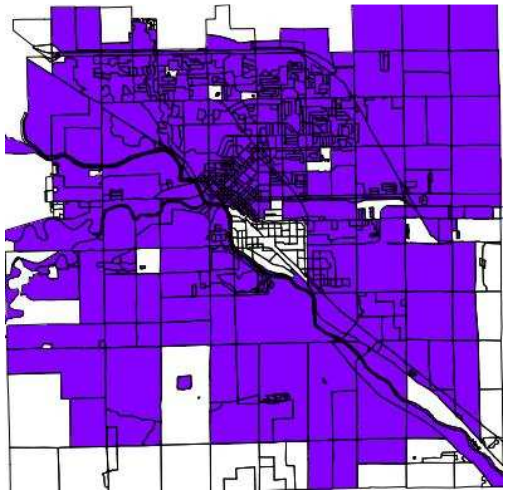

HxCDD

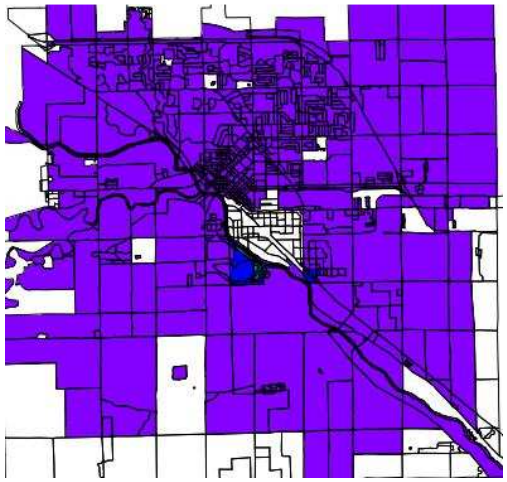

HpCDD

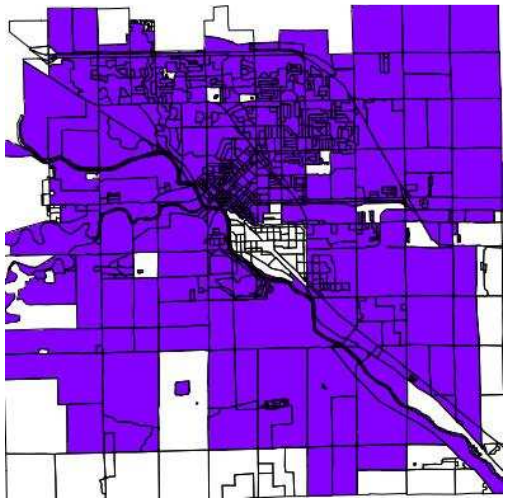

OCDD

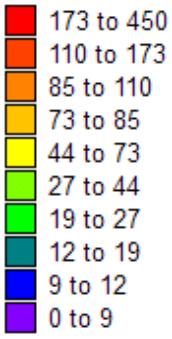

Figure 7.5 a. Predictions of average concentrations of dioxin congeners as TEQ equivalents at census block level (ppt).

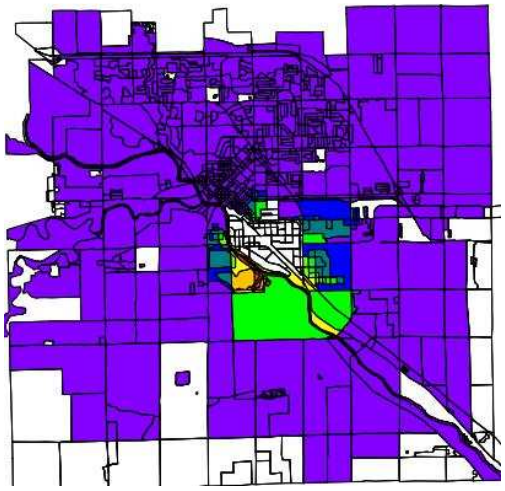

TeCDF

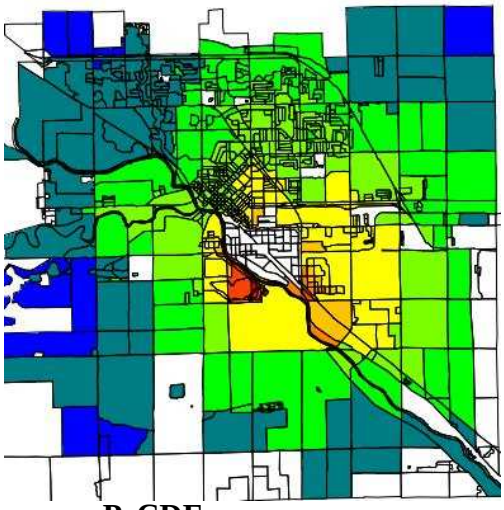

PeCDF

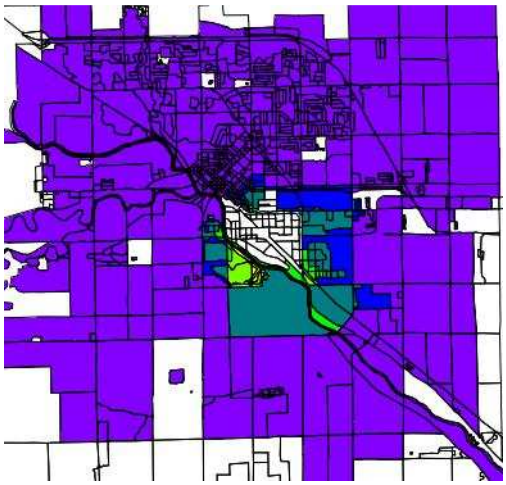

HxCDF

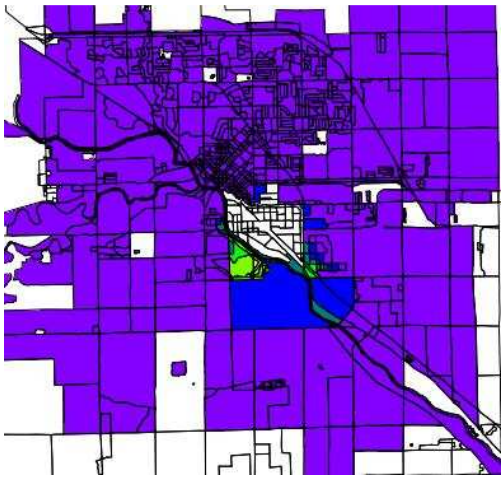

HpCDF

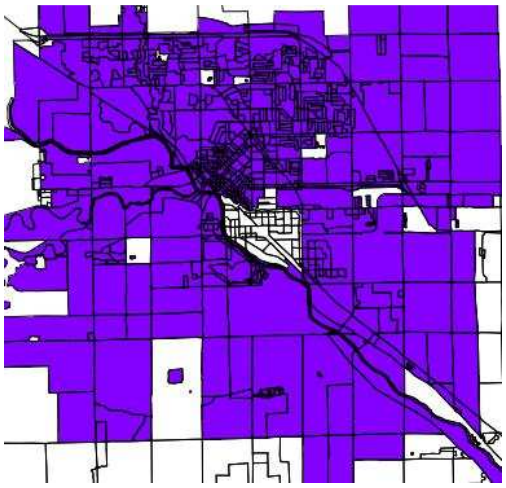

OCDF

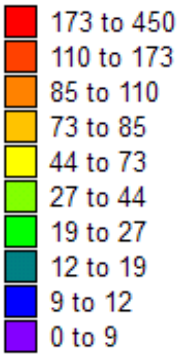

Figure 7.5 b. Predictions of average concentrations of furans congeners as TEQ equivalents at census block level (ppt).

Figure 7.6 (a,b) represents the census block averaging of TEQs predicted by AERMOD coupled with geostatistical model using the emission of 1983and the 51 UMDES soil samples (b) and by ISCT3 coupled with geostatistical model using 53 MDEQ soil samples as described in chapter 4*(8)*. A few observations can be made: (i) the extent of the 'soil plume' is more close to the plant based on AERMOD air dispersion model than the plume based on ISCT3 air dispersion models; (ii) the extent of contamination of the highest TEQ areas around the plant is similar, indicating that the geostatistical model is robust and is not significantly influenced by the deposition models.

When scatter-plotting the averaging TEQ predictions on census blocks of the two mentioned modeling works, additional observations are to include such that: ISCT3air dispersion based model predicted higher TEQ values up to about 70 ppt than those resulted from AERMOD air dispersion based model (Figure 7.7). The higher predicted TEQ values from ISCST3 based model to AERMOD based model were distributed further out of the plant. On the contrary, AERMOD based model predicted much higher TEQs, over 70 ppt than what ISCST3 based model could predict in the close vicinity of the plant. The overlaid cumulative distribution functions of the two data sets, UMDES51 used by AERMOD based model and MDEQ53 used by ISCST3 based model (Figure 7.8) can help to explain these observations. As depicted in Figure 7.8, below value of about 70 ppt, the MDEQ soil data set are higher than that of the UMDES data per any quantile of the distributions. These lower segments of the distributions likely scattered far away from the plant. ISCST3 based model used the MDEQ soil data set to regress with ISCST3's deposition fluxes interpolated higher TEQs values further away from the plant than the

AERMOD based model which employed the UMDES data set to regress with AERMOD's deposition fluxes. At the upper tails of the distributions (above 70 ppt), the UMDES soil data set are higher than the MDEQ soil data set at every quantile of the distributions (Figure 7.8). These higher TEQ values of the UMDES data set likely distributed immediately close to the plant, leading to the higher TEQs predicted by AERMOD based model.

(a) (b)

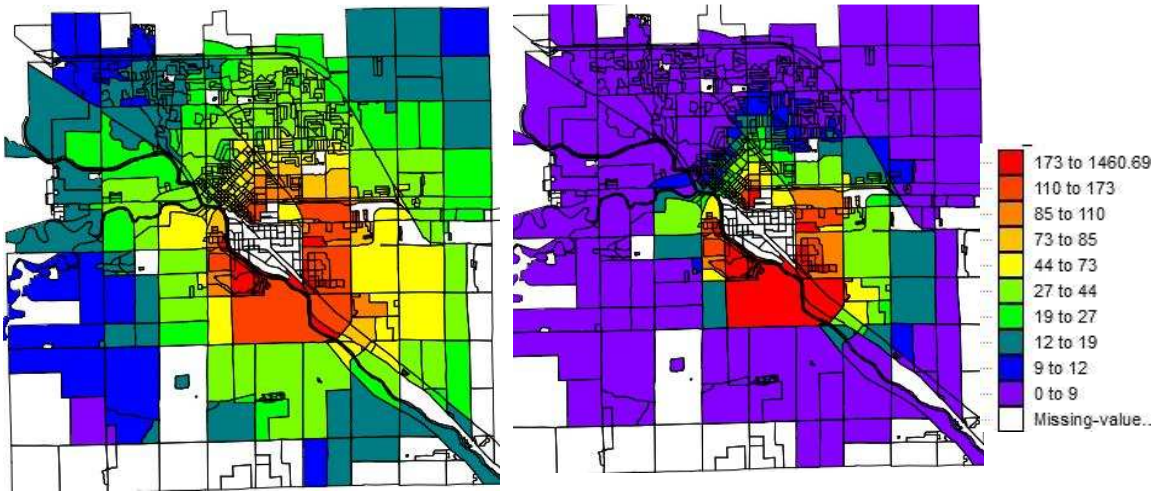

Figure 7.6 (a,b). Mean values of TEQ predictions at census block level (a): TEQ deposition modeled using ISCST3; and (b): TEQ deposition modeled using AERMOD.

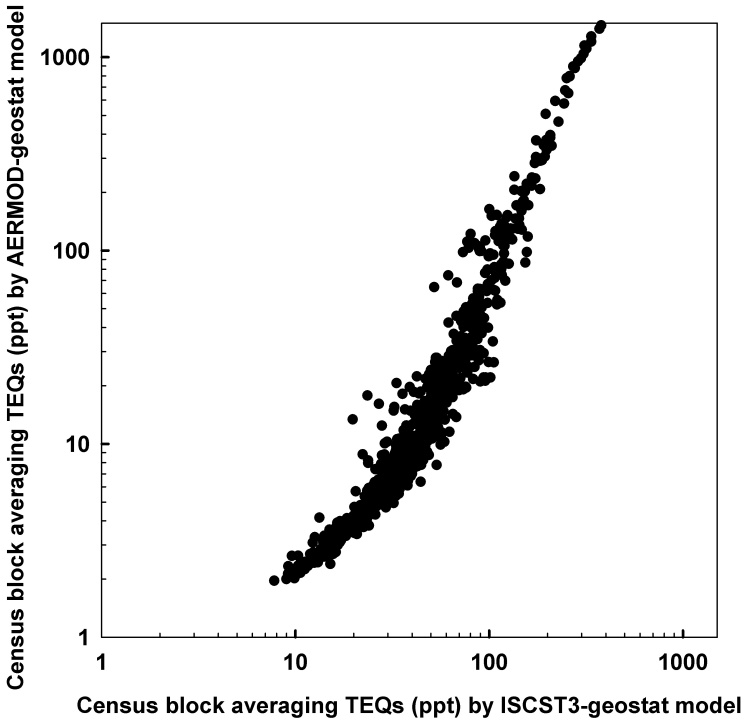

Figure 7.7. Scatter plot of mean TEQs at census block level with deposition modeling using ISCST3 (on x-axis) and using AERMOD (on y-axis).

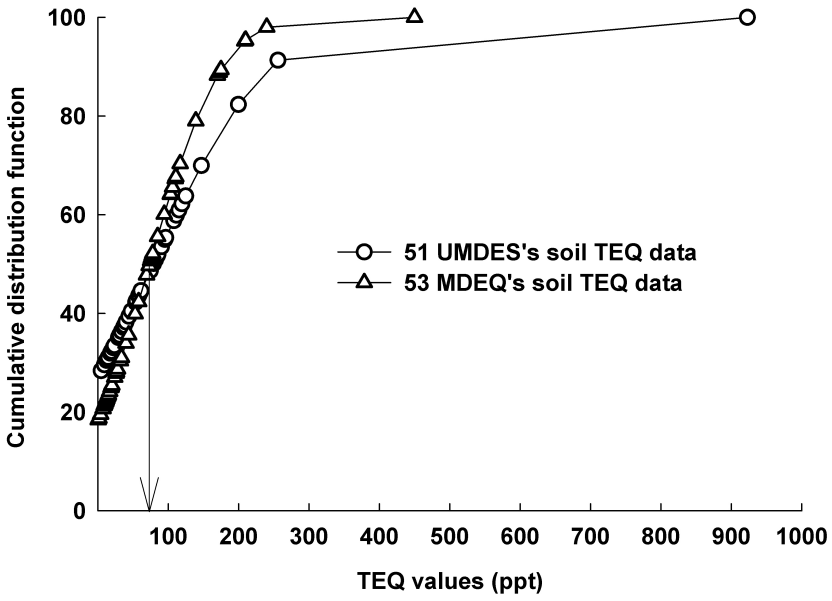

Figure 7.8. Cumulative distribution functions of UMDES 51 soil TEQ data and MDEQ 53 TEQ soil data.

Validation of dioxin congener's prediction. Each of the 51 UMDES data was compared to the distribution of 100 TEQ values simulated at the closest grid node. Modified box plots in Figure 7.9 (a-c) summarize the results for all 51 sampled locations, repeatedly for 10 dioxin and furan congeners. At each of the 51 locations, a vertical bar was plotted representing the 25–75 quantile range of the distribution of 100 simulated realizations (local distribution). The minimum and maximum simulated values are bounded by lines over the vertical bar. The true value of the soil data at that location is denoted by dark triangle symbol. On the x-axis of each sub-figure, the distance to the incinerator is given. Generally, the true soil values tend to fall within the upper tail of the simulated local distributions for locations which are close to the source incinerator. Further from the source, the true soil values are better captured within the 25-75th quantile range (Figure 7.9(a-c)).

The predicted concentrations of all dioxin congeners and the two furan congeners, TeCDF and OCDF (Figure 7.9 c) showed similar distributions at all 51 locations. When the predicted and measured concentrations are compared, the model was capable of capturing the trends of the boxplots across the 51 sampled locations. Some dissimilarities were noted. For example, at the first two sampled locations closest to the stack, the model underestimated the soil measurements; at a distance of about 4200 m, the model over predicted the real measurements. The predicted soil concentrations of PeCDF and HxCDF showed differently such that real soil measurements were mostly captured within the range of 25th and 75th percentiles of the distributions.

Interestingly, at further distance from the incinerator stack, the predictions of dioxins and furans better captured the true values. Specifically, dioxin congeners are predicted

within 25^{th} and 75^{th} quantile ranges of the distributions of 100 simulated values out to the distance of 4500m from the incinerator. This quantile range (25^{th}-75^{th}) is also called the 0.5-probability interval (0.5-PI). Furans however are better predicted in the 0.5-PI only in the range from 4500 to 7000 m from the incinerator. Elsewhere, the predictions fluctuated strongly. Overall, the observed trends in dioxins and furans predictions mimic the distributions of soil congener data at 51 locations (Figure 7.10 (a-b)).

Figure 7.10a and 7.10b show the distribution of dioxin congeners at 51 locations as a function of distance to the smoke stack. It can be seen that from 4500 m, the dioxin congener concentrations gradually decrease and deviate about the median values (0.5-PI). While we observed furan congeners are strongly variable again from 7000 m away of the smoke stack. The model under predicted the soil data at locations close to the stack where we observed the highest values of soil data.

Appendix 7.1 provides details of the computation for the number of true values that fall into the interval p-PI of the local distribution (100 realizations at one sampling location) for the 10 selected dioxins and furans.

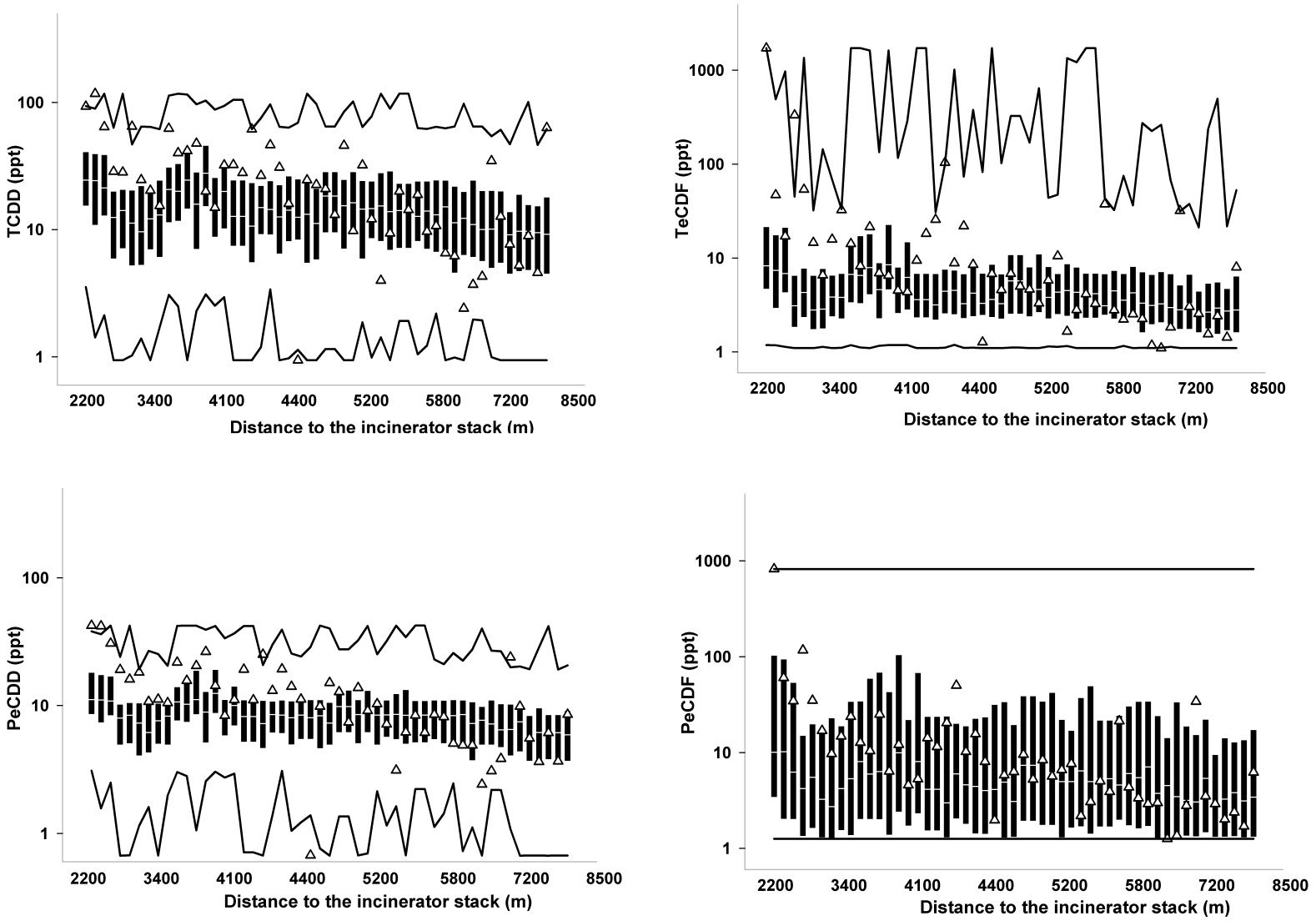

Figure 7.9a. Box plots of the distributions of 100 simulated TCDD, TeCDF, PeCDD and PeCDF values at the closest grid nodes to the location of the 51 UMDES samples (values denoted by open triangles).

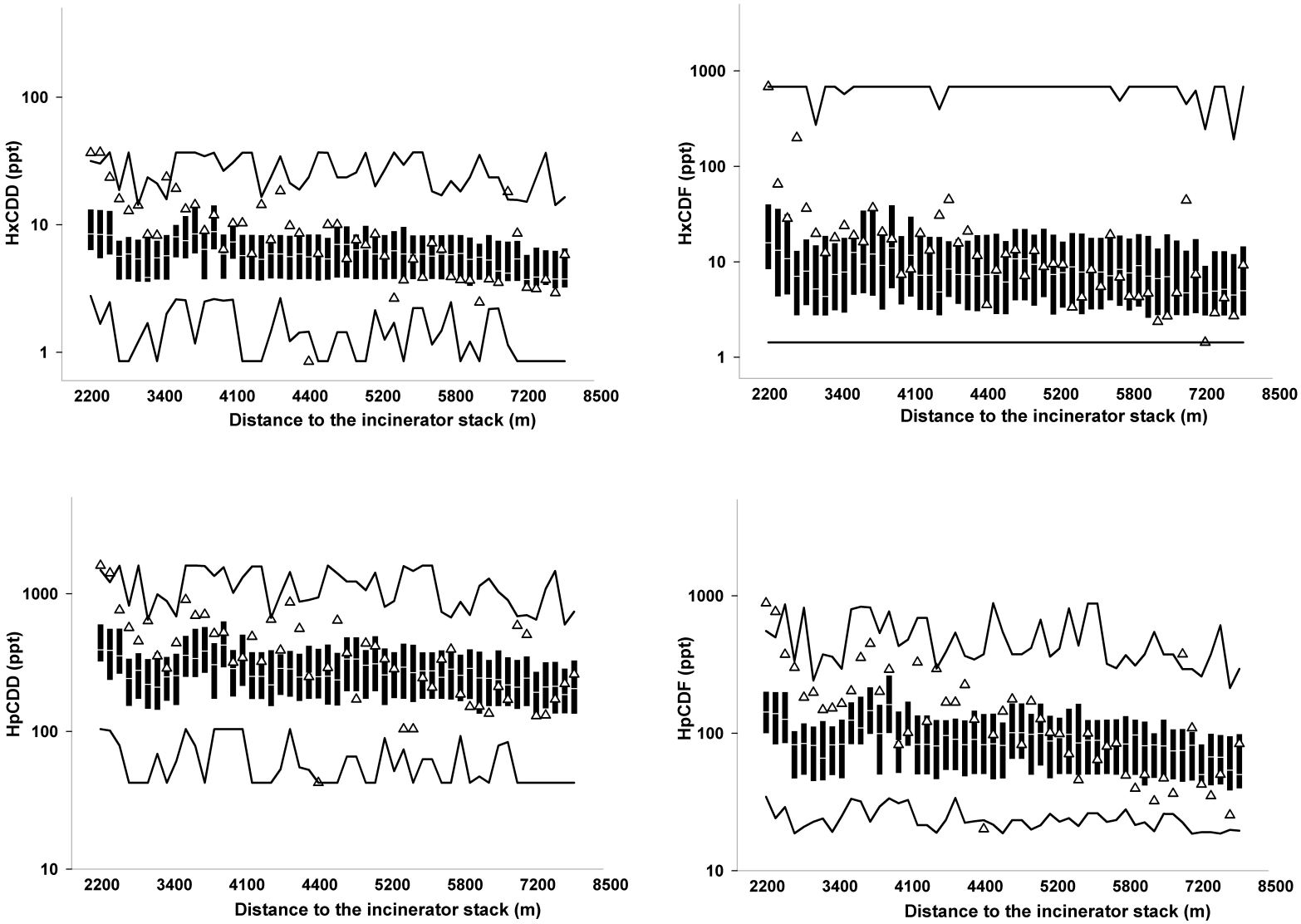

Figure 7.9b. Box plots of the distributions of 100 simulated HxCDD, HxCDF, HpCDD and HpCDF values at the closest grid nodes to the locations of the 51UMDES samples (values denoted by open triangles).

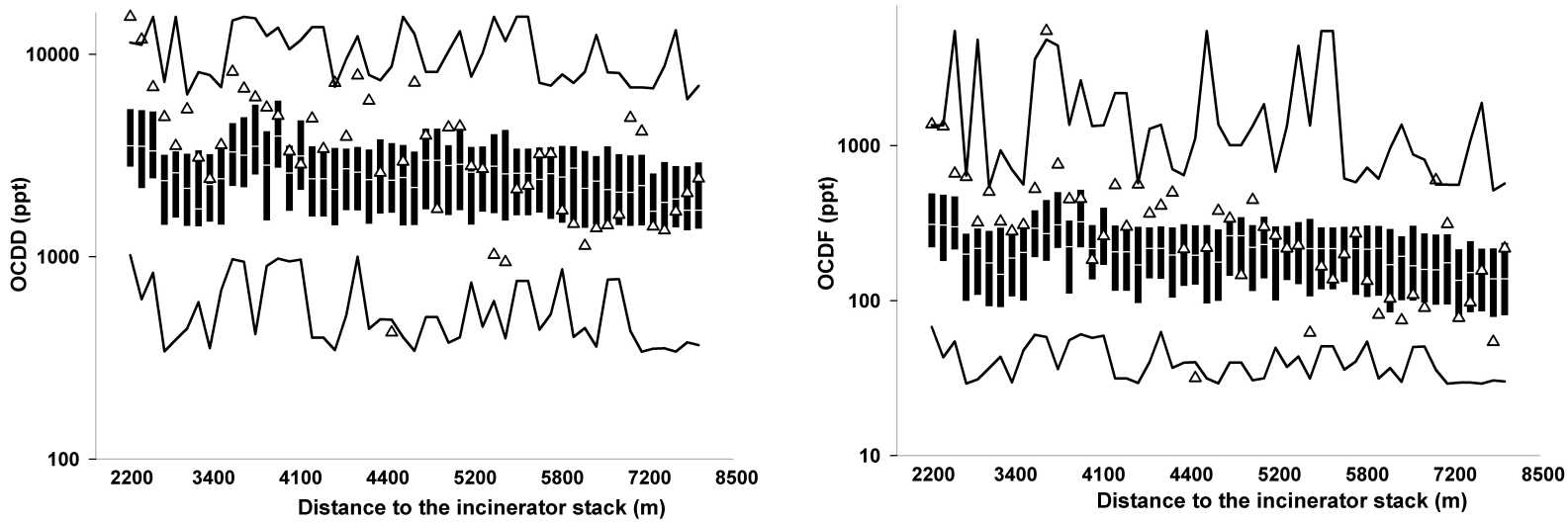

Figure 7.9c. Box plots of the distributions of 100 simulated OCDD and OCDF values corresponding at the closest grid nodes to the location of the 51 UMDES samples (values denoted by open triangles).

Boxplot of Figure 7.9 (a,b,c) are modified, composing of vertical bar for 25^{th} – 75^{th} range, minimum and maximum value are lines connected and median value is presented by a white mark on each vertical bar.

(a) (b)

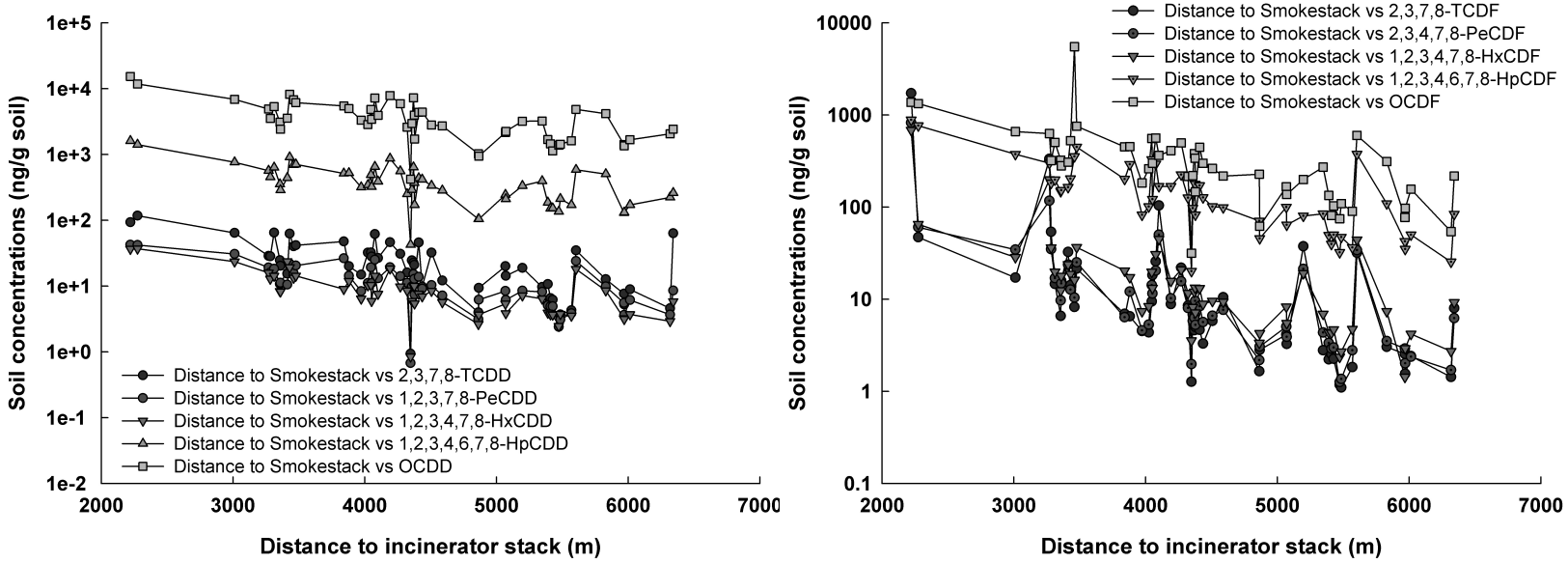

Figure 7.10 (a,b). Distributions of soil dioxin congener (a) and soil furan congener (b) concentrations at 51 locations as function of the distance to the smoke stack.

Model Uncertainty. Sequential Gaussian Simulation was used in previous work *(7, 8, 29)* , and indicated that inclusion of sample locations in geospatial analysis, a regression step between available soil samples and deposition fluxes predicted by air dispersion models in this study, yielded more accurate prediction as compared to the aspatial based approach. We repeated the validation of the model uncertainty in terms of model accuracy and precision in predicting soil dioxin congeners at the 51 known soil locations.

At each of the known locations, we obtained 100 realizations of congener concentrations. The conditional cumulative distribution function (ccdf) at that location is obtained, allowing computations of a series of symmetric p-probability intervals (p-PI) bounded by (1-p)/2 and (1+p)/2 quantiles of that ccdf *(29)*. For example, the 0.5-PI is bounded by the lower and upper quartiles (25-75%). Nine PIs were computed for 0.1, 0.2, 0.3 to 0.9 p intervals in the whole ccdf distribution [0,1]. A distribution is deemed accurate if the fraction of the true values that fall into the p interval exceeds p for all p in [0,1]*(30)*. As for the 0.5-PI, a correct model would indicate that there is a 0.5 probability that the actual measured congener concentration value at that location falls into that interval or, equivalently, that over the study area 50% of the 0.5-PI include the true value. The ccdf of 100 simulated concentrations at each location for each dioxin congener is called the local distribution.

Similarly, a cdf of the available 51 measurements of each dioxin congener across all locations is called the global distribution. The probability interval of the global distribution (the 51 soil available data) was plotted against the empirical probability interval of the local distribution (100 simulated values at grid node that is closest to the

sampling location) to quantify the accuracy of the model of uncertainty (expected vs. measured fractions of values).

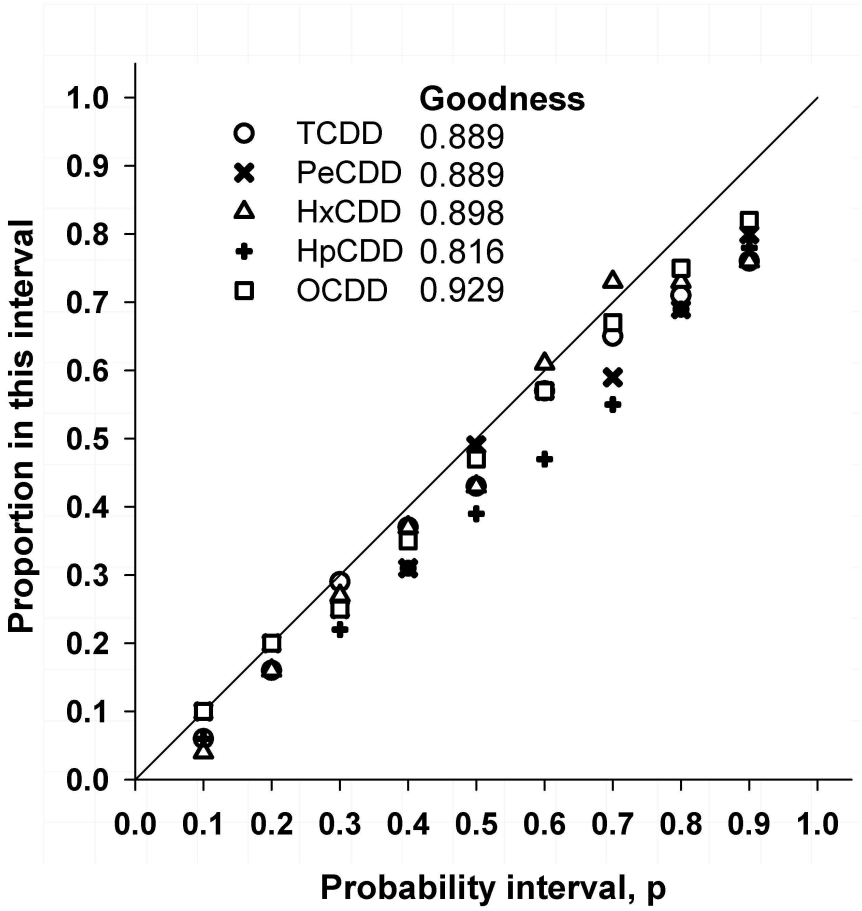

Figure 7.11a. Accuracy plot of dioxin congeners

The accuracy plots (Figure 7.11a, 7.11b) show that, except for PeCDF and HxCDF, the concentrations of the dioxin and furan congeners were predicted with similar accuracy. For example, the observed TCDD (Figure 7.11.a) values are included in the 0.3-PI for 29% of the 51 available measurements (expected proportion=30%). TeCDF, PeCDF and HxCDF predictions at 0.3-PI (Figure 7.4.b) are accurate as the expected

fractions of true values in this interval exceeded 0.3. The 45 degree diagonal line provided in each accuracy plot indicates that, if a point falls above the line, the model prediction at its corresponding PI is accurate. If points of the scattergram are below the 45 diagonal line, the model is said inaccurate as the portion of the true values are lesser than expected as those probability intervals (Figure 7.11a, 7.11b at the intervals of 0.6, 0.7, 0.8 and 0.9-PIs).

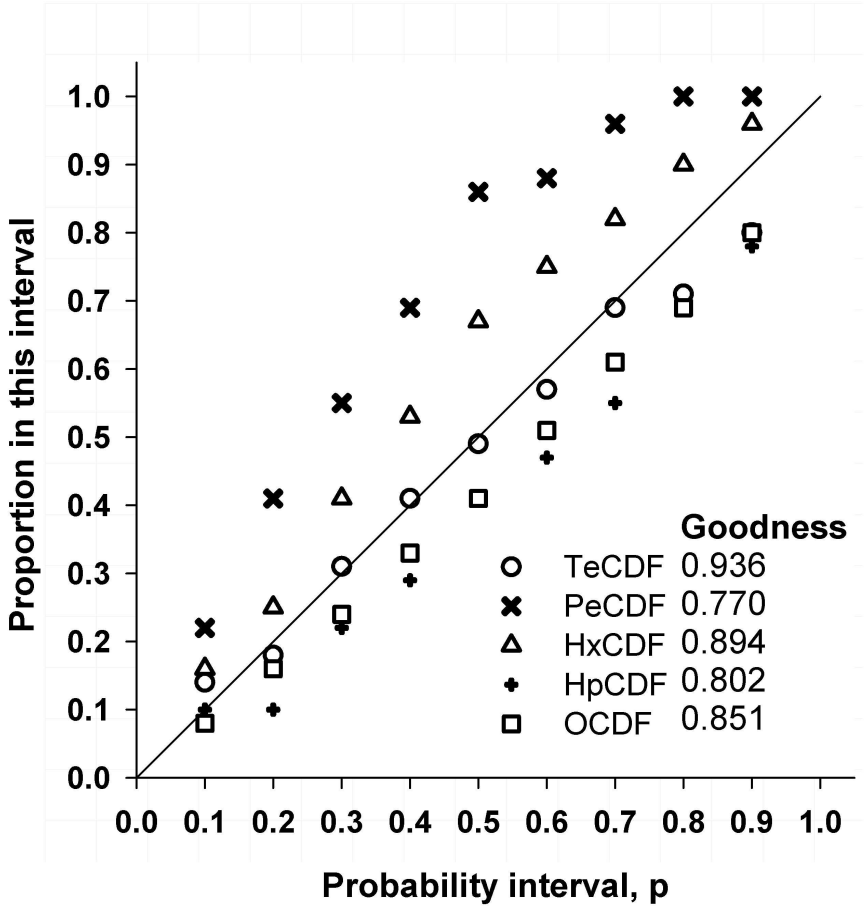

Figure 7.11b. Accuracy plot of 5 furan congeners

Inaccuracy cases might be due to the fact that the global distributions of measured values have a number of outliers with high values. In order to assess the inaccuracy cases, the goodness of fit for each congener was computed. Goodness of 1 represents both 100% accuracy and precision. Based on the results in figure 7.11a, the predictions for dioxins are more accurate and precise than those for furans. Predictions for PeCDF and HxCDF are the worst (Figure 7.11b).

Not only should the true (measured) congener values fall into the probability interval (PI) according to the expected probability *p*, but this interval should be as narrow as possible to reduce the uncertainty about that value. The average width of these local PIs should also be smaller than the global PI inferred from the sample histogram. The scatter plots in Figure 7.12a (dioxins) and Figure 7.12b (furans) indicate that, for all congeners (except for PeCDF and HxCDF), at all probabilities p, the local PIs are indeed narrower than the corresponding global PIs. This means that the geostatistical model of uncertainty is more precise than an aspatial model that ignores the location of soil samples. This observation validates the use of a geospatial model to interpolate the deposition data from the incinerator.

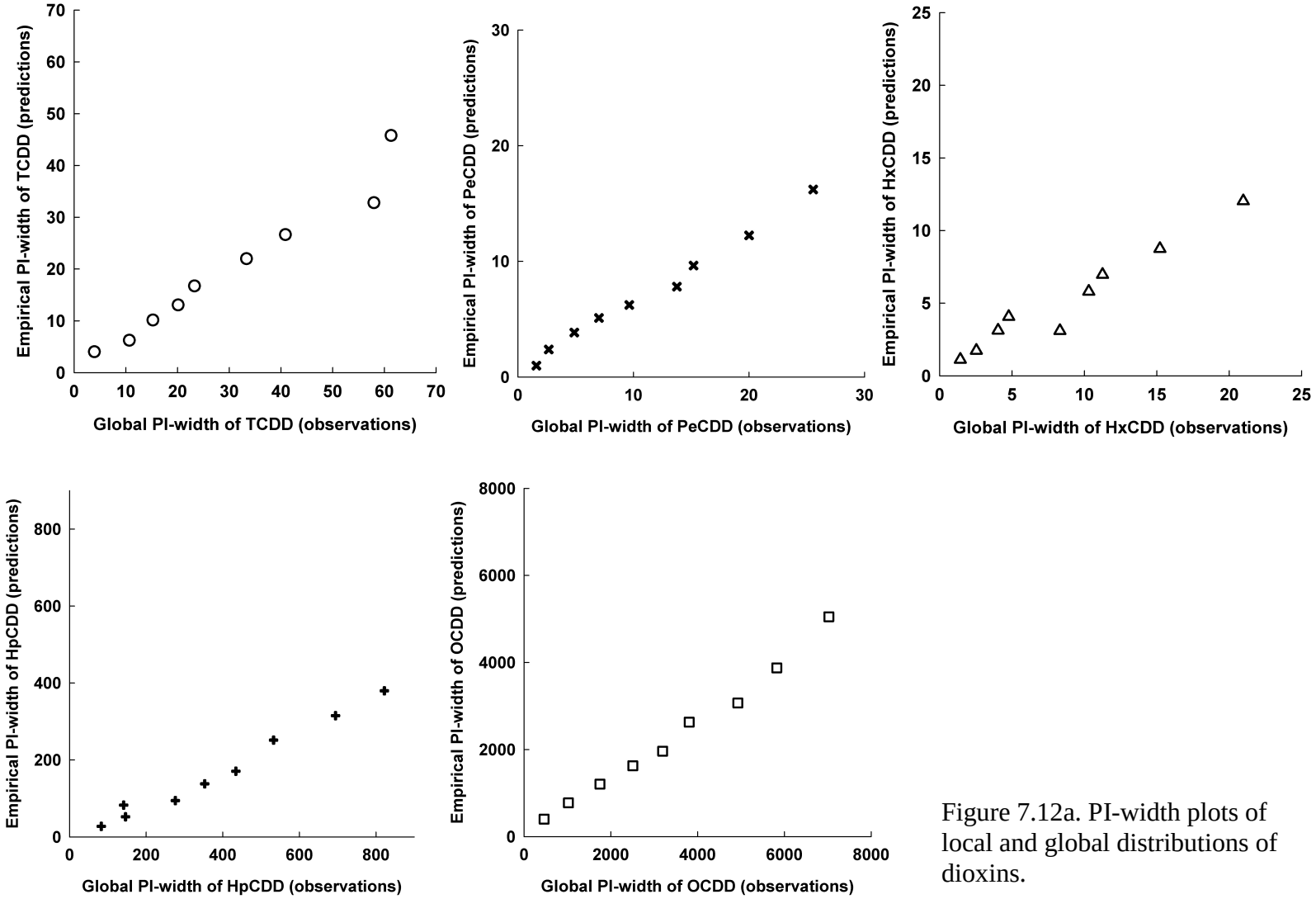

Figure 7.12a. PI-width plots of local and global distributions of dioxins.

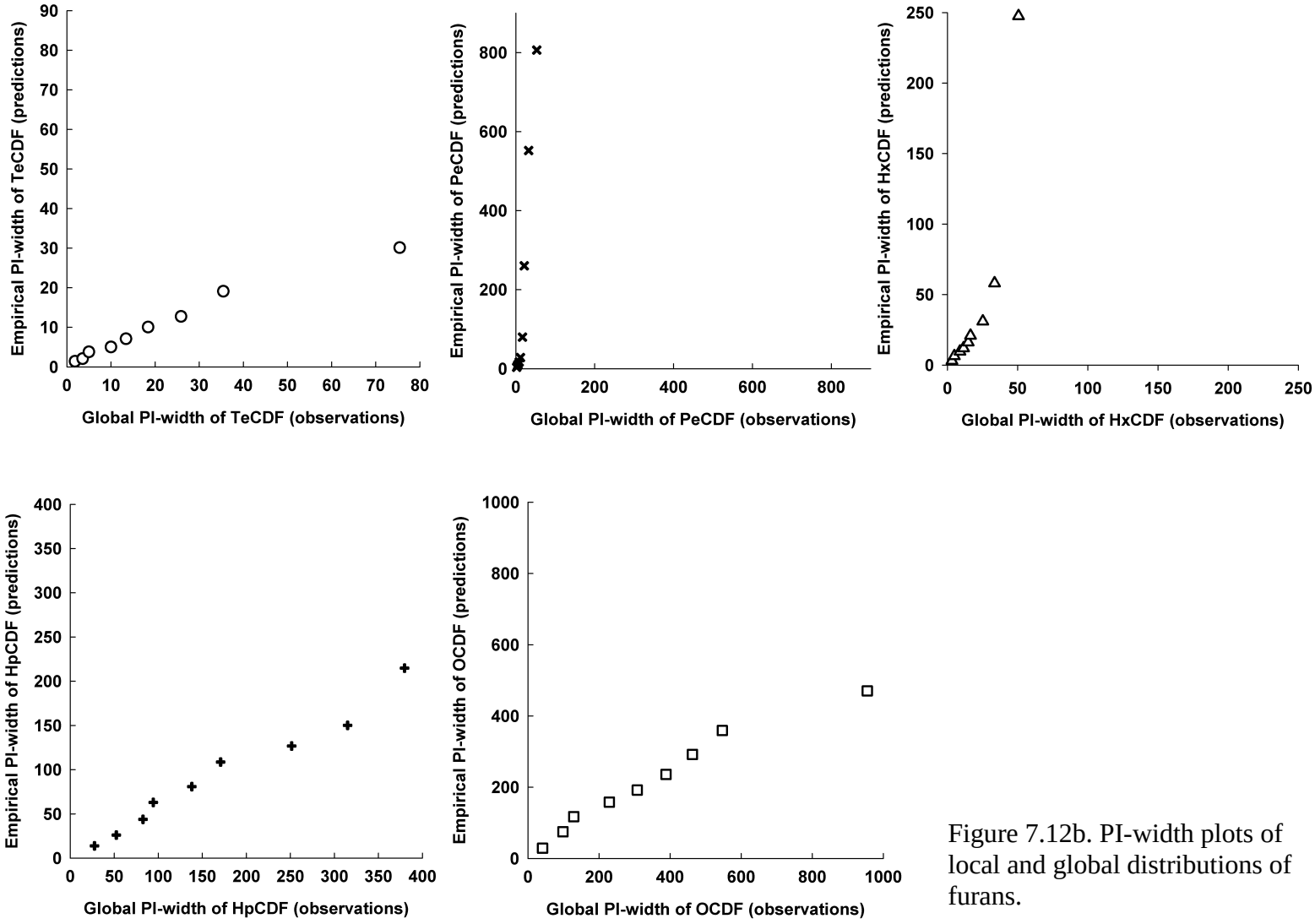

Figure 7.12b. PI-width plots of local and global distributions of furans.

7. 4. Conclusion

This chapter reported and discussed the geostatistical modeling and validation of soil concentrations of 10 dioxin and furan congeners. The predictions of concentrations at 51 sampling locations are moderately accurate and precise for all congeners, except for PeCDF and HxCDF. Close to the plant, the true soil measurements fall into the upper tail (above 75^{th} quantile) of the cumulative distributions of model predictions. Interestingly, the model predictions are more accurate at further distance from the incinerator source, reflecting the variability of the true soil measurements. Point-simulated values of soil congeners were predicted to be high proximate to the plant, whereas the extent of contamination appears to be directed towards higher values south of the plant. The point simulated plume predicted by ISCST3 for TEQ concentration however also extended north of the plant *(7)*. The different shape and extent of plumes predicted by the AERMOD coupled geostatistical model (as compared to the ISCST3 coupled geostatistical model) is likely due to the available 51 UMDES soil data (as compared to the 53 MDEQ data), or the meteorological data set chosen. Lastly, considering that the correlation between wet and dry deposition and actual measured soil data was higher for congener-specific/AERMOD models (0.4-0.8) than for TEQ/ISCT3 models (<0.4), the former better predicts the soil value trends and is a better test of the hypothesis as to whether the soil contamination is driven by incinerator emissions deposition.

Appendix 7.1: Number of UMDES observations that fall within a series of confidence intervals defined by the quantiles of the distribution of 100 simulated congener values. Goodness indicators are provided.

Chemical	Probability interval, PI	Empirical PI	No. of true values fall in to PI	Empirical PI width	[emp.PI-PI]	Weight	Goodness
	0.1	0.06	3	4.04	0.04	2	
	0.2	0.16	8	6.26	0.04	2	
	0.3	0.29	15	10.15	0.01	2	
	0.4	0.37	19	13.06	0.03	2	
	0.5	0.43	22	16.74	0.07	2	
	0.6	0.57	29	22.01	0.03	2	
	0.7	0.65	33	26.64	0.05	2	
	0.8	0.71	36	32.81	0.09	2	
	0.9	0.76	39	45.79	0.14	2	
TCDD							**0.889**
	0.1	0.1	5	0.99	0	1	
	0.2	0.2	10	2.39	0	1	
	0.3	0.25	13	3.85	0.05	2	
	0.4	0.31	16	5.11	0.09	2	
	0.5	0.49	25	6.23	0.01	2	
	0.6	0.57	29	7.81	0.03	2	
	0.7	0.59	30	9.64	0.11	2	
	0.8	0.69	35	12.25	0.11	2	
	0.9	0.8	41	16.21	0.1	2	
PeCDD							**0.889**

Chemical	Probability interval, PI	Empirical PI	No. of true values fall in to PI	Empirical PI width	[emp.PI-PI]	Weight	Goodness
	0.1	0.04	2	1.12	0.06	2	
	0.2	0.16	8	1.74	0.04	2	
	0.3	0.27	14	3.13	0.03	2	
	0.4	0.37	19	4.07	0.03	2	
	0.5	0.43	22	3.1	0.07	2	
	0.6	0.61	31	5.81	0.01	1	
	0.7	0.73	37	6.97	0.03	1	
	0.8	0.73	37	8.75	0.07	2	
	0.9	0.76	39	12.03	0.14	2	
HxCDD							**0.898**
	0.1	0.06	3	12	0.04	2	
	0.2	0.2	10	26.08	0	1	
	0.3	0.22	11	42.84	0.08	2	
	0.4	0.31	16	63.03	0.09	2	
	0.5	0.39	20	81.31	0.11	2	
	0.6	0.47	24	108.6	0.13	2	
	0.7	0.55	28	125.69	0.15	2	
	0.8	0.69	35	150.1	0.11	2	
	0.9	0.78	40	214.76	0.12	2	
HpCDD							**0.816**
	0.1	0.1	5	401.8	0	1	
	0.2	0.2	10	776.58	0	1	
	0.3	0.25	13	1207.06	0.05	2	
	0.4	0.35	18	1628.67	0.05	2	
	0.5	0.47	24	1962.69	0.03	2	
	0.6	0.57	29	2631.14	0.03	2	
	0.7	0.67	34	3069.58	0.03	2	
	0.8	0.75	38	3878.09	0.05	2	
	0.9	0.82	42	5051.29	0.08	2	
OCDD							**0.929**

Chemical	Probability interval, PI	Empirical PI	No. of true values fall in to PI	Empirical PI width	[emp.PI-PI]	Weight	Goodness
	0.1	0.14	7	1.43	0.04	1.00	
	0.2	0.18	9	2.09	0.02	2.00	
	0.3	0.31	16	3.81	0.01	1.00	
	0.4	0.41	21	5.03	0.01	1.00	
	0.5	**0.49**	**25**	**7.11**	0.01	2.00	
	0.6	0.57	29	10.05	0.03	2.00	
	0.7	0.69	35	12.74	0.01	2.00	
	0.8	0.71	36	19.1	0.09	2.00	
	0.9	**0.8**	41	**30.12**	0.10	2.00	
TeCDF							**0.936**
	0.1	0.22	11	3.79	0.12	1.00	
	0.2	0.41	21	7.59	0.21	1.00	
	0.3	0.55	28	10.72	0.25	1.00	
	0.4	0.69	35	17.01	0.29	1.00	
	0.5	0.86	44	28.35	0.36	1.00	
	0.6	0.88	45	80.21	0.28	1.00	
	0.7	0.96	49	260.52	0.26	1.00	
	0.8	1.00	51	552.29	0.20	1.00	
	0.9	1.00	51	806.69	0.10	1.00	
PeCDF							**0.770**

Chemical	Probability interval, PI	Empirical PI	No. of true values fall in to PI	Empirical PI width	[emp.PI-PI]	Weight	Goodness
	0.1	0.16	8	3.09	0.06	1.00	
	0.2	0.25	13	6.38	0.05	1.00	
	0.3	0.41	21	9.63	0.11	1.00	
	0.4	0.53	27	12	0.13	1.00	
	0.5	0.67	34	16.21	0.17	1.00	
	0.6	0.75	38	20.88	0.15	1.00	
	0.7	0.82	42	31.04	0.12	1.00	
	0.8	0.9	46	58.08	0.10	1.00	
	0.9	0.96	49	247.57	0.06	1.00	
HxCDF							**0.894**
	0.1	0.1	5	13.86	0.00	1.00	
	0.2	0.1	10	26.08	0.10	2.00	
	0.3	0.22	11	43.84	0.08	2.00	
	0.4	0.29	15	62.94	0.11	2.00	
	0.5	0.41	21	80.84	0.09	2.00	
	0.6	0.47	24	108.6	0.13	2.00	
	0.7	0.55	28	126.71	0.15	2.00	
	0.8	0.69	35	150.1	0.11	2.00	
	0.9	0.78	40	214.76	0.12	2.00	
HpCDF							**0.802**
	0.1	0.08	4	29.04	0.02	2.00	
	0.2	0.16	8	74.95	0.04	2.00	
	0.3	0.24	12	117.46	0.06	2.00	
	0.4	0.33	17	158.24	0.07	2.00	
	0.5	0.41	21	192.01	0.09	2.00	
	0.6	0.51	26	235.88	0.09	2.00	
	0.7	0.61	31	292.15	0.09	2.00	
	0.8	0.69	35	359.38	0.11	2.00	
	0.9	0.8	41	470.46	0.10	2.00	
OCDF							**0.851**

References

(1) EPA, U., User's Guide for the AMS/EPA Regulatory Model - AERMOD. **2006**

(2) EPA, U., User's Guide for the Industrial Source Complex (ISC 3) Dispersion Models **1995,** Vol. 1

(3) EPA/OSW, 1996 National Dioxin Database. **1996**.

(4) Dyke, P. H.; Amendola, G., Dioxin releases from US chemical industry sites manufacturing or using chlorine. *Chemosphere* **2007,** 67, (9), S125-S134.

(5) EPA, Soil Screening Survey At Four Midwestern Sites **1985**, 163.

(6) EPA, U. *Michigan Dioxin Studies Dow Chemical Building 703 Incinerator Exhaust And Ambient Air Study*; 1987.

(7) Goovaerts, P.; Trinh, H. T.; Demond, A.; Franzblau, A.; Garabrant, D.; Gillespie, B.; Lepkowski, J.; Adriaens, P., Geostatistical modeling of the spatial distribution of soil dioxins in the vicinity of an incinerator. 1. Theory and application to Midland, Michigan. *Environmental Science & Technology* **2008,** 42, (10), 3648-3654.

(8) Goovaerts, P.; Trinh, H. T.; Demond, A. H.; Towey, T.; Chang, S. C.; Gwinn, D.; Hong, B.; Franzblau, A.; Garabrant, D.; Gillespie, B. W.; Lepkowski, J.; Adriaens, P., Geostatistical modeling of the spatial distribution of soil dioxin in the vicinity of an incinerator. 2. Verification and calibration study. *Environmental Science & Technology* **2008,** 42, (10), 3655-3661.

(9) MDEQ *Part 201 Generic Soil Direct Contact Criteria* Michigan Department of Environmental Quality Environmental Response Division: 1998.

(10) Garabrant, D. H.; Franzblau, A.; Lepkowski, J.; Gillespie, B. W.; Adriaens, P.; Demond, A.; Ward, B.; LaDronka, K.; Hedgeman, E.; Knutson, K.; Zwica, L.; Olson, K.; Towey, T.; Chen, Q. X.; Hong, B. L., The University of Michigan Dioxin Exposure Study: Methods for an Environmental Exposure Study of Polychlorinated Dioxins, Furans, and Biphenyls. *Environmental Health Perspectives* **2009,** 117, (5), 803-810.

(11) Perry, S. G.; Cimorelli, A. J.; Paine, R. J.; Brode, R. W.; Weil, J. C.; Venkatram, A.; Wilson, R. B.; Lee, R. F.; Peters, W. D., AERMOD: A dispersion model for industrial source applications. Part II: Model performance against 17 field study databases. *Journal of Applied Meteorology* **2005,** 44, (5), 694-708.

(12) Rosenbaum, A.; Hartley, S.; Holder, C.; Turley, A.; Graham, S., Nitrogen Dioxide (NO2) Exposure Assessment in Support of US EPA's NAAQS Review: Application of AERMOD and APEX to Philadelphia County. *Epidemiology* **2008,** 19, (6), S344-S345.

(13) Hill, R.; Taylor, J.; Lowles, I.; Emmerson, K.; Parker, T., A new model validation database for evaluating AERMOD, NRPB R91 and ADMS using krypton-85 data from BNFL Sellafield. *International Journal of Environment and Pollution* **2005,** 24, (1-4), 75-87.

(14) Hanna, S. R.; Egan, B. A.; Purdum, J., Evaluation of the ADMS, AERMOD, and ISC3 dispersion models with the OPTEX, Duke Forest, Kincaid, Indianapolis and Lovett field datasets. *International Journal of Environment and Pollution* **2001,** 16, (1-6), 301-314.

(15) EPA, U. *Comparison of regulatory design concentrations AERMOD vs ISCST3, CTDMPLUS, ISC-PRIME*; 2003.

(16) Floret, N.; Viel, J. F.; Lucot, E.; Dudermel, P. M.; Cahn, J. Y.; Badot, P. M.; Mauny, F., Dispersion modeling as a dioxin exposure indicator in the vicinity of a municipal solid waste incinerator: A validation study. *Environmental Science & Technology* **2006,** 40, (7), 2149-2155.

(17) Yoshida, K.; Ikeda, S.; Nakanishi, J.; Tsuzuki, N., Validation of modeling approach to evaluate congener-specific concentrations of polychlorinated dibenzo-p-dioxins and dibenzofurans in air and soil near a solid waste incinerator. *Chemosphere* **2001,** 45, (8), 1209-1217.
(18) Maantay, J. A.; Tu, J.; Maroko, A. R., Loose-coupling an air dispersion model and a geographic information system (GIS) for studying air pollution and asthma in the Bronx, New York City. *International Journal of Environmental Health Research* **2009,** 19, (1), 59-79.
(19) Trembly, M. G.; Amendola, G. A., Dow Chemical Building 703 incinerator exhaust and ambient air study. Final report. In 1987; p Pages: 308.
(20) MDEQ, Meteorological Data Support Document. In Michigan Department of Environmental Quality: 2009.
(21) MDEQ, Michigan Geographic Data Library. In Michigan Department of Information Technology: 2009.
(22) EPA *Michigan Dioxin Studies Atmospheric Sampling Fact Sheet*; 1983.
(23) Inc., S. I. *SAS/STAT User's Guide* Fourth Edition, Vol. 2; SAS Institute Inc.: Cary, NC, 1989.
(24) Deutsch, C. V., Journel A.G., *GSLIB Geostatistical Software Library and User's Guide*. Second edition ed.; Oxford University Press 1992.
(25) TerraSeer *STIS (Space-Time Intelligence System)*, 1.6.002.
(26) Goovaerts, P., *Geostatistics for Natural Resources Evaluation*. Oxford University Press 1997.
(27) Koester, C. J.; Hites, R. A., Wet and Dry Deposition of Chlorinated Dioxins and Furans. *Environmental Science & Technology* **1992,** 26, (7), 1375-1382.
(28) Van den Berg, M.; Birnbaum, L. S.; Denison, M.; De Vito, M.; Farland, W.; Feeley, M.; Fiedler, H.; Hakansson, H.; Hanberg, A.; Haws, L.; Rose, M.; Safe, S.; Schrenk, D.; Tohyama, C.; Tritscher, A.; Tuomisto, J.; Tysklind, M.; Walker, N.; Peterson, R. E., The 2005 World Health Organization reevaluation of human and mammalian toxic equivalency factors for dioxins and dioxin-like compounds. *Toxicological Sciences* **2006,** 93, (2), 223-241.
(29) Goovaerts, P., Geostatistical modelling of uncertainty in soil science. *Geoderma* **2001,** 103, (1-2), 3-26.
(30) Deutsch, C. V., *Direct assessment of local accuracy and precision.* Kluwer Academic Publishing: Dordrecht, 1997; p 115–125.

Chapter 8

Conclusions and Recommendations

Conclusions

Dioxins as 2,3,7,8-TCDD, 1,2,3,7,8-PeCDD, 2,3,4,7,8-PeCDF are the most toxic pollutants. Dioxin pollution in the ambient air or on the ground may be partially due to the emission of dioxins from old industrial waste incinerators. Dioxins are hydrophobic compounds thus are often associated with airborne particles once they are emitted from the incinerator stack. Dry and wet depositions of dioxins associated particles are the two removal pathways of dioxins in the atmosphere. Less chlorinated dioxin congeners such as tetra and penta dioxins partition into the gaseous phase of the atmosphere at higher extent than the more chlorinated dioxins such as hepta and octa congeners. Portions of dioxins partitioned into the gaseous phase are also removed from the atmosphere by ways of dry and wet depositions. Air dispersion models such as ISCST3 and AERMOD can predict the amount of dioxin depositions in gaseous and particulate phase by dry and wet deposition mechanisms. As in our studies, dry deposition of dioxin in particulate phase is a dominant removal pathway. Depositions occur closely to the point source, especially with the case of wet deposition. We tested two air dispersion models, ISCST3 and AERMOD with different choices of model inputs such as dioxin emission rates, dioxin

particle size distributions, and meteorological data. The site specific meteorological data (wind speed, wind direction, temperature, among others) are likely the controlled variables to the air dispersion modeling results of air concentrations and dry and wet deposition fluxes.

Dry and wet deposition fluxes of dioxin TEQ and dioxin congeners are regressed against the actual soil measurements as a step of coupling air dispersion model with geostatistical model. The coupling model simulates 100 dioxin concentrations at every receptor, allowing to probabilistically quantifying the distributions of TEQ and dioxin congeners. As a result, we could obtain various forms of dioxin deposition maps for several purposes. For an example, averaging dioxin predictions on census block level with computed probability of exceeding threshold TEQ value were used as a guideline to the UMDES soil sampling in Midland area.

Although deposition fluxes predicted by AERMOD with the best available input data showed an improvement in compared to the results from ISCST3 model, however when coupled with geostatistical model, the combining model might not yet a better model in predicting spatial distribution of dioxins. Our studies showed that available soil measurements, employed in the geostatistical model, might have a strong impact on the accuracy of model predictions. Variability in values of the soil data set and in sampled locations is to be considered. Cross-validation of dioxin predictions using the available dioxin measurements can only obtain a moderate accuracy if the measurements were preferentially samples at locations where high TEQ values were expected, as in 51 UMDES samples.

Suggestions for further research

As indicated by our study results, the following recommendations are made to better quantify spatial distribution of dioxins:

- Emission profiles of dioxin congeners and TEQ are to be measured correctly from the incinerator stack. Actual emission rates of dioxins as inputs to the air dispersion model would allow a good estimate of ambient air concentration and depositions on the ground.
- Meteorological data need to be preprocessed in compatible formats for air dispersion models and to contain no missing data in order to run the air dispersion model smoothly. The meteorological data should be collected on site or as close as possible to the modeling area.
- Actual soil measurements used in geostatistical analysis and cross-validation are not much preferential and not having extreme high values. The more soil data collected the better model predictions can be expected.